GEDIZ UNIVERSITY ★ GRADUATE SCHOOL OF SCIENCE ENGINEERING AND TECHNOLOGY

ELECTRICAL EQUIVALENT CIRCUIT MODELLING OF DYE SENSITIZED SOLAR CELLS

M.Sc. THESIS

Elif Şeyda ÇAKMAK
(60071110)

Department of Electrical and Electronic Engineering

Nanotechnology Programme

Thesis Advisor: Asst. Prof. Dr. Ömer MERMER

March 2014

GEDİZ ÜNİVERSİTESİ ★ FEN BİLİMLERİ ENSTİTÜSÜ

BOYA DUYARLI GÜNEŞ PİLLERİNİN ELEKTRİKSEL EŞDEĞER DEVRE MODELLEMESİ

YÜKSEK LİSANS TEZİ

Elif Şeyda ÇAKMAK
(60071110)

Elektrik Elektronik Mühendisliği Anabilimdalı

Nanoteknoloji Programı

Tez Danışmanı: Yar. Doç. Ömer MERMER

Mart 2014

Elif Şeyda Çakmak, a **M.Sc.** student of **Graduate School of Nanotechnology** student ID **60071110**, successfully defended the **thesis** entitled **"Electrical Equivalent Circuit Modelling of Dye Sensitized Solar Cells (DSSCs)"**, which she prepared after fulfilling the requirements specified in the associated legislations, before the jury whose signatures are below.

Thesis Advisor :   **Asst. Prof. Dr. Ömer Mermer**   ....
                       Gediz University

Jury Members :   **Asst.Prof. Dr. Ömer Mermer**   ....
                     Gediz University

                     Asst.Prof. Dr. Melih Palandöken   ....
                     Gediz University

                     Asst.Prof. Dr. Mustafa Can   ....
                     Izmir Katip Çelebi University

Date of Submission : 15 December 2013
Date of Defense :   20 January 2014

To my spouse and parents,

FOREWORD

TABLE OF CONTENTS

ABBREVIATIONS

BHJ	:	Bulk Heterojunction
CSDM	:	Conventional Single Diode Model
DSC	:	Dye Sensitised Solar Cell
DSSC	:	Dye Sensitised Solar Cell
EQE	:	External Quantum Efficiency
HOMO	:	Highest Occupied Molecular Orbital
HSC	:	Hybride Solar Cell
IPCE	:	Incident Photon to Charge Carrier Efficiency
IQE	:	Internal Quantum Efficency
ISC	:	Inorganic Solar Cell
LHE	:	Light Harvesting Efficiency
LUMO	:	Lowest Unoccupied Molecular Orbital
OC	:	Open Circuit
OSC	:	Organic Solar Cell
SC	:	Short Circuit
STC	:	Standard Test Conditions (1000W/m²,25°C)

LIST OF TABLES

LIST OF FIGURES

ELECTRICAL EQUIVALENT CIRCUIT MODELLING OF DYE SENSITIZED SOLAR CELLS

SUMMARY

Although, development of solar cell technology highly depends on material research at the very primary stage of this science, to improve industrial feasibility of solar cell devices, understanding behaviors of devices is vital. Models help to simplify device behaviors for specific aims. Modeling electrical behaviors by modeling current-voltage characteristic of device under different conditions is crucial to understand cell itself, to integrate it into arrays and circuits, and to avoid from mismatches.

There are variety types of electrical equivalent circuit models proposed in literature. Most of them have Schottky diodes, shunted and serial resistances, as well as a current source representing illumination dependant photocurrent. Due to the transcendental structure of nonlinear diode equation, decision on solution method is an issue. To get amenable values there are many analytical and computational methods are proposed in literature.

In order to have an idea about cell, the accuracy of parameters that are extracted from the solution of circuit model is important. The accuracy of parameters are excessively depends on the model and its solution method.

Thus, methods and models should be tested with a lot of I-V data got from different types of cells, under different conditions. In this study, physical background of dye synthesized solar cells is explained and the simplest model (single diode model) in literature is used to develop a model under consideration of different illuminations and applied to the different DSSCs' numerated from 1 to 6.

BOYA DUYARLI GÜNEŞ PİLLERİNİN ELEKTRİKSEL EŞDEĞER DEVRE MODELLEMESİ

ÖZET

Başlangıçta güneş pil teknolojileri tamamen malzeme bilimine bağımlı olarak yürütülmüşse de, günümüz teknolojisinde cihazın davranışını anlamak endüstriyel fizibilitesini arttırmak açsından daha büyük önem kazanmıştır. Cihaz davranışlarını basite indirgemek ve anlamak için çeşitli modelleri kullanılır. Cihazın farklı koşullardaki elektriksel davranışlarının, yani akım gerilim cevabının modellenmesi, cihazın modüllere ve çeşitli devrelere entegrasyonunda cihazı tanımlamak adına ve uyuşmazlıkları önlemek adına önemlidir. Literatürde pek çok elektriksel eşdeğer devre modelleme çeşidi kullanılmıştır. Bunlar çoğunluğu Schottky diyotlara, paralel ve seri dirençlere ve bunlara ek olarak da devrenin akımında ışığa duyarlı olarak oluşan değişimi modelleyen fotoakım kaynağına sahiptir. Doğrusal olmayan diyot denkleminin transandantal yapısı nedeniyle modellerin çözüm metotlarına karar vermek de başlı başına bir problem oluşturmaktadır. Güvenilir sonuçlar elde edebilmek için, literatürde analitik ve bilgi sayımsal pek çok metot önerilmiştir. Güneş hücresi hakkında bilgi edine bilmek için eşdeğer devre modelinin çözümünde elde edilen parametrelerin tutarlı olması çok önemlidir. Parametrelerin doğruluğu ise tamamen seçilen model ve çözüm metodunun doğru olmasına bağlıdır. Bundan dolayı önerilecek modellerin ve metotların çeşitli güneş hücrelerinden farklı durumlar altında elde edilmiş pek ok sayıda akım-gerilim verileri ile test edilmiş olması model ve metodun doğruluğuna karar verebilmek açısından önemlidir. Bu çalışmamızda, ön bilgi olarak boya duyarlı güneş pillerinin fiziksel altyapısından kısaca bahsedilmiş ve çalışma prensibi anlatılmıştır. Sonrasında, yapılan modelleme için literatürde kullanılan en temel model, bir diyotlu eşdeğer devre modeli seçilmiştir. Seçilen model 1'den 6'ya kadar numaraladığımız farklı boya duyarlı güneş pili verilerine uygulanılarak, farklı aydınlatmalar için tutarlılığını sürdürecek şekilde geliştirilmiştir.

1. INTRODUCTION

Although sustainable energy has been a problem for human being from time to time; after industrial revolution, savage consumption of traditional energy sources such as fossil fuels and coals has given rise to environmental pollution, deforestation and species extinction implicitly. Due to the fact, some vital problems such as global warming and serious energy crisis have occurred on all over the World. To fix all these environmental and economical problems people should aim to use the renewable energy sources immediately.

Throughout the Earth's beginning, Sun is the most effective energy source of the nature. In this century, it is rising once again as the most promising renewable energy source of the future. As it is stated "More energy from sunlight strikes Earth in 1 hour than all of the energy consumed by humans in an entire year." [1]. Therefore, harvesting only miniscule amount of the energy reaching Earth may solve most of the energy problem of humanity without harming environment.

"Photovoltaic Cells" (PVCs) in other words "solar cells" are devices in which photons converted into electricity. Although, photovoltaic effect (generation of potential energy under illumination) was discovered by Alexandre Edmond Becquerel in 1839 [2,3] and photoconductivity (conduction triggered by illumination) was discovered in 1873 by Willoughby Smith, first real silicon solar cell was made in Bell Laboratories in 1953, which had enough efficiency to convert sufficient energy for daily electrical equipments [4].

Throughout the first invention of the solar cell, scientists have been seeking to invent easier, cheaper more efficient ways to harvest energy from Sun for decades. Therefore, evolution of solar cells has been rapidly growing. Besides, it has been benefiting from revolution in other technologies such as semiconductor electronics, organic electronics or nanotechnologies. These are categorized under three generation stemmed from their technological roots [5]: 1st generation solar cells are bulk p-n junction semiconductor cells. This generation so far has the highest

conversion efficiency records as it can be seen in (figure-1.1). 2nd generation solar cells are based on thin film technology. It is clear in (figure-1.1) that thin film solar cells are second generation not exactly because of their invention age but thanks to their higher technology production process. Since 2nd generation cells need only few amount of material, they have lower production cost and unfortunately lower efficiency. 3rd generation of solar cells is based on nanotechnology. They are made of mesoscopic (nanostructured) materials, which are purely organic, or mixture of organic and inorganic materials. Hence, even though currently this generation has lowest efficiency records of the cells (figure-1.1), combining their limitless number of material combinations ability and flexible design capability with its low cost and easy mass production opportunity, 3rd generation cells may drastically change their trajectory. To illustrate, as it is show in (figure-1.1) growth of the efficiencies of organic solar cells and dye sensitized solar cells seems very promising for almost ten years old technologies.
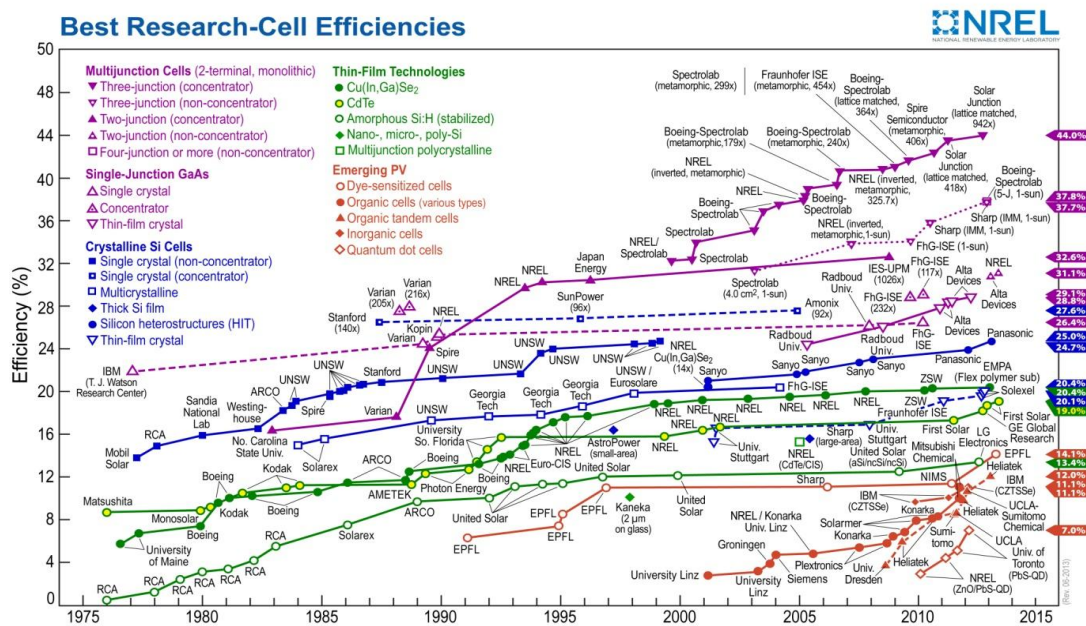
Figure 1.1 : Best Research-Cell Efficiencies statistics of National Renewable Energy Laboratory of America [6]

Although, development of solar cell technology highly depends on material research at the very primary stage of this science, to predict and solve technical problems into design as well as to improve industrial feasibility of solar cell devices, understanding behaviors of devices is vital [7]. Models help to simplify device behaviors for specific aims. Solar cells' behaviors are mainly modeled in two types. These are

optical and electrical behaviors. Modeling optical behaviors of a cell is beneficial to understand photons behavior and to increase efficiency with optimizing optical features of device [8]. On the other hand, modeling electrical behaviors by modeling current-voltage characteristic of device under different conditions is crucial to understand electrons behavior and to integrate it into arrays and circuits to harvest electricity efficiently and to avoid from mismatches [9].

There are variety types of electrical equivalent circuit models proposed in literature. Most of them have Schottky diodes, shunted and serial resistances, as well as a current source representing illumination dependant photocurrent [10-24]. Some of these models have additional diodes to model specific electrical behavior [10,22] or electrical behavior under dark condition [11-14]. A few of them also are trying to model AC behavior of their cell with adding some capacitances [17-21] or inductances to increase AC understanding [14].

Ideally, a perfect model should be decided and solved truly with its all parameters under consideration of every condition (such as under temperature, time, illumination changes) to get a real conclusion about device behavior. However, due to the transcendental structure of nonlinear diode equation, even decision on solution method is an issue. To get amenable values, many analytical and computational methods are proposed in literature [26-33].

In order to have an idea about cell, the accuracy of parameters that are extracted from the solution of circuit model, such as I_{ph} (photo current), R_s (serial resistance),R_{sh} (shunt resistance), n (ideality factor), I_o (saturation current) is important. Thus, the accuracy of parameters are excessively depends on the model and its solution method.

Due to this paradoxical situation, methods and models should be tested with a lot of I-V data got from different types of cells, under different conditions. Considering the solar cell models in the literature, it can be easily noticed that different types of solar cells with different working principles are modeled with same electrical circuit models, since they have similar shape of I-V curve but in different scales. In this study, physical background of dye synthesized solar cells is explained and the simplest model (single diode model) in literature is used to develop a novel model

under different illumination conditions and applied to the different DSSCs'
numerated from 1 to 6 [33].

2. SOLAR CELLS

The purpose of solar cells and photovoltaic devices is to convert sunlight into electricity. Solar cell could be defined by two-sectioned working principle on a black-box level. First, the sunlight is absorbed and afterwards the absorbed energy is converted into electrical power between two contact points (Figure 2.1).
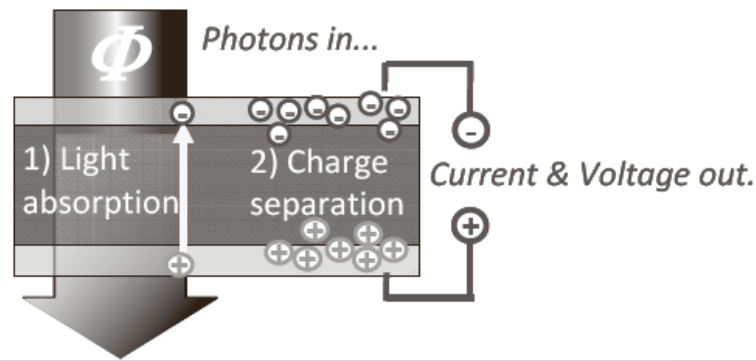
Figure 2.1 : Black-box picture of the two-sectioned working principle in photovoltaic devices: Light absorption & Charge separation [35].

The light harvesting efficiency (LHE) is defined as the fraction of light that is absorbed in the active constituent of photovoltaic device. Once designating the solar cell device's light harvesting efficiency, both the light absorbed by layers and the light reflected at the front-contact of the solar cell device (R) should be calculated.

Internal quantum efficiency (IQE) is the proportion of the charge carriers created inside the cell to the photons absorbed by the cell. So, the process inside the device is encapsulated in IQE of the solar cell device. External quantum efficiency (EQE), which is also known as incident photon to converted electron (IPCE) is the proportion of the charge carriers created inside the cell to the incident photons reaching to the cell [98]. EQE can be subtracted from the Equation 2.1 as product of LHE and IQE [34].

$$\mathbf{EQE(\lambda, V) = \big(1 - R(\lambda)\big).\,LHE(\lambda).\,IQE(\lambda, V)} \tag{2.1}$$

There is another common parameter to measure efficiency of a solar cell is the power conversion efficiency (η). It is the ration of the maximum electrical output power to

the power of the incident light. Summary of the historical events are demonstrated in Figure 2.2 with the important names and dates [36-40].
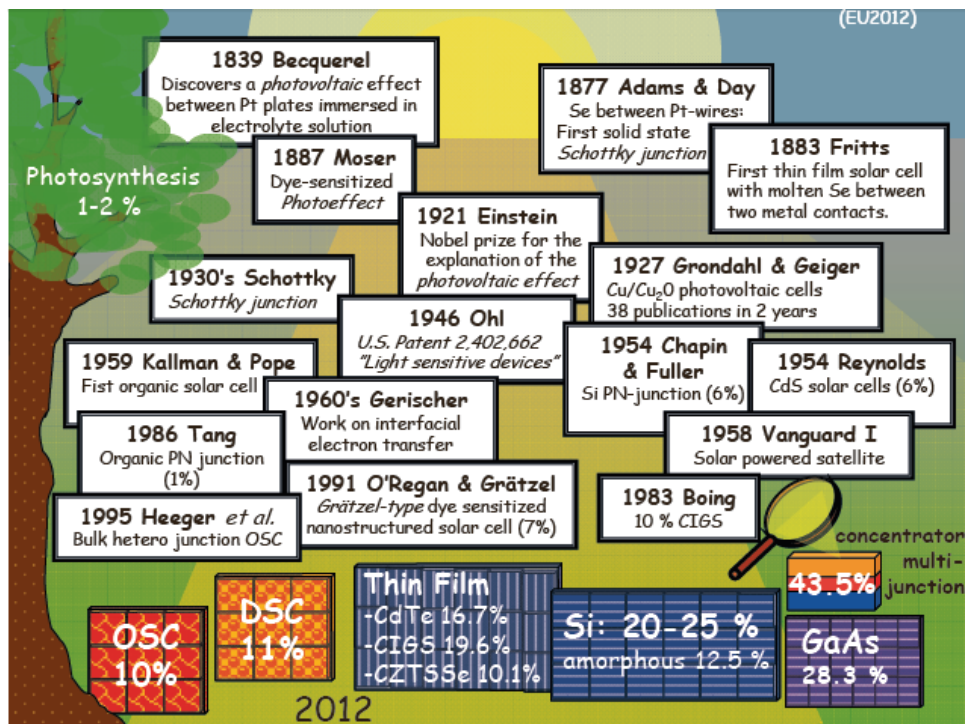
Figure 2.2 : Brief summary of chronologically important dates and names in solar cell history and efficiencies of different types of solar cell devices. [41].

Many different types of solar cell devices are available in the literature and on the market. The ones differentiated from each other in terms of materials are used for light harvesting and also in the conversion processes of absorbed photons into free electrons and holes. In order to select different types of lab-scale solar cells, current record efficiencies are included in Figure 2.2.

Solar cells including inorganic semiconductors for light harvesting can be classified as inorganic solar cells (ISCs) [42]. On the other hand, organic solar cells (OSCs) and dye sensitized solar cells (DSCs) are solar cells that have included different organic compounds (polymers and dyes) for light harvesting. There are similarities and differences between ISCs, OSCs and DSCs. Technology types and comparison will be briefly mentioned in the following chapters. This overview does not reflect upon the technological importance of the respective device technology. Introduced

information about OSC and DSC and technologies relevant for the type of HSC-devices are examined.

2.1 Inorganic Solar Cells

In order to reflect the technological importance of silicon solar cells, they are usually stated as 1st generation solar cells. The stimulation for technological development that is driven by Chapin, Fuller and Pearson in 1954 was the invention of a 6% efficient silicon p-n-junction [38]. By the help of continuously improved technology, in lab-scale devices; increases device efficiency up to 25% [41]. Due to the fact that the silicon's absorption coefficient is comparatively low and in order to get sufficient light harvesting a layer of 150 m material is required. For that reason, high purity grade silicon must be fabricated. Yet, this process will be energy intensive and costly.

Reynolds et al. has also reported a 6% efficient CdS solar cell in 1954 [40]. CdS solar cells are called as 2nd generation solar cells according to their technologies. By comparison to silicon, these technologies has higher absorption coefficients $\alpha(\lambda)$. In consequence, these types of devices are hereinafter referred to as thin film solar cells and it requires less material. This type involves amorphous Si, CdS, CdTe, Cu-InSe$_2$ (CIS), CuInGaSe$_2$ (CIGS), and CuZnSnS/Se (CZTS) [44,45]. According to achievement in lab-scale devices, the efficiencies for these types reached 20% [41].

For both silicon and thin film inorganic solar cells an electric field applied at the function between p-type and n-type inorganic semiconductors is considered as the main reason of charge separation, which is illustrated in Figure 2.3 (left) [45]. On the other hand, diffusion current has reasonable impact on current flow under some occasions such as low electric field and instant energy shortages.
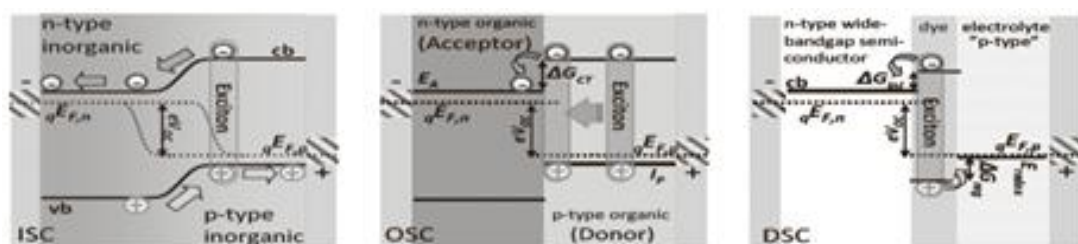
Figure 2.3 : Analogy of an inorganic solar cell, an organic solar cell and a dye-sensitized solar cell. Concerted from ref [45].

2.2 . Organic Solar Cells

In the 1960's the significant progress of inorganic solar cells is influenced organic device researchers. They utilized organic dyes and pigments to harvest solar energy, and called the devices organic solar cells (OSCs). In the 1980's an OSC with %1 efficiency is decleared by Tang. It had a junction made up of p-type and n-type organic semiconductors as it is demonstrated in Figure 2.3(middle)[36].

Harvested light create excitons into the bulk organic semiconducting materials. A thermodynamic offset is necessary to convert excitons into holes and electrons at the junction between n-type and p-type material. Therefore, exciton diffusion length LXD is a limiting factor for OSC device performance.

In order to overcome the limitation of the diffusion length, bulk-heterojunction (BHJ) OSCs are invented [46]. BHJ-OSC devices have n-type and p-type organic semiconductors as a deposited mixture. Phase separation and domain size are accured after co-deposition of the deposited mixture.

As an example of the impact of the BHJ approach onto efficiency of OSCs, although, organic tandem cells, which utilize small-molecular organic materials, have reached efficiencies of 8.3% in recent times [47], Mitsubishi Chemicals reported that efficiencies of the BHJ organic solar cells are recently achieved up to 9.2% [48]. More information about OSC can be found in literature [45,49,50].

2.3 Dye Sensitized Solar Cells

DSSCs are also referred as "Artificial Photosynthesis", due to the fact that even though the potential of organic dye to harvest light has been known before, first attempt to harvest light via dye sensitized semiconductor was from ZnO based chlorophylls8. Although the first configuration of the contemporary DSSC dates back to the late 1980s [51], in 1991 rational work of Grätzel and O'Regan first proved that DSSCs have capability to be the popular alternative energy source of the future [37]. Ru-based dyes are very common to use for DSSC devices. However, the highest efficiency reached with this type of dyes is around 11.5% [52]. Recent

studies showed that higher efficiencies can be obtained by using different combinations, such as Zn-based dye and Co-based electrolyte pair DSSC with a higher efficiency exceeding 12% [53].

The power conversion efficiency of DSC is not good enough when it is compared to other inorganic 1st and 2nd generation solar cells but it is superior then inorganic solar cells at some points. For example, efficiencies of inorganic solar cells change around 20% in the temperature range of 25-65°C that is the ordinary operation condition for photovoltaic devices. On the other hand, DSSCs are virtually independent from the temperature changes in this temperature range [54]. Since DSSC is less sensitive to the incident angle of the photon propagation, it is even better than polycrystalline Si solar cells for diffuse sunlight or cloudy weathers. Thus, DSCs does not require solar tracking systems unlike the inorganic solar cells.

Although the mass production system for DSSCs is not available yet, it is predicted that mass production of DSSCs will reduce the cost more than other thin film device production processes. Nevertheless, it is requires research about low cost and abundant materials available to use for more efficient DSC devices.

Unlike inorganic solar cells, DSCs are do not demand expensive and energy consuming high vacuum systems and material purification steps. Besides, materials used for organic based solar cells are biocompatible and most of them abundantly available. Thus, energy harvesting can be expanded up to the terawatts without shortage of the material [55]. This provides DSCs an advantage over the 2 major competitive thin-film photovoltaic technologies - CdTe and CuIn(As)Se; which are made up of highly toxic supplements of small abundance in nature.

Another necessity for all types of photovoltaic cells is long-term durability. different extensive studies has approved that the DSCs can satisfy the durability requirements for commercial solar cells to put up with outdoor operation for 20 plus years[33]. Under consideration of these advantages, it can be easily seen that DSC has the potential to be the powerful candidate of large-scale photovoltaic systems.

The chlorophylls are dyes in green leaves using photon energy to generate electrons and that triggers the sequential reactions to converts solar energy into the chemical energy. Complete of these reactions called photosynthesis. The Dye Sensitized Solar

Cell (DSC a.k. a. DSSC) has similar working principle with plant photosynthesis to generate energy from sunlight. To illustrate, each plant leaf is a photochemical cell that generates biological materials by using solar energy. The plants of the world produce the all foods which 100 times more than human needs in all over the world. Nevertheless, this photosynthesis process of the plants harvests only 0.002-0.05% of the solar energy reached to the ground of the Earth [55].

The DSSC whose working principle is illustrated in Figure 2.4 has different operation process then other photovoltaic devices that use different mediums for carrier generation (dye) and carrier transport (TiO2 nano-particles). The operation steps are the following [56].
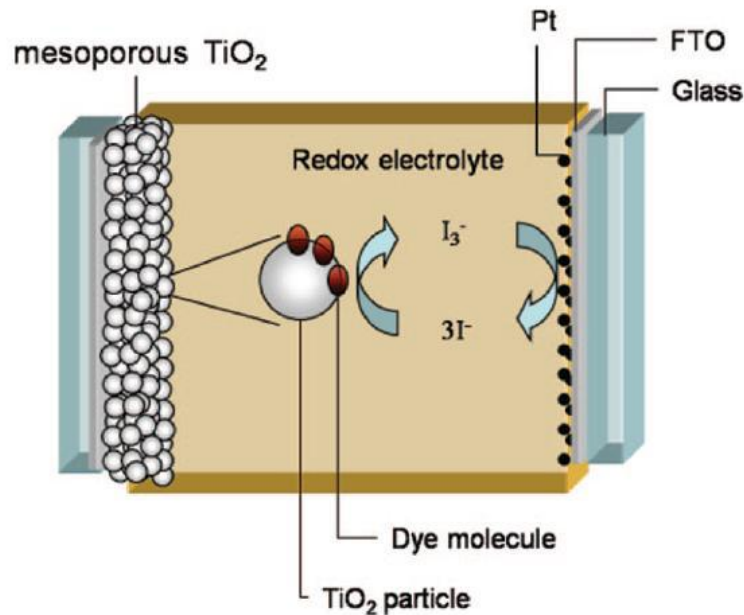
Figure 2.4 : Dye Solar Cell's working principle [58].

2.3.1 Excitation

After the photon energy is absorbed by the sensitizer dye molecule, electrons are excited from ground state (S) to the excited state (S*). In general, dye molecules has the absorption range around 720 nm with 1,72 eV photon energy. The lifetime of the excited electron is in the order of nanosecond.

$$S + h\vartheta \rightarrow S^* \tag{2.2}$$

$$S^* \rightarrow S^+ + e^- \tag{2.3}$$
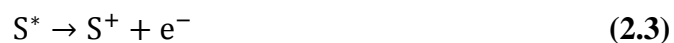
2.3.2 Injection

The sensitized dye molecules are adsorbed on semiconductor molecule which has high energy band gap such as TiO_2 in common. After excitation, dye molecules gain ability to transfer an electron to the conduction band of semiconductor. The dye becomes oxidized (S^+) due to the electron injection caused by the internal electric field of the nanoparticles. In order to get an efficient injection, the lowest unoccupied molecular orbital (LUMO) of the dye molecule has to be around 0.3 V above the conduction band of the TiO_2.

2.3.3 Diffusion in TiO_2

In DSSCs diffusion in TiO_2 is the dominant electron transport mechanism. Since, the nanoporous TiO_2 layer made up of spherical anatase particles. Diameter of these particles around 25 nm. As a result of the oxygen vacancies inside the TiO_2 lattice, the layer is weakly n-doped (charge carrier concentration 10^{16} cm^{-3}). Thus, because of the too miniscule size of the TiO_2 particles to built up an electric field in macroscopic scales, electron diffuses in to the electrode by trapping and de-trapping mechanism.

2.3.4 Iodine Reduction

The electron travelling through the counter electrode from the outer circuit decreases the iodine in the electrolyte to the tri-iodide, while platinum layer on the back electrode acts as a catalyst. The iodine reaction:

$$I_3^- + 2e^- \rightarrow 3I^- \tag{2.4}$$

On the other side, there is another reduction occurs at the excited dye molecules during the recombination of the photo-generated electrons. In order to achieve charge transfer efficiently, the iodine reduction of the counter electrode has to be orders of magnitude faster than recombination at the photoelectrode/electrolyte interface.

2.3.5 Dye regeneration

The highest occupied molecular orbital (HOMO) of the dye, which is regenerating its original form, is refilled by the reduced iodide ion and ready for electron regeneration again. Photoanode reaction:

$$2I^- \rightarrow I_2 + 2e^- \tag{2.5}$$

This reaction avoids the increase of S^+, which could cause the returns from the conduction band electrons to the dye molecules. The difference between the Fermi level of the semiconductor and redox potential of the mediator equals to the maximum output voltage [58].

Hence, DSSC device harvests energy from light and generate electricity without causing any permanent physical or chemical deformation on device mechanism [56].

3. EQUIVALENT CIRCUIT MODELING

Equivalent circuit models are widely used by researchers and manufacturers to get understand and simulate the transportation of photo-charge carriers in the solar cells. With utilizing these models, they extract parameters, which represent some of the characteristic features of the cell. These features can be related with the chemical composition of the cell, physical structure or even manufacturing technology of the cell [20]. The detailed understanding of the charge carrier transportation mechanism inside the cell can be achieved, if deeper examinations of the physical meaning inside the equivalent circuit parameters are performed under different characteristic features.

There are variety types of electrical equivalent circuit models proposed in literature. Most of them have Schottky diodes, shunted and serial resistances, as well as a current source representing illumination dependant photocurrent [10-24]. Some of these models have additional diodes to model specific electrical behavior [10,22] or electrical behavior under dark condition [11-14]. A few of them also are trying to model AC behavior of their cell with adding some capacitances [17-21] or inductances to increase AC understanding [14].

Although there are several equivalent models proposed in literature, some of them, such as single and double diode models, are approving their validity for different type of solar cells under specific conditions. Conventional single diode model (CSDM) is widely used from the most researchers to extract parameters under different illuminations and temperatures for semiconductor solar cells [27-29,59-63] and organic solar cells [11,12,15,29,31,45,64-66] as well as dye sensitized solar cells [5,17-20,67-69] in the literature. CSDM is the oldest method stemmed from the physical similarity of the well-known diode structure and p-n junction silicon solar cells. Due to the fact that, many of the referred studies about equivalent circuit modelling are method improvement studies [7,10,25,28,29,32,62], trying to find more efficient, easy and accurate method to solve intrinsic equation of the model, applied on conventional silicon solar cells. There are also commercial simulators,

such as Model 4200-SCS, using single diode model under their interface to simulate semiconductor solar cells [63] Since, organic solar cells and DSSCs are new technologies; researchers have applied this conventional model into their experimental data or extracted data from other research papers to improve their device efficiencies or solution methods. Before covering the CSDM, electrical basics of solar cells are described.

3.1 Electrical Basics of Solar Cells

Basic electrical characteristics have common properties in the literature. When they are measured in the dark condition, the current vs. voltage (I-V) characteristics of inorganic and organic solar cells resemble the exponential response of simple p-n junction diode. In addition to this diode behavior, shining light on a solar cell generates a photocurrent, and the I-V characteristic under illumination is ideally the combination of the dark characteristic and the photocurrent. The I-V characteristics of an ideal solar cell can be described by the Schottky equation with an additional photocurrent term, I_{ph} (3.1).

$$I = I_{ph} - I_0 \left(\frac{\exp V_d}{n V_{th}} - 1 \right) \tag{3.1}$$

$$V_{th} = kT/e \tag{3.2}$$

where I is the current, V is the applied voltage, I_0 is the reverse saturation current of the ideal diode, *e* is the elementary charge, n is the ideality factor, "k" is the Boltzmann constant, and "T" is temperature in Kelvin (K).

Figure 3.1 shows the current vs. voltage and power vs. voltage for an idealized solar cell in the region of power generation. Positive power that is product of voltage and current indicates power generation in the solar cell. P_{max} which is product of I_{max} and V_{max} is the maximum power that solar cells can be produced The most important performance parameters that can be found from the I-V curve of a device under a known illumination are open-circuit voltage (V_{oc}), short-circuit current (I_{sc}), fill factor (FF), and power conversion efficiency (η)[70]. All these parameters will be explained in the following subsections.
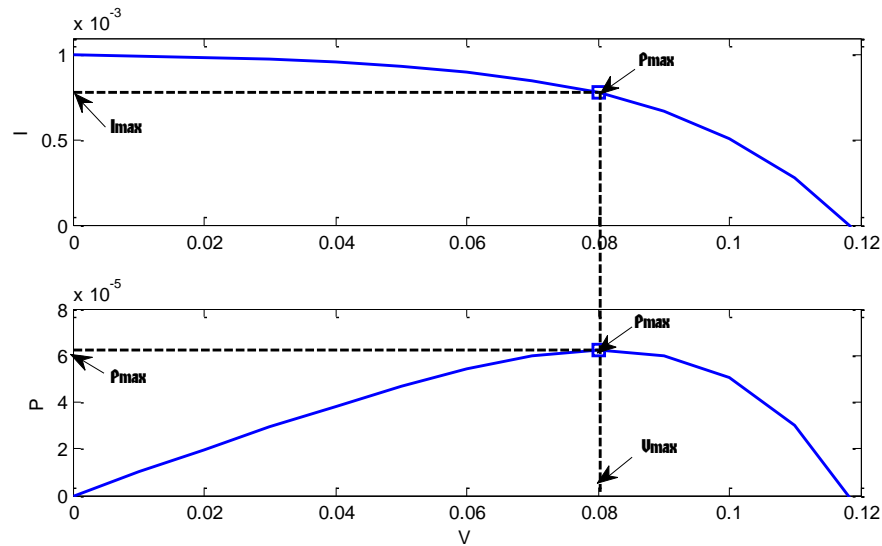
Figure 3.1 : Graphs of current and power as a function of voltage for a solar cell along with key parameters.

3.1.1 Open circuit voltage

The open-circuit voltage V_{oc} is the voltage across the solar cell when current equals zero, which is the same as the device being open-circuited. Because I = 0, no power is actually produced at this voltage. However, the open circuit voltage indicates the boundary for voltages at which power can be produced. The V_{OC} can also be thought of as the point at which the photocurrent generation and dark current processes compensate one another.

3.1.2 Short circuit current

Similar to open circuit voltage, the short-circuit current I_{sc} is the current when applied voltage equals to zero, which is the same conditions as the two electrodes of the cell being short-circuited together. Again, there is no power produced at this point, but the I_{sc} does mark the onset of power generation. In ideal solar cells, the I_{sc} will be the same as the photocurrent I_{ph}. However, it will be seen in the following chapter that several effects can lower the I_{sc} from this ideal value (see Chapter 4.2.2).

3.1.3 Fill factor

While V_{oc} and I_{sc} indicate the boundaries of power production in a solar cell, the maximum power produced P_{max} occurs at the voltage V_{max} and current I_{max} where

the product of I and V is at a maximum ,as shown in Figure 3.1. Because of the diode behavior of solar cell and additional resistance and recombination losses, I_{max} and V_{max} are always less than I_{sc} and V_{oc} , respectively [3]. The fill factor (FF) describes these differences and is defined as follow.

$$FF = \frac{I_{max}V_{max}}{I_{SC}V_{OC}} \qquad (3.3)$$

The fill factor describes how close P_{max} come to the boundaries of power production of I_{SC} and V_{OC} and also indicates the sharpness of the bend in the exponential I-V curve that connects I_{SC} and V_{OC}. Since higher FF is related to higher maximum power, high FF is desired; however, the diode-like behavior of solar cells results in FF always being less than one.

3.1.4 Power conversion efficiency

The most important performance parameter of a solar cell is the power conversion efficiency (η). It is defined as the ratio of the output electrical power to the intensity of incident irradiance I_L (light power per unit area). Because the point where the cell operates on the I-V curve changes depending on the load, the output power depends on the load. For consistency, the maximum output power is used for calculating efficiency. In equation form, efficiency is written as follows

$$\eta = \frac{FF \times J_{SC} \times V_{OC}}{I_L} \times 100\% \qquad (3.4)$$

This equation clearly shows that FF, I_{sc}, and , V_{oc} have direct effects on the efficiency [71]. Power conversion efficiency is important since it determines how effectively the space occupied by a solar cell is being used and how much area must be covered with solar cells to produce a given amount of power. Since larger areas require more resources to cover with solar cells, higher efficiency is often desirable. However, efficiency and cost for each solar cell cell must be balanced for improving the related technologies.
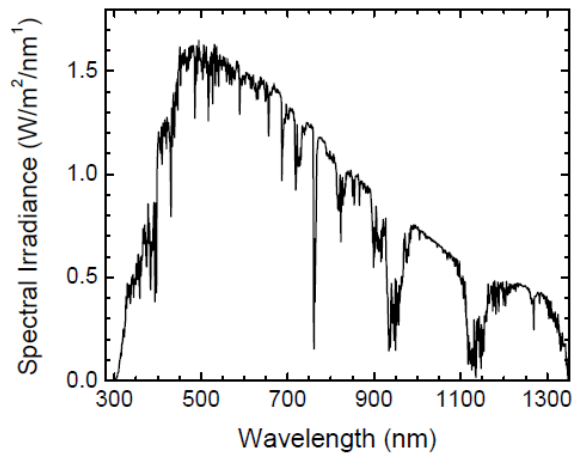
Figure 3.2 : Spectral irradiance of the AM1.5 G solar spectrum up to 1,350 nm [24].

Because solar cells do not absorb and convert photons to electrons at all wavelengths with the same efficiency, power conversion efficiency depends on the power and spectrum of the light. Between various solar cells, a standard spectrum must be chosen for the calculation of efficiency. Although the spectrum of the sunlight at the earth's surface varies with location, cloud coverage, and other factors, the AM1.5 G spectrum in Figure 3.2 is the most commonly used standard spectrum for measuring and comparing the performance of solar cells[33].

3.2 Conventional Single Diode Model (CSDM)

Modeling based on circuit analyses, is a controlling tool for designing and simulating high performance DSSC. The accurate values of these modeling parameters could provide the precise quantitative relationship between DSSC performance and DSSC physical structure, chemical composition or manufacture processing [20]. Several models of a DSSC are proposed in the literature. Although, most of them are modeled by conventional single diode, a few are declared by model with double diodes. The conventional single diode model is shown in Figure 3.3 . There are four important parameters in this model i.e. serial resistance (R_s), shunt resistance (R_{sh}) and diode's parameters ideality factor (n) and saturation current (I_0).
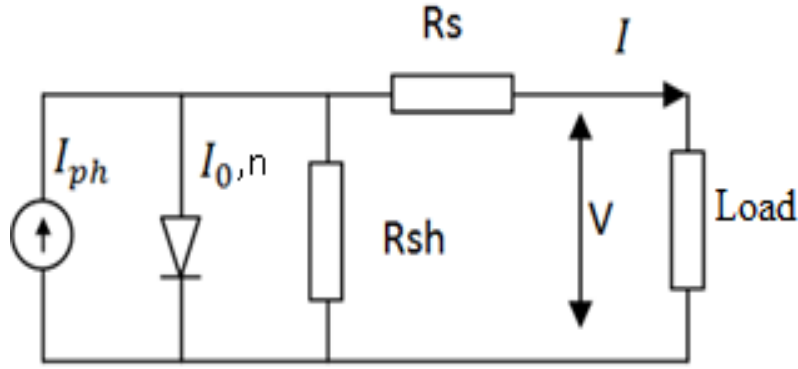
Figure 3.3 : Conventional single diode equivalent circuit model.

The single diode circuit analysis for a conventional solar cell can be extended to evaluate the electrical mechanism of DSSC. The relation between current and voltage in this circuit is given by the following equation.

$$I = I_{ph} - I_0 \left(\frac{\exp(V+IR_s)}{nV_{th}} - 1 \right) - \frac{V+IR_s}{R_{sh}} \tag{3.5}$$

This equation is similar to I-V relation of ideal solar cell except two extra resistances. I_{ph} , V_{th} , n, Io were also explained previously in chapter 3.1.

Conventional single diode model has been reported many times by various researches. Groups of Koide and Han analyzing the electrical processes of the DSCs with electrochemical impedance spectroscopy (EIS) propose a single diode model with a shunted and three serial resistances as well as two capacitances shunted to two of the serial resistances to model AC behavior of the cell [18,19]. However, EIS spectra measurement need more time and more experience to interpret its graphics. On the other hand, Guliani et al use the same model illustration with Koide and Han in their paper but in order to perform the model to find required parameters they ignore the capacitances and put a resistance equal to the sum of the three serial resistance instead of them [17]. After all, they performed the lambert-w function to find parameters onto the conventional model (CSDM). In 2009, Hanmin et al perform the conventional single diode model to utilize an improved method to estimate the parameters [67]. They examine the dynamic response of the DSSCs and compare it with the response of the silicon solar cell in 2011, by changing the speed of sweeping of the bias power supply applied on the cell, which is the method commonly used to extract I-V measurements of solar cells [30]. As a result, they illustrated the drastic impact of the stepwise speed of the testing system on the I-V

curve of the DSCs, it has not any considerable effect on I-V curve of the silicon solar cell instead. In order to model this dynamic behavior of DSCs, the group added two capacitances to the CSDM which are shunted to each resistance. Hanmin and Danyang use the model they improved in 2011 onto extracted data from literature and compare its accuracy with the other's. However, It can be deduced from the fitting graphics showed in the article that they ignored the capacitances during the modeling process and thus literally they used the conventional model to find parameters. Recently, Guliani and his group calculated the dynamic model of the circuit used by groups of Koide and Han by inserting the capacitance equations founded via EIS into the lambert-w function [72]. acetic acid treatment effectively reduces the DSSC's series resistance, R_s, and improves DSSC short-circuit current Isc according to the research of Masaki [68]; 4t-butylpyridine increase the resistance of DSSC, R_{sh}, to achieve the elevation of DSSC's open circuit voltage, Voc; Hoshikawa found the addition of LiI in the electrolyte leaded to Voc reduction, and same as t-BuPy [69].

Beside conventional single diode model, double diodes model have been also studied by many groups in the literature. Tripathi and his colleagues were proposed a double diode dynamic model [14]. In this complicate model, there are three resistances and two of them are shunted by capacitances and a Warburg impedance serial connected to the serial resistances. Besides, there is an inductive pathway shunted to the serial resistances, which consist of an inductance and a serial resistance. In this model, interfaces of the DSSC is represented by electrical components, however, this model requires EIS and lots of calculation, time and afford to simulate a cell.

3.2.1 Serial resistance

Serial resistance R_s represents total of the noise resistances, such as contact resistance and charge transfer resistance inside the semiconductor material [56]. High serial resistance decreases the fill factor and maximum power output. Besides, very high serial resistance may also reduce the short circuit current. On the other hand, it does not affect the open circuit voltage, since when the circuit is open the total current flow through the serial resistance is zero. According to the literature, the inverse slope of the I-V curve at the open-circuit point provides the approximate value of the serial resistance [10,11,14,73]. However, although this approximation

might works in inorganic solar cells due to their low ideality factor, in our research it has been evinced that this approximation may give wrong results for dye sensitized solar cells that have extremely high ideality factors. Relevant information will be given in chapter 4.2.3 with details.
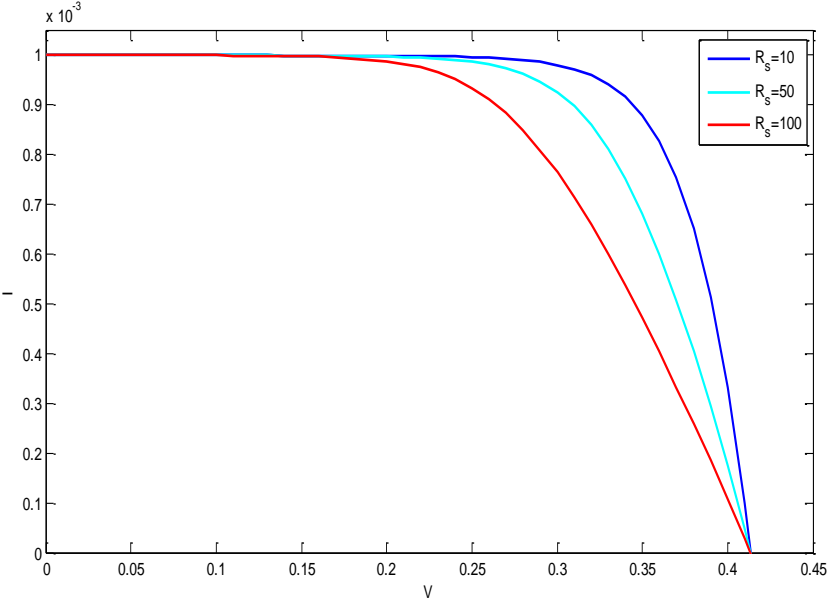
Figure 3.4 : I-V response of solar cell for different serial resistances.

3.2.2 Shunt resistance

Shunt resistance, R_{sh} represents the leakage current inside the cell. Low shunt resistance causes significant power loss, due to the alternate current path created by low shunt resistance for the photocurrent generated by cell. In addition, it affects the fill factor and open circuit voltage as well as maximum power output implicitly. According to many of the methods in literature, approximate value of the shunt resistance can be extracted from the slope of the I-V curve at the short circuit point [10,11,14,18,73]. (see chapter 4.2.1)
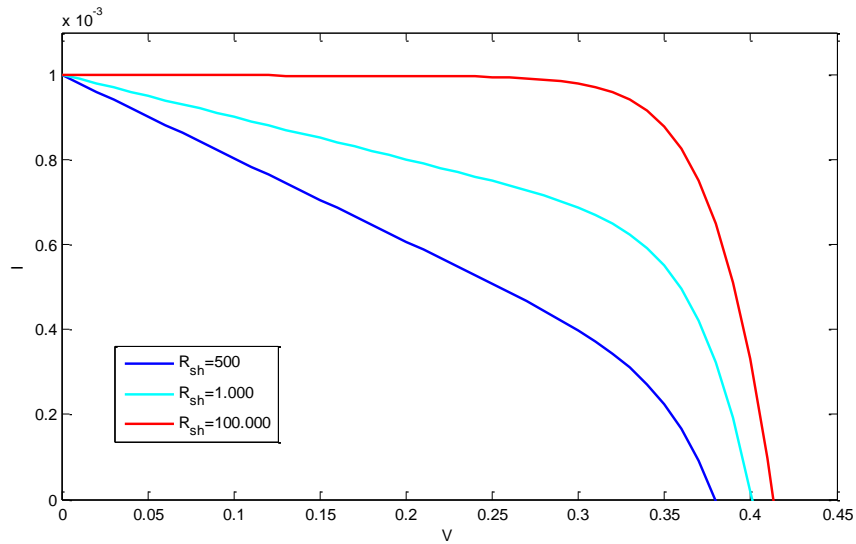
Figure 3.5 : I-V response of solar cell for different shunted resistances

3.2.3 Ideality factor

The diode ideality factor, n, is a parameter that describes how closely the I-V curve resembles to the theoretical model. DSSC diode factors range from 1 (close to the ideal case) to 2 depending on the type of carrier recombination in the cell. As it is demonstrated in Figure 3.6 a diode factor greater than unity on the I-V curve suggests higher V_{oc}'s implying a greater efficiency. However, this may not be the case since the diode factor is related to other parameters in the solar cell and indeed, it may decrease the performance of the cell through a corresponding decrease in fill factor.
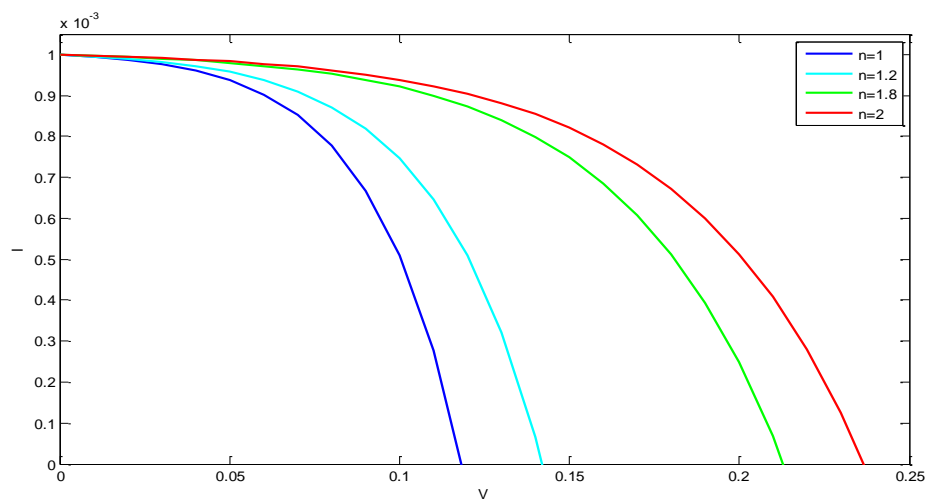
Figure 3.6 : I-V response of solar cell for different ideality factors.

3.2.4 Saturation current

The saturation current, which is also referred as dark current, represents the parasitic losses relevant with the capability of the solar cell to hold charge separation and thus suppress recombination losses as a function of voltage. Pinholes in the TiO_2 are one of the major contributors to these losses. These pinholes stems from the interfaces between the electrolyte and the back conducting oxide. The saturation current is also relevant to the shunt resistance, since both are a quantity of recombination losses in the cell.
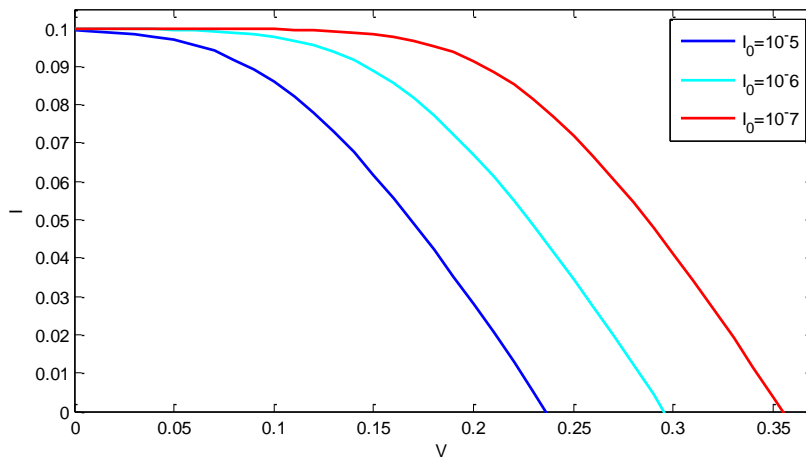
Figure 3.7 : I-V response of solar cell for different saturation currents.

As it is illustrated in Figure 3.7 its effect on the I-V curve is similar to changes in the diode factor. An increase in the saturation current reduced the V_{oc} which leads to a reduction in the cell efficiency. This is because under an ideal scenario the V_{oc} indicates the point where the rate of injected carriers is equal to the rate of recombination in the solar cell. When another source of recombination (at the TCO interface) is included, the equilibrium between photogeneration and recombination of carriers will occur at a decreased bias voltage [74]. The relation between V_{oc} and the I_0 can be written as shown in Equation 3.6 [10].

$$V_{OC} = \frac{kT}{q} \ln \frac{I_{sc}}{I_0} \tag{3.6}$$

4. METHODS TO EXTRACT ELECTRICAL PARAMETERS OF SINGLE DIODE MODEL

4.1 Methods in the Literature

The knowledge of model parameters from measured current–voltage characteristics is crucially important for the quality control and improvement of the performance of the solar cells. There are different methods to solve Eq. 3.5 resulting in different approximation mathematical models. due to the transcendental structure of the equation, decision on solution method is not easy. The different mathematical models generally include parameters that are provided by photovoltaic modules manufacturers. For this, numerous methods have been proposed in the literature to determine different parameters [3,7,10,17,22,25-28,29-32]   These parameters are usually the saturation current, the series resistance, the ideality factor, the shunt conductance and the photocurrent.

According to Wolf and Rauschenbach, there are three I-V characteristics of photovoltaic cells can be determined by different methods. These characteristics are the photovoltaic output characteristic, the p-n junction characteristic, and the rectifier forward characteristic [75]. Different methods applied on different characteristics of the same I-V provides different results because of the effects of the cell internal series resistance. Gerardo et al proposed a method in 1982 to determine R_s [76]. This method uses the area under the I-V curve in the proposed R_s equation. As an integration advantage of that, it is reducing the data errors by using the graphical feature of device. A similar method is also used to calculate R_s by a commercial solar cell simulator called Model 4200-SCS (Semiconductor Characterization System) in recent years [63]. Phang et al suggested an analytical method in 1984. To reduce calculation time, he derives analytical expressions from experimental data and makes some approximations and assumptions depend on the pre-known parameter results. Results are accurate for grey and blue solar cells when it is compared with the results gathered by an iterative method as it is indicated in article. Chegaar et al presents a

simple and successful method for evaluating the characteristic parameters in illuminated solar cells. The approach involves the use of an auxiliary function and a computer-fitting routine. Author, applied the method on I-V measurement of a commercial silicon solar cell, a module and a plastic solar cell to approve the validity of the method. There is another method is applied onto conventional single diode model in order to obtain intrinsic and extrinsic parameters of illuminated solar cells [31]. The method is depends on calculating the Co-content function (CC) from the exact explicit analytical solutions of the illuminated current–voltage characteristics. The resulting CC is showed with a purely algebraic function of current and voltage. Coefficients of this function provide the model parameters with a bi-dimensional fitting. Hruska et al utilized the curve fitting toolbox of MATLAB and converted implicit circuit equation into the explicit equation with the assistance of Lambert W function. They successfully applied the method on the experimental data of p-n junction solar cells [32]. This article applies the proposed method on to KC200GT solar array. Nominal information from the array datasheet is used to fit three experimental remarkable points (I_{sc},V_{oc},P_{max}) without any need to guess or estimate other parameters except ideality factor, n. It uses iteration methods and algorithm to solve transcendental equations and to adjust the model [27].

4.2 Lambert-W Function: Exact Solution of the Model Equation

Lambert-W function is used in literatures to solve circuit equations, because it is enables to convert transcendental equations into explicit functions. To illustrate; Lambert-W function is used to solve circuit equation, additionally circuit function is separated into 5 different parts which is called Co-content functions and results are compared with other approaches using plastic solar cell IV results [31]. In another study Lambert-W function is applied a double diode solar cell model as an example of curve fitting solution of W function on diode equations. References can be used to reach another double diode model and mathematical source of Lambert-W function [32]. Beside, Lambert-W function is also used to model ITO/PEDOT:PSS/P3HT:PCBM/Al organic solar cells with s-shape I-V output with double diode approach and unlike the way used in our proposed solution, Lambert-W function is applied to the voltage equation [22]. Parameters of Nontreated and Carboxylic-Acid-Treated Dye Sensitized Solar Cells are analytically extracted by

using Lambert-W function onto circuit equation as well as parmeter equations such as R_{sh}, V_{oc}, I_{sc} [17].

In our study the circuit Equation 3.5 is converted to an explicit current equation including Lambert-W function. The equation is solved and it is found the optimal parameters to mimic the electrical output of DSSCs we applied. The general solution of Lambert-W function is:

$$\text{a: } \ln(A + Bx) + Cx = \ln(Dx) \qquad \rightarrow \qquad \text{b: } x = \frac{1}{C} W \left[\frac{CD}{B} \exp \left(\frac{AC}{B} \right) \right] - \frac{A}{B} \qquad \textbf{(4.1)}$$

Equation 3.5 is rewritten as Eq. 4.2a to resemble equation 4.1.a in which 'I' is assumed to be 'x',

$$\frac{I(R_{sh}+R_s)}{I_0 R_{sh}} + \frac{V}{I_0 R_{sh}} - \frac{(I_{ph}+I_0)}{I_0} = -\exp \left[\frac{(V+IR_s)}{nV_{th}} \right] \qquad \textbf{(4.2a)}$$

And its logarithm is taken,

$$\ln \left(-\frac{I(R_{sh}+R_s)}{I_0 R_{sh}} - \frac{V-R_{sh}(I_{ph}+I_0)}{I_0 R_{sh}} \right) = \frac{V}{nV_{th}} + \frac{IR_s}{nV_{th}} \qquad \textbf{(4.2b)}$$

By taking all 'I' to the left and logarithm to the right required equation is obtained :

$$\ln \left(-\frac{I(R_{sh}+R_s)}{I_0 R_{sh}} - \frac{V-R_{sh}(I_{ph}+I_0)}{I_0 R_{sh}} \right) - \frac{IR_s}{nV_{th}} = \ln \left(\exp \left(\frac{V}{nV_{th}} \right) \right) \qquad \textbf{(4.2c)}$$

And necessary parameters to solve equation are:

$$A = \frac{R_{sh}(I_{ph}+I_0)-V}{I_0 R_{sh}} \text{ , } B = -\frac{(R_{sh}+R_s)}{I_0 R_{sh}} \text{ , } C = -\frac{R_s}{nV_{th}} \text{ , } D = \exp \left(\frac{V}{nV_{th}} \right) \qquad \textbf{(4.3)}$$

After insertion of the founded parameters in to the general solution, an explicit solution of the single diode circuit equation is extracted:

$$I = -\frac{nV_{th}}{R_s} W \left[\frac{R_{sh}R_s I_0}{nV_{th}(R_{s}+R_{sh})} \exp \left(\frac{V}{nV_{th}} - \left(-\frac{R_{sh}(I_{ph}+I_0)-V}{R_{s}+R_{sh}} \right) \frac{R_s}{nV_{th}} \right) \right] + \frac{R_{sh}(I_{ph}+I_0)-V}{R_{s}+R_{sh}} \qquad \textbf{(4.4)}$$

4.2.1 A simple method to determine model parameters

Although we are obtained an explicit Equation 4.4 by using Lambert-W function, we need a consistent method to obtain required parameters R_s, R_{sh}, I_{ph}, V_{oc}, I_0, n, in equation.

As it is mentioned in previous chapter, according to the literature [10,11,14,17,25,26,28,73] serial resistance can be found graphically from the slope at OC point;

$$R_S = -\left(\frac{dV}{dI}\right)_{V=V_{oc}} \qquad (4.4)$$

Also, shunt resistances can be obtained similarly from the slope at SC point;

$$R_{sh} = -\left(\frac{dV}{dI}\right)_{I=I_{sc}} \qquad (4.6)$$

In general, these graphical results are used as initial values not direct result to determine real resistances in most of the models.

Approximating photocurrent which results from

$$R_{Sh} \gg R_S \qquad (4.7)$$

assumption;

$$I_{ph} \cong I_{sc} \qquad (4.8)$$

is very conventional and easy method extracted from I-V measurements of the devices [18,23,25,26,30,65,71].

The simplest and accurate way to decide diode parameters n and I_0 is using numerical fitting methods to correlate theoretical and experimental I-V (For more information about codes see Appendix 1.A).

4.2.2 Improvement of the method

To evaluate this method we ignored how complex the physical structure of DSSCs and focused its model, single diode circuit with a circuit analyzer's point of view and reconsidered the equation 4.5, 4.6 and 4.7.
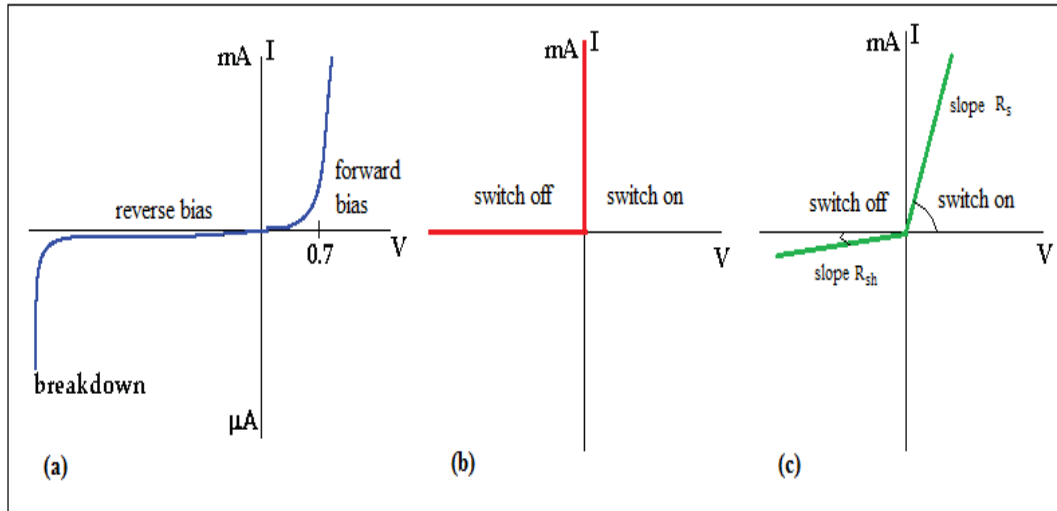
Figure 4.1 : (a) I-V curve of an ideal Schottky Diode, (b) I-V curve of an ideal diode, (c)I-V curve of an ideal diode connected with a serial and a shunt resistances.

Figure 4.1(a) shows I-V curve of an ideal Schottky (p-n junction) diode we use in our model (Eq. 3.1). Ideal diode could also be considered as a switch; which is on when bias voltage is positive and switch off when the bias voltage is negative as it is illustrated in Figure 4.1(b). If a serial and a shunted resistance are inserted into the ideal circuit, we get an output resembles sketched in Figure 4.1(c).

Under reverse bias, shunted resistance can be graphically obtained from the slope of negative voltage. For PV cells we assumed the assumption in Eq. 4.8. Thus, slope of the I-V curve can be used to find R_s approximately. However, as it is shown in Figure 4.2 especially for high n values or very low I_{sc} values, curve may not be stabilized at the point of OC. Thus, obtaining R_s from the slope of I-V at the point of OC might be misleading. In our study I-V data from the highest voltage, end of the datas are used, to have accurate results from all data we have.

Similarly, to obtain R_{sh} graphically, we used a few data from reverse part and the SC point to avoid from the breakdown point of the diode and to get accurate results.
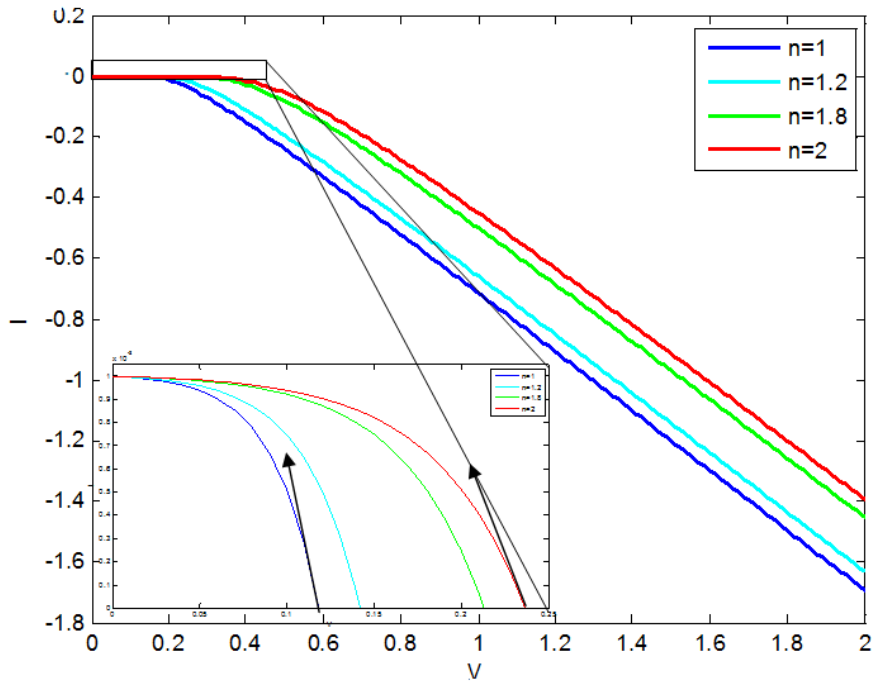
Figure 4.2 : Picture depicts that slope of forward bias equal when Rs is same. Inner picture shows difference of the slopes of different "n" s at OC.

On the other hand, in our approach using approximation 4.10 into the method isn't found efficient. Since some solar cells, specifically new invented DSSCs or organic solar cells may have high serial resistances or low shunted resistances as well. In this case, this approximation was harmful for the accuracy of our fit results. Therefore, the equation

$$I_{ph} = I_{sc} \left(\frac{R_s + R_{sh}}{R_{sh}} \right) \tag{4.9}$$

From literature [11] inserted into Eq. 4.4 and R_s is added into the fit parameters beside I_0 and n.

4.2.3 Improvement of the model under consideration of illumination dependences

Although single and double diode dynamic models in literature could increase accuracy under dynamic situations [14,17-21,67,72] and the double diode model of Thripathi might be very useful to have comprehensive understanding of physical dynamics inside a DSSC, required process and calculation are difficult and time consuming to one who wants a simple way to simulate his cell and extract parameters. Thus, "The simplest is the best!" is our motto to improve the conventional single diode model without inserting any additional component.

Improvement of the model is required to have accurate results throughout the all I-V data including negative current and voltage for different illuminations in a short time. However, if diode parameters are extracted for every illumination of a device, as it is applied in conventional models, having reasonable and predictable information is hardly possible. Therefore, in most of the conventional models, researchers model every single illumination data with a different circuit by attaining Rs, Rsh, n and I_o for each of them. Thus, one could not have an idea about parameters of an unmeasured illumination.

Beside, Marcelo at al. are applied diode parameters of silicon solar cell which they obtained from the extracted I-V data measured by Kyocera KC200GT in nominal conditions (1000W/m², 25°C) [27]. In our research, remarkable improvement is achieved by applying the nominal condition diode parameters to all illumination data we have. Also the improved model is the kernel of our ICS simulators.

Despite, characteristic relation between amount of illumination and Isc easily stands out in literatures [77-80]. Few of them touch on the relation between illuminations and shunt resistance or serial resistance.

4.2.3.1 Illumination dependence of I_{sc}

As it is know from pictures of articles and datasheets such as figure 4.3,
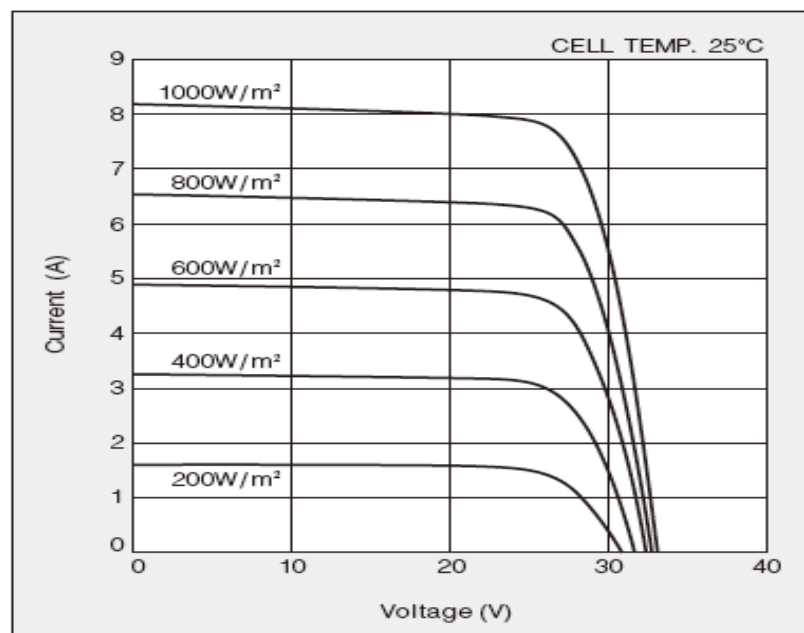
Figure 4.3 : I-V characteristic of photovoltaic module KC200GT under different illuminations [81].

29

when illumination increases I_{sc} also increases [7,14,16,64,66,78,82]. Moreover, there is an almost linear relation between I_{sc} and I_L expressed as $I_{sc}^{\gamma \approx 1} \alpha I_L$ by Yoo et al [12] and as it is demonstrated in other articles [78,79]. The linear relation between illumination and short circuit current of DSSC's used in this study can be seen in Figure 4.4. Beside, in our method an error number is added to ignore some measurement errors (See Chapter 5.3).
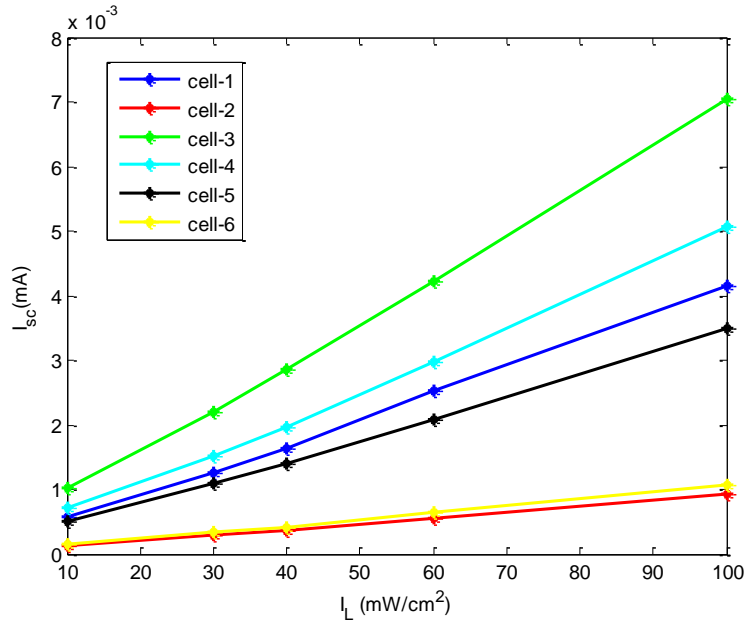
Figure 4.4 : I_L-I_{sc} graphics of six DSSCs used in our study.

4.2.3.2 Illumination dependence of Rs

As it is described in Chapter 4.2.2 Rs can be found from inverse slope of I-V curve around high voltage. For different illuminations it slightly differs from each other. In the review of Moliton and Nunzi an increasing linear relationship between $(R_S + R_{Sdark})^2$- I_L is depicted [16]. Although, from the Yoo's et.al. table of finding R_s decreasing while I_L increasing, they conclude that "R_s is relatively unchanged" [12]. Also, a semiconductor characterization system, Model 4200SCS, uses an approximate R_s for the simulation of parameters for different illuminations [63].

For DSSCs used in our study a regular relationship valid for all cells between R_s - I_L could not be found and it can be considered relatively unchanged for most of them (See Chapter 5).

4.2.3.3 Illumination dependence of R_{Sh}

When R_{sh} is found with graphical approach mentioned in Chapter 4.2.2 a nonlinear inverse relation between R_{sh}-I_L can easily be observed. This relationship depicted in review of Moliton and Nunzi as $\left(\frac{1}{R_{sh}^2}\right) \alpha\, I_L$ for the polimer cell of Alem et al [16,81]. In other article this relatonship is proposed more physical approach as a shunted resistance equation (Eq. 4.10) for polymer solar cells:

$$\left(\frac{cp\, A\, n_e\, q\, \mu}{d} + \frac{1}{R_{Shdark}}\right)^{-1} = R_{Sh} \tag{4.10}$$

In Equation 4.10 cp is contact permeability, n_e is charge carrier density which is illumination dependent coefficient, q is electron charge number, μ is mobility and d is the thickness [48]. Despite Equation 4.10 might give a direct result, it require too much information which makes the equation hard to solve especially for solar cells produced with novel metarials. There is another approach which we inspired from is

$$\left(\frac{1}{R_{Sh}} + \frac{1}{R_{Shdark}}\right)^{-1} \alpha\, I_L \tag{4.11}$$

proposed by Yoo et al.[22].

4.3 Illumination Sensitive Equivalent Circuit Model

Under the consideration of all improvements an illumination sensitive equivalent circuit model is proposed in Figure 4.5 and circuit equation is depicted at Equation 3.5 is rewritten to point its illumination dependency in Equation 4.12.
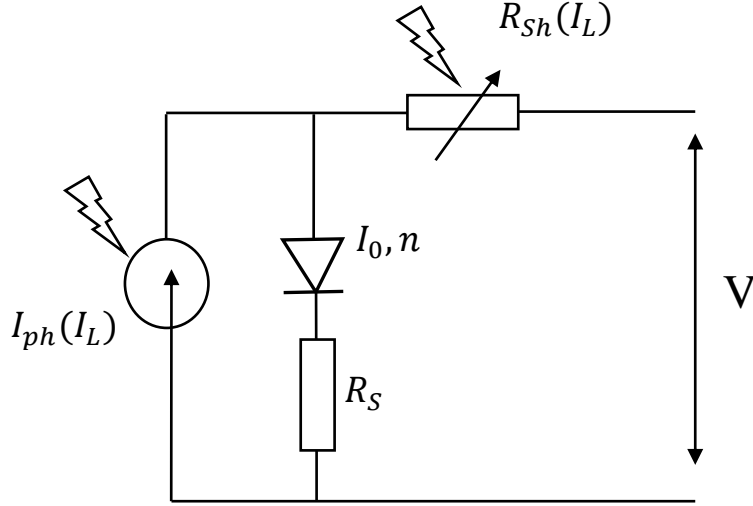
Figure 4.5 : Improved model illustration as an equivalent circuit.

$$I = I_{sc}(I_L)\left(\frac{R_s + R_{sh}(I_L)}{R_{sh}(I_L)}\right) - I_0\left(\frac{\exp(V + IR_s)}{nV_{th}} - 1\right) - \frac{V + IR_s}{R_{sh}(I_L)} \qquad (4.12)$$

This changes can be inserted into the Lambert-W Equation 4.4:

$$I =$$

$$-\frac{nV_{th}}{R_s}W\left[\frac{R_{sh}(I_L)R_sI_0}{nV_{th}(R_s + R_{sh}(I_L))}\exp\left(\frac{V}{nV_{th}} - \left(-\frac{R_{sh}(I_L)\left(I_{sc}(I_L)\left(\frac{R_s + R_{sh}(I_L)}{R_{sh}(I_L)}\right) + I_0\right) - V}{R_s + R_{sh}(I_L)}\right)\frac{R_s}{nV_{th}}\right)\right] +$$

$$\frac{R_{sh}(I_L)\left(I_{sc}(I_L)\left(\frac{R_s + R_{sh}(I_L)}{R_{sh}(I_L)}\right) + I_0\right) - V}{R_s + R_{sh}(I_L)} \qquad (4.13)$$

5. RESULTS

5.1 Results of Simple Method

In a nut shell, R_s and R_{sh} are found from inverse slope at OC and SC points of I-V graph of solar cells and I_{ph} is approximated as I_{sc} in simple method mentioned in Chapter 4.2.1. In this chapter, unsuccessful result of simple method is shown for Cell-1 to depict how our improvement affected the results. We also applied this simple method for other solar cells and fitting results did not show in this thesis for the sake of simplicity.
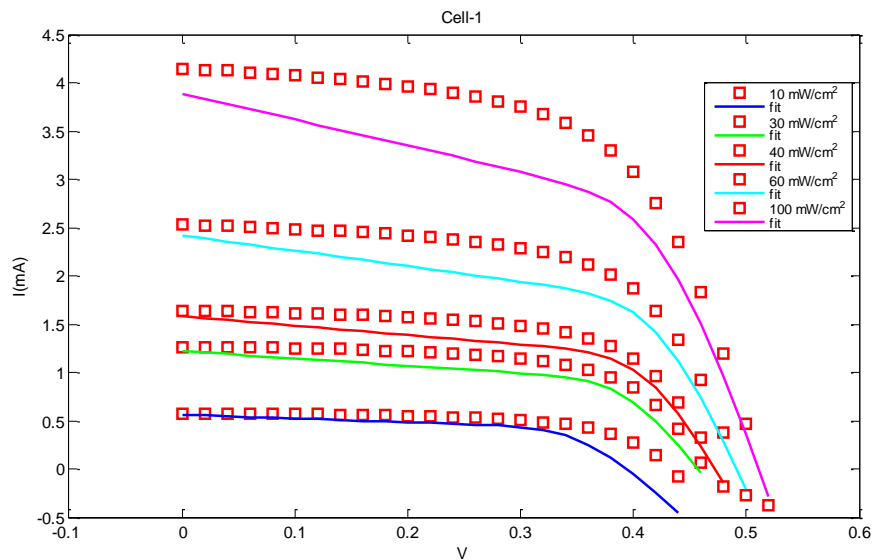
Figure 5.1 : Result of simple method before improvement.

Figure 5.1 shows fitting results and experiemental data for cell-1 solar cell. As it is shown in Figure 5.1 simple method could not fitted to the experimental data. On the other hand, simple information parameters such as FF, V_{oc}, I_{sc}, η which are directly obtained from measured I-V data is achieved by this method and both improved method and model. This informations are listed below for the six cells from Table 5.1 to 5.6.

Table 5.1 : Simple parameters of Cell-1

Irradiance	V_{oc}	I_{sc} (mA)	FF	η
10mW/cm²	0.4400	0.5765	0.6187	0.0157
30mW/cm²	0.4600	1.2658	0.6362	0.0123
40mW/cm²	0.4800	1.6404	0.6204	0.0122
60mW/cm²	0.5000	2.5309	0.6055	0.0128
100mW/cm²	0.5200	4.1493	0.5801	0.0125

Table 5.2 : Simple parameters of Cell-2

Irradiance	V_{oc}	I_{sc}(mA)	FF	η
10mW/cm²	0.3600	0.1313	0.5149	0.0024
30mW/cm²	0.4000	0.2908	0.5414	0.0021
40mW/cm²	0.4000	0.3695	0.5536	0.0020
60mW/cm²	0.4200	0.5517	0.5490	0.0021
100mW/cm²	0.4400	0.9183	0.5633	0.0023

Table 5.3 : Simple parameters of Cell-3

Irradiance	V_{oc}	I_{sc} (mA)	FF	η
10mW/cm²	0.5400	1.0217	0.6737	0.0372
30mW/cm²	0.5600	2.2084	0.6626	0.0273
40mW/cm²	0.5600	2.8538	0.6577	0.0263
60mW/cm²	0.5800	4.2252	0.6236	0.0255
100mW/cm²	0.5800	7.0404	0.5988	0.0245

Table 5.4 : Simple parameters of Cell-4

Irradiance	V_{oc}	I_{sc} (mA)	FF	η
10mW/cm²	0.4800	0.7070	0.6922	0.0235
30mW/cm²	0.5000	1.5226	0.6802	0.0173
40mW/cm²	0.5200	1.9648	0.6548	0.0167
60mW/cm²	0.5200	2.9786	0.6510	0.0168
100mW/cm²	0.5400	5.0802	0.6038	0.0166

Table 5.5 : Simple parameters of Cell-5

Irradiance	V_{oc}	I_{sc} (mA)	FF	η
10mW/cm²	0.5200	0.4990	0.6241	0.0162
30mW/cm²	0.5400	1.1049	0.6450	0.0128
40mW/cm²	0.5600	1.4065	0.6305	0.0124
60mW/cm²	0.5600	2.0866	0.6395	0.0125
100mW/cm²	0.5800	3.4954	0.6177	0.0125

Table 5.6 : Simple parameters of Cell-6

Irradiance	V_{oc}	I_{sc} (mA)	FF	η
10mW/cm²	0.3600	0.1462	0.4977	0.0026
30mW/cm²	0.4000	0.3303	0.5188	0.0023
40mW/cm²	0.4200	0.4230	0.5086	0.0023
60mW/cm²	0.4400	0.6478	0.5170	0.0025
100mW/cm²	0.4600	1.0637	0.5096	0.0025

5.2 Results of Method Improvement

When Equation 4.8 is used in equivalent circuit equation 4.4 improvemen at SC point
is obtained. This improvement is illustrated in Figure 5.2
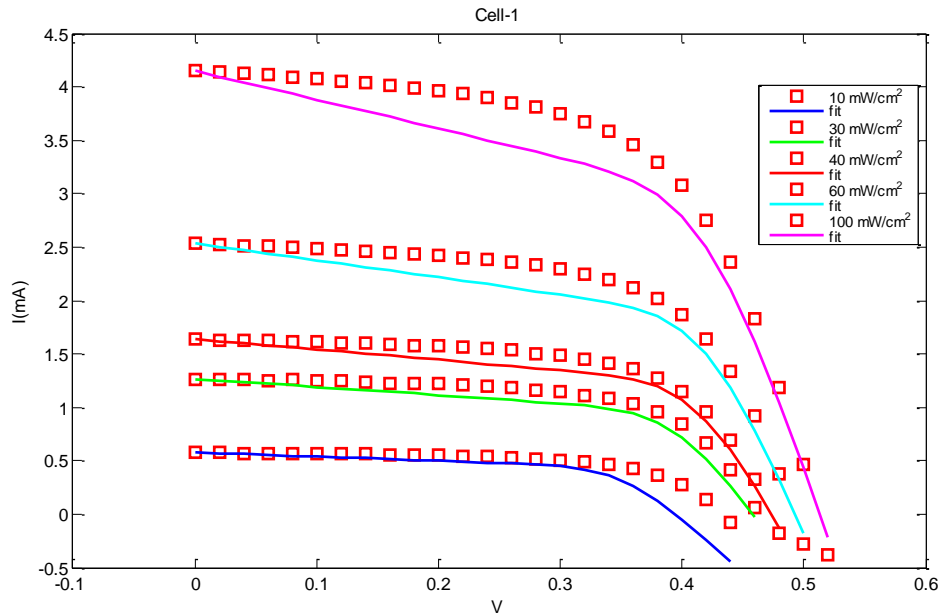
Figure 5.2 : Effect of Iph improvement is shown on Cell-1 data.

Resistance extraction is also improved by finding R_s from the inverse slope around
high voltage and adding R_s in to the fit parameters as a start point to extract R_s fit
result, and by extracting R_{sh} from negative voltage at the point of SC (Chapter 4.2.2).
Improved method is applied by using optimization method in MatLab (See App.A.1).
When improvement is applied to model, a radical improvement is observed through
whole fitting curve. I-V fitting results of improved method is shown in graphics from
Figure 5.3 to Figure 5.15 for six different DSSCs invented and measured by Mustafa

Can in his PhD study [87]. Method is applied for 10W/cm², 30W/cm², 40W/cm², 60W/cm² and 100W/cm² illumination intensities and two different type of sketch are used to illustrate accuracy of method. These are positive part demonstration and logarithmic demonstration for complete I-V curve. Results of four parameters obtained from method are show in tables (Table 5.7 – Table 5.12) in comparison to model improvement findings.

Figure 5.3 : Method Improved I-V fitting results of positive part for Cell-1.

Figure 5.4 : Method Improved logarithmic I-V fitting result of complete experimental data of Cell-1

Figure 5.5 : Method Improved I-V fitting results of positive part for Cell-2.

Figure 5.6 : Method Improved logarithmic I-V fitting result of complete experimental data of Cell-2.

Figure 5.7 : Method Improved I-V fitting results of positive part for Cell-3.

Figure 5.8 : Method Improved logarithmic I-V fitting result of complete experimental data of Cell-3.

Figure 5.9 : Method Improved I-V fitting results of positive part for Cell-4.

Figure 5.10 : Method Improved logarithmic I-V fitting result of complete experimental data of Cell-4.

Figure 5.11 : Method Improved I-V fitting results of positive part for Cell-5
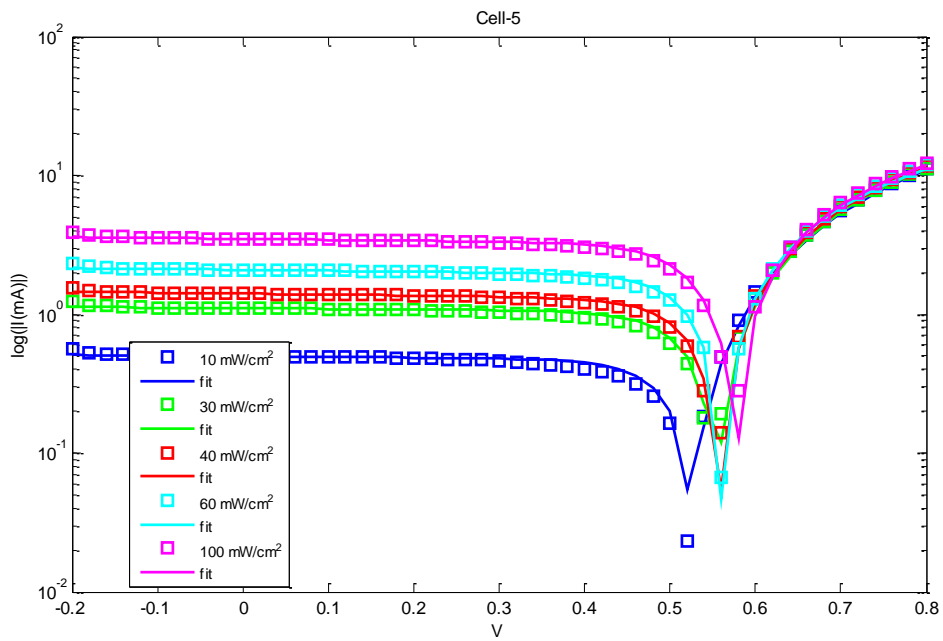
Figure 5.12 : Method Improved logarithmic I-V fitting result of complete experimental data of Cell-5.
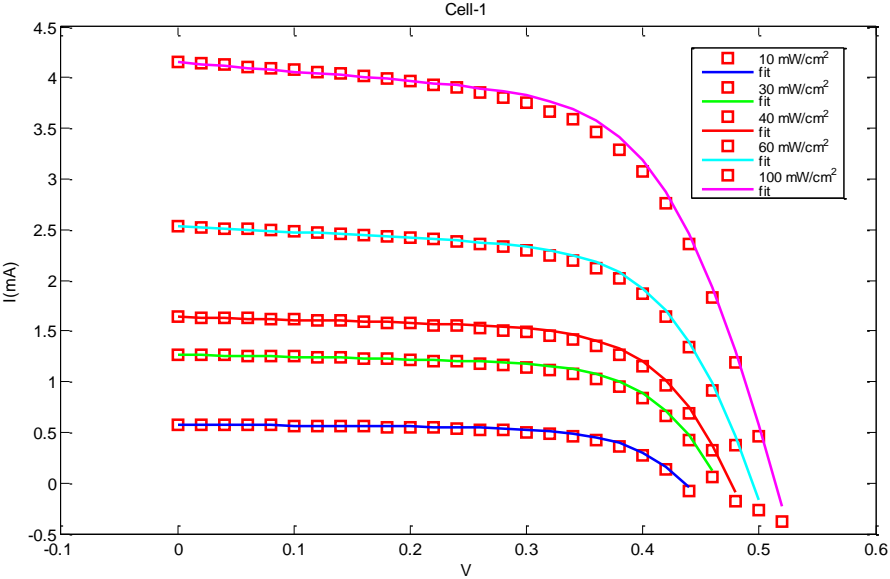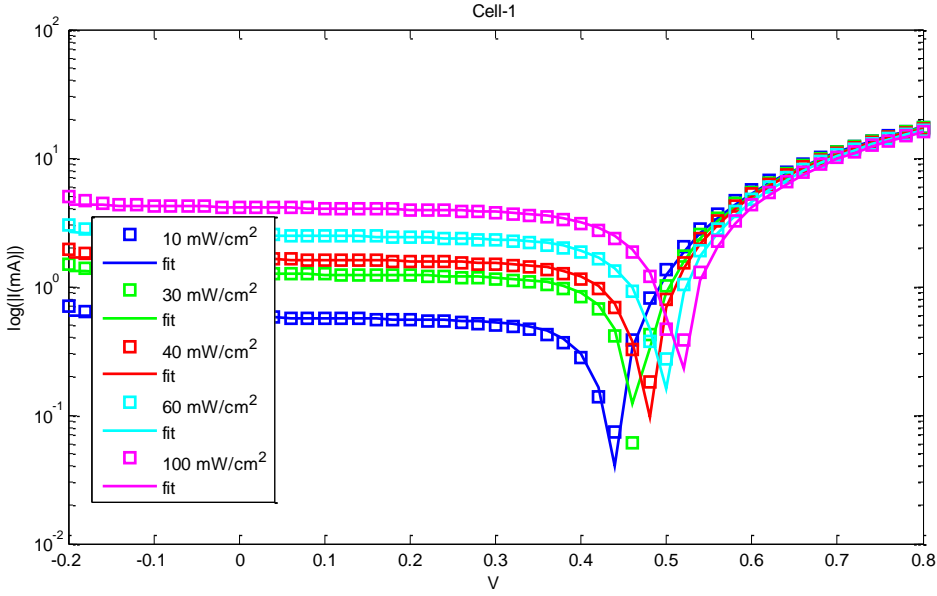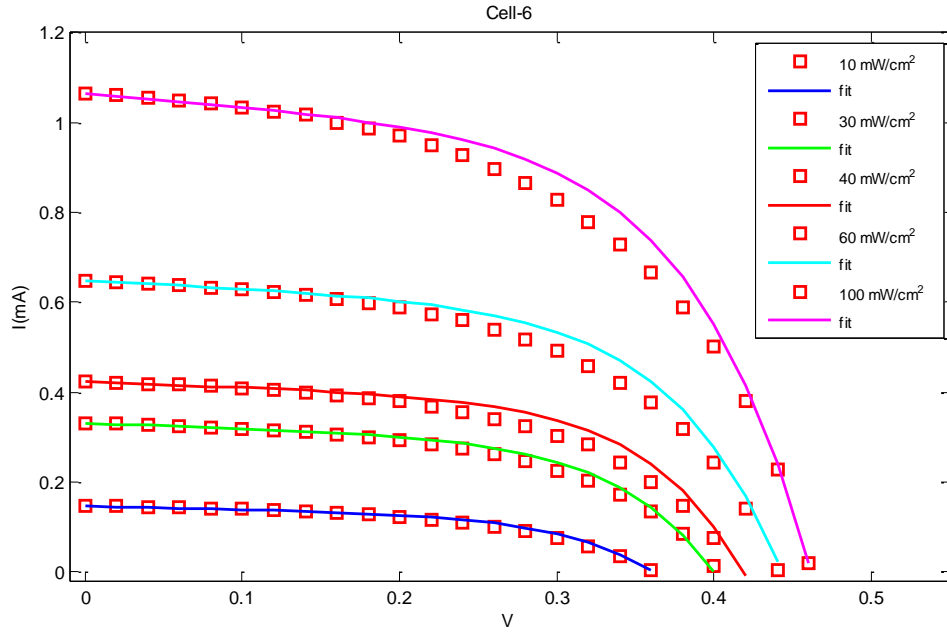
Figure 5.13 : Method Improved I-V fitting results of positive part for Cell-6.
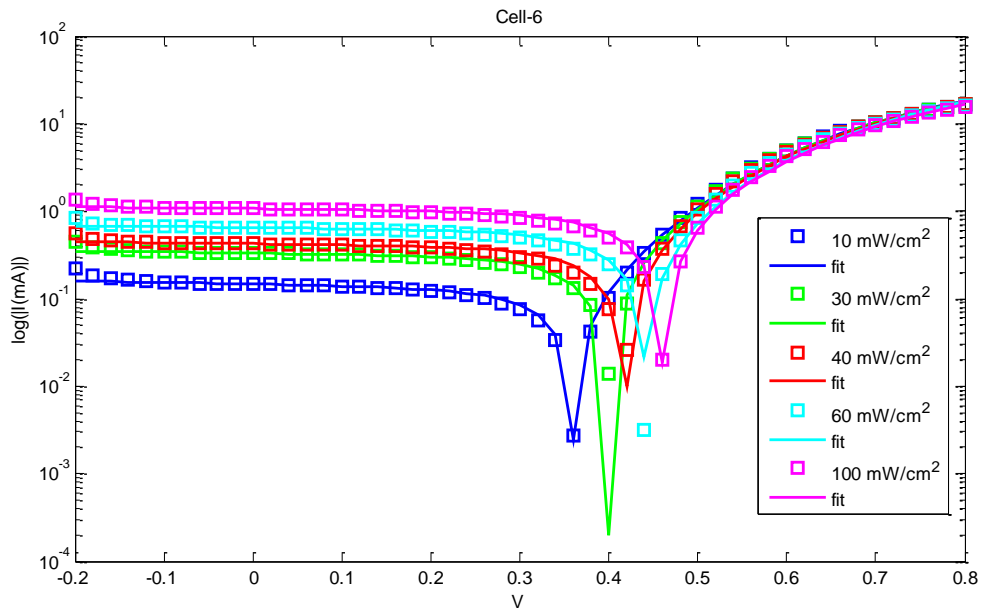
Figure 5.14 : Method Improved logarithmic I-V fitting result of complete experimental data of Cell-6.

5.3 Results of Model Improvement

As it is described in Chapter 4.2.3 if device model is considered a system includes irradiance relations in it and as it is shown in comparison tables in Chapter 5.5 that, when diode parameters of different irradiances are very closed to each other, better results are achived as it is illustrated (Figure 5.15 – Figure 5.26). Also, a regular

relation between R_{sh} and illumination is obtained to the fixed diode usage for different illuminations (Table 5.7 – Table 5.12) as it is illustrated (Figure 5.26 – Figure 5.32). It is also drastically reduced the iteration time (See Table 5.13).
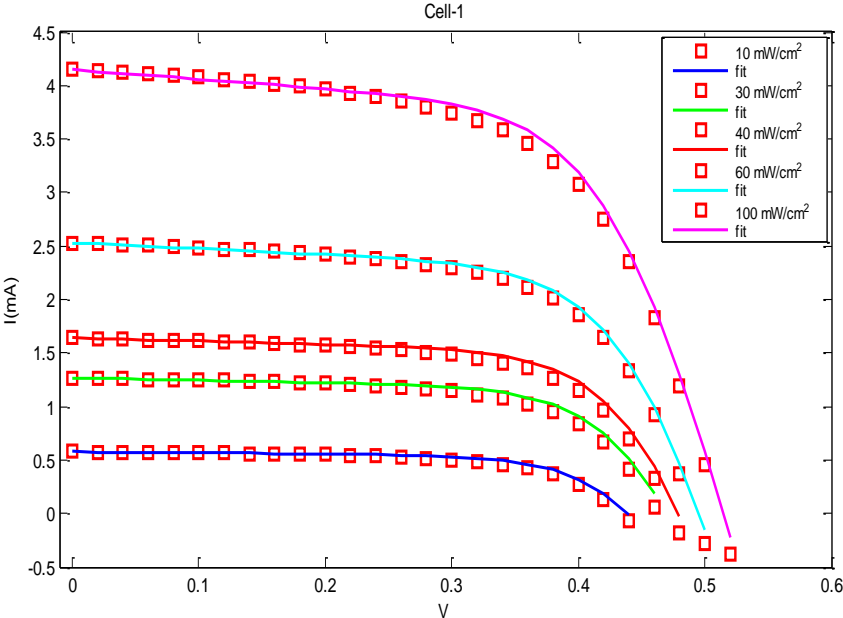
Figure 5.15 : Model improved I-V fitting results of positive part for Cell-1.
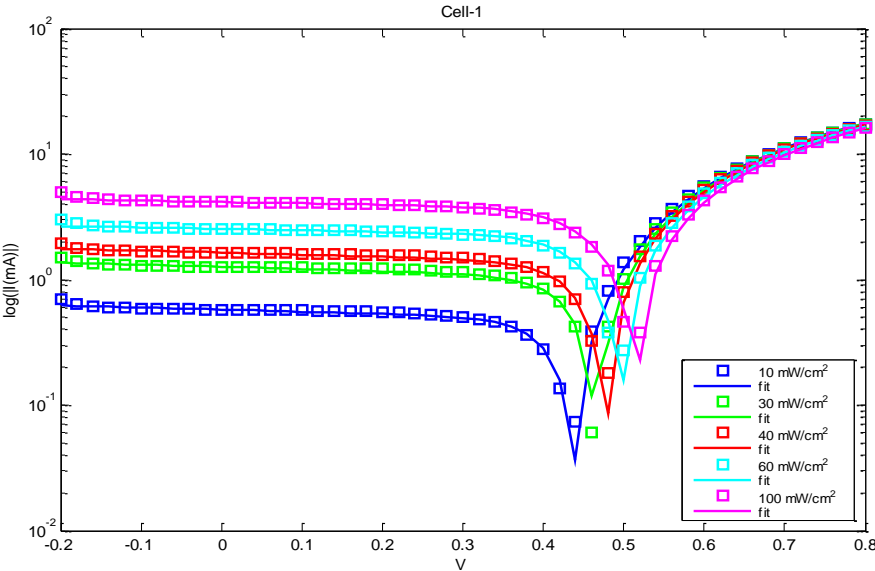
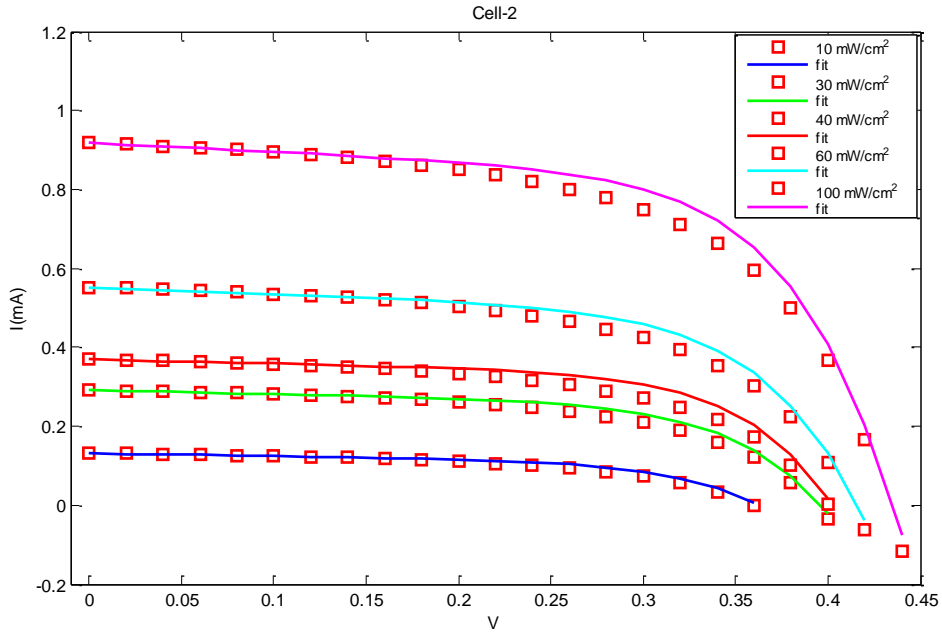**Figure 5.16 :** Model improved logarithmic I-V fitting result of complete experimental data of Cell-1.
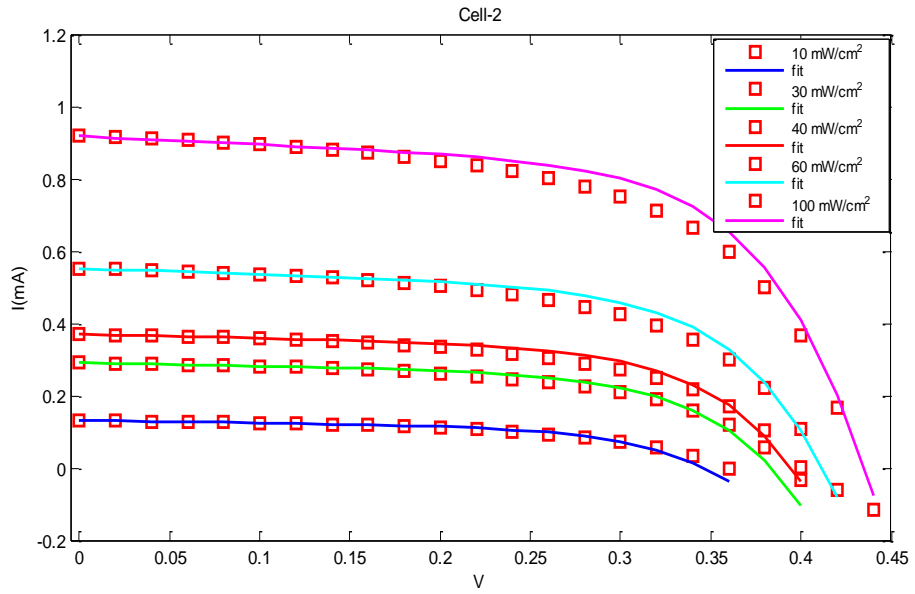
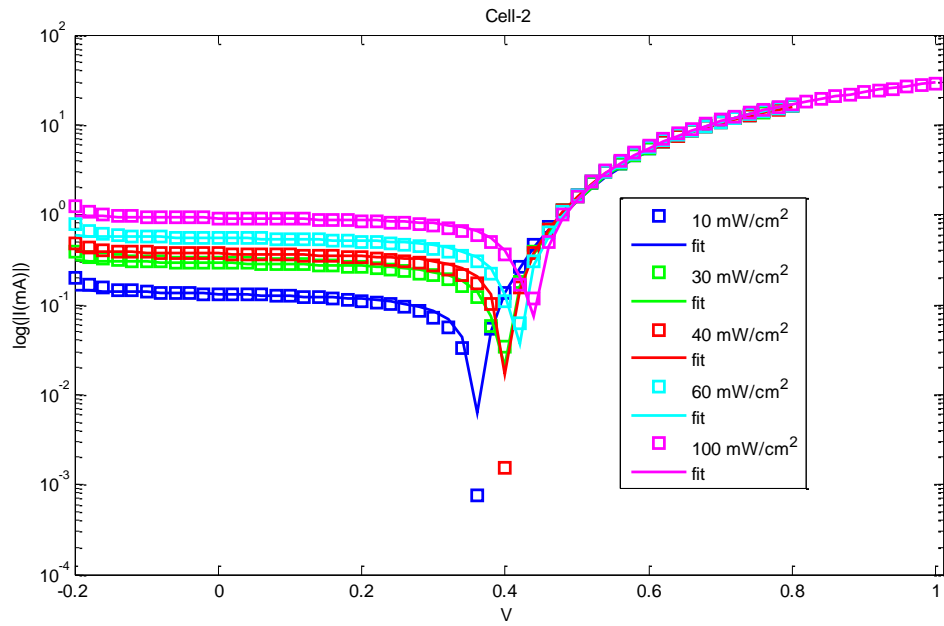**Figure 5.17 :** Model improved I-V fitting results of positive part for Cell-2.
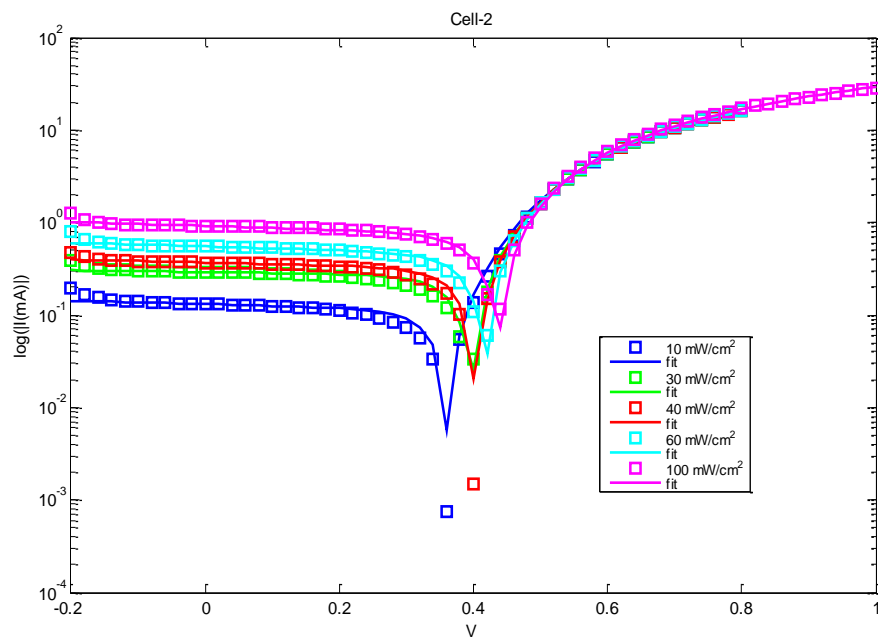
Figure 5.18 : Model improved logarithmic I-V fitting result of complete experimental data of Cell-2.
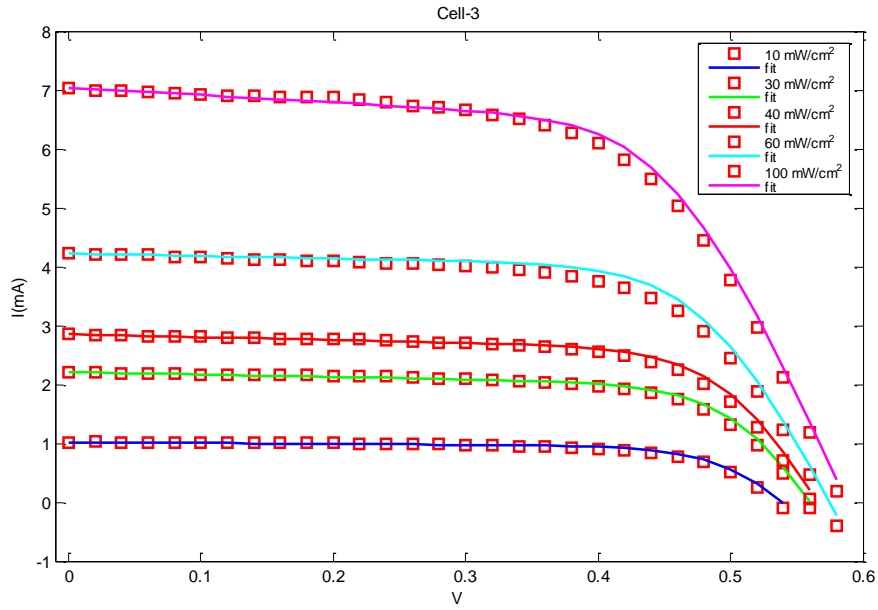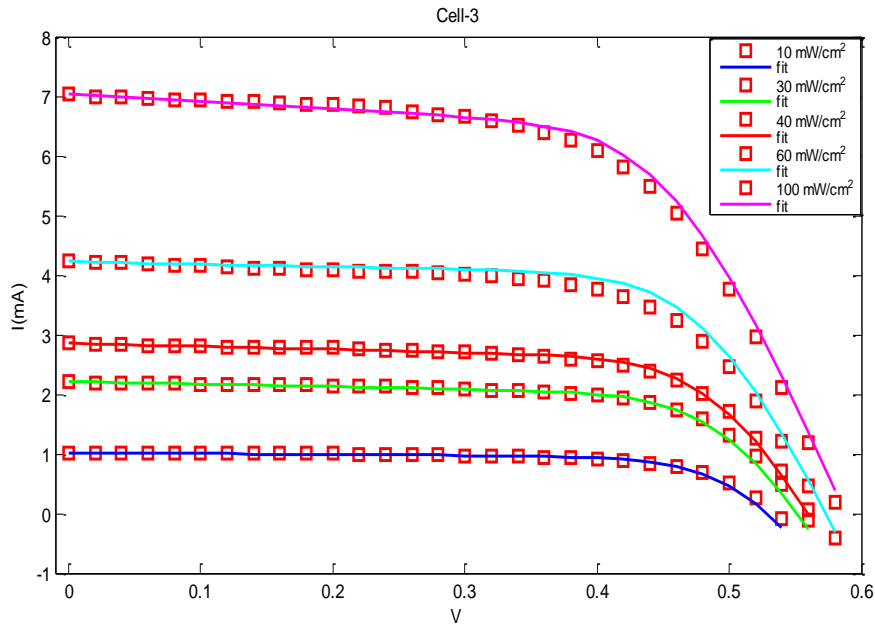
Figure 5.19 : Model improved I-V fitting results of positive part for Cell-3.
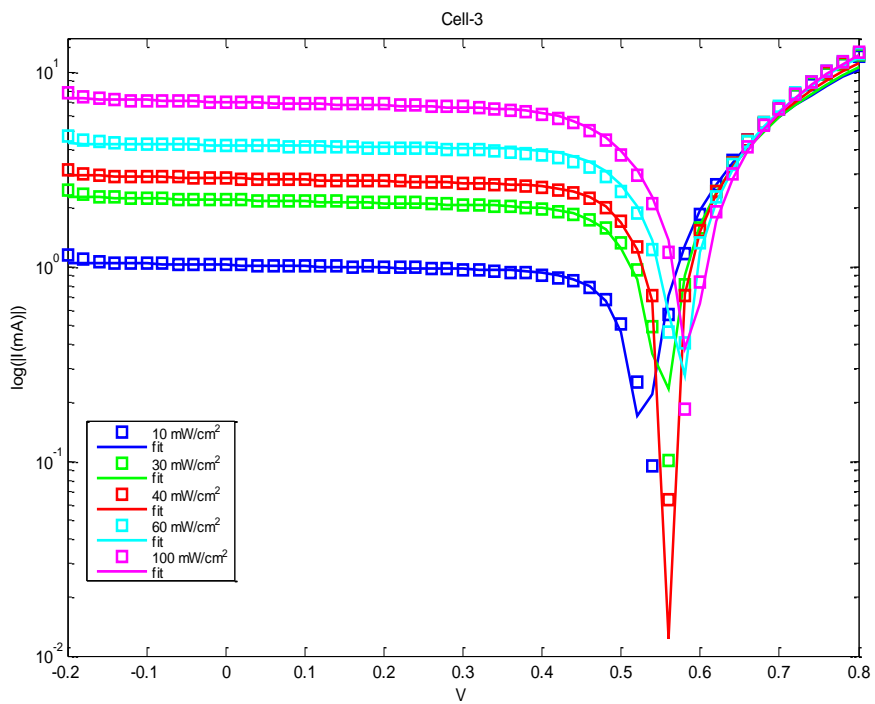
Figure 5.20 : Model improved logarithmic I-V fitting result of complete experimental data of Cell-3.
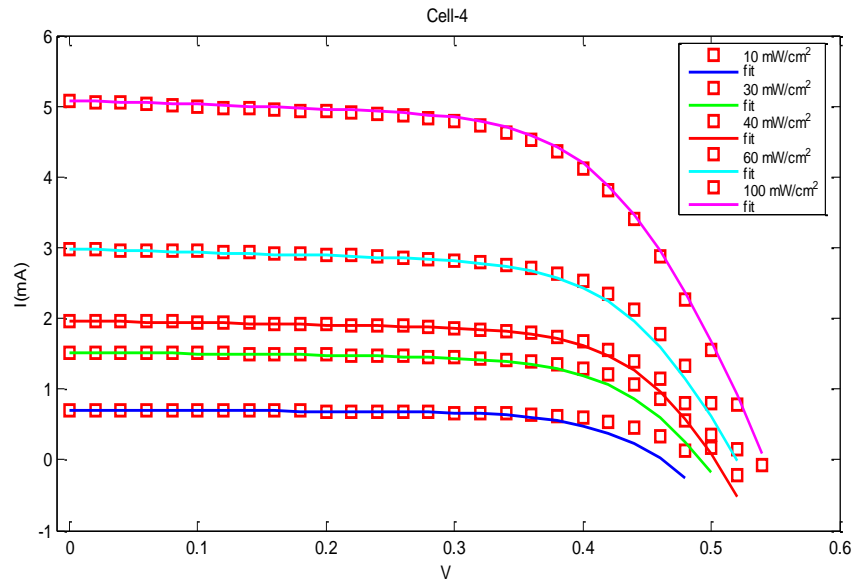
Figure 5.21 : Model improved I-V fitting results of positive part for Cell-4.
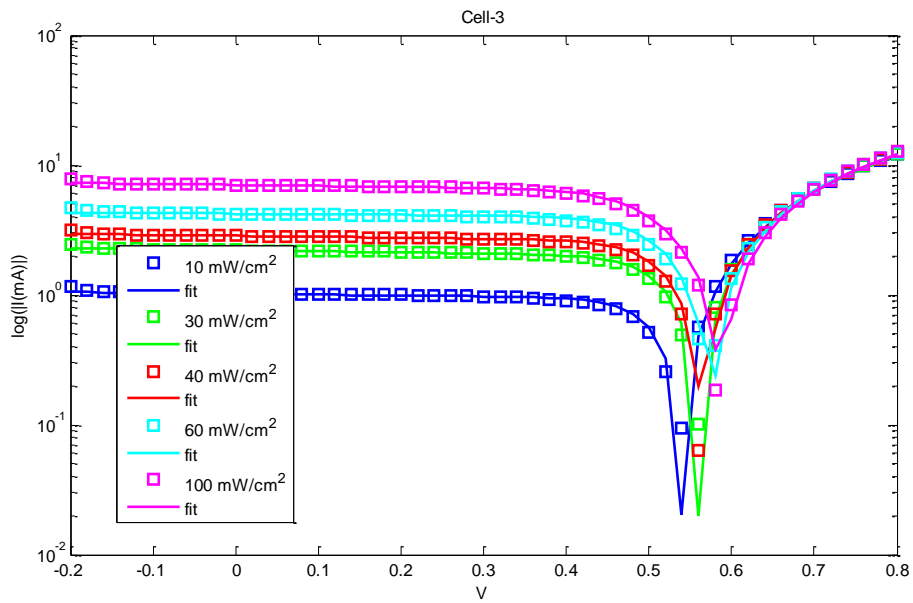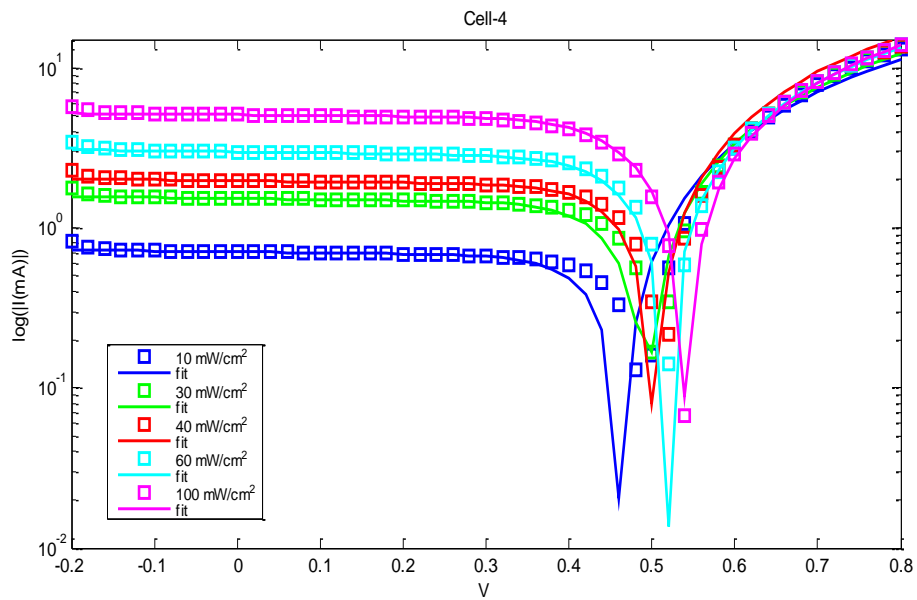

Figure 5.22 : Model improved logarithmic I-V fitting result of complete experimental data of Cell-4.
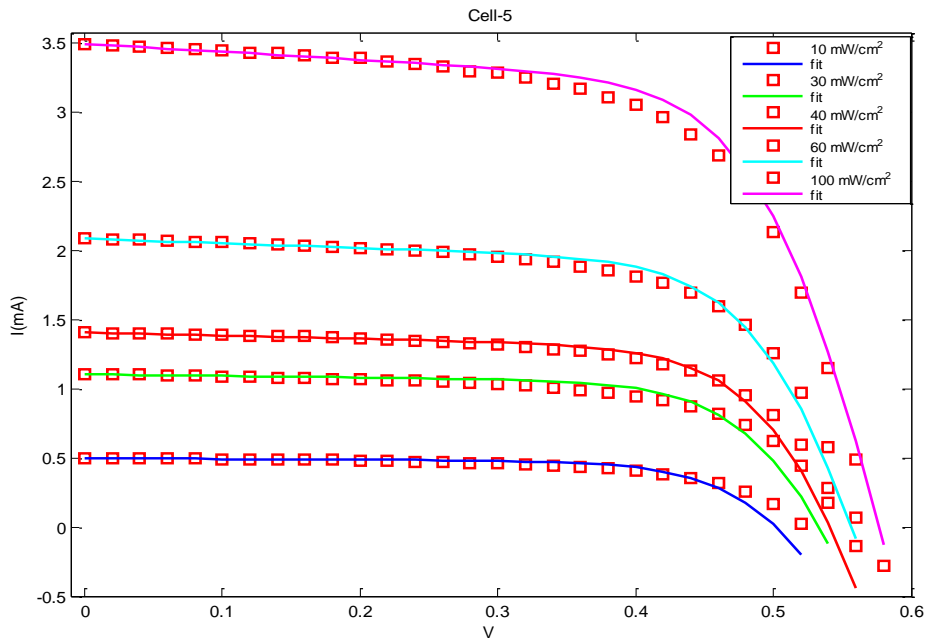
Figure 5.23 : Model improved I-V fitting results of positive part for Cell-5.
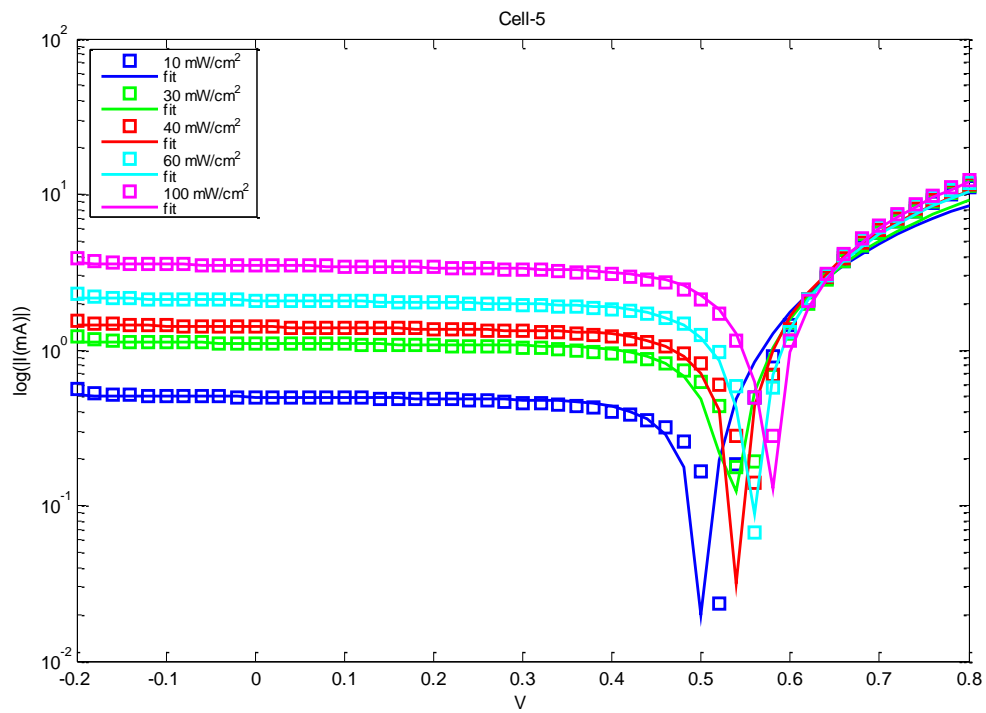
Figure 5.24 : Model improved logarithmic I-V fitting result of complete experimental data of Cell-5.
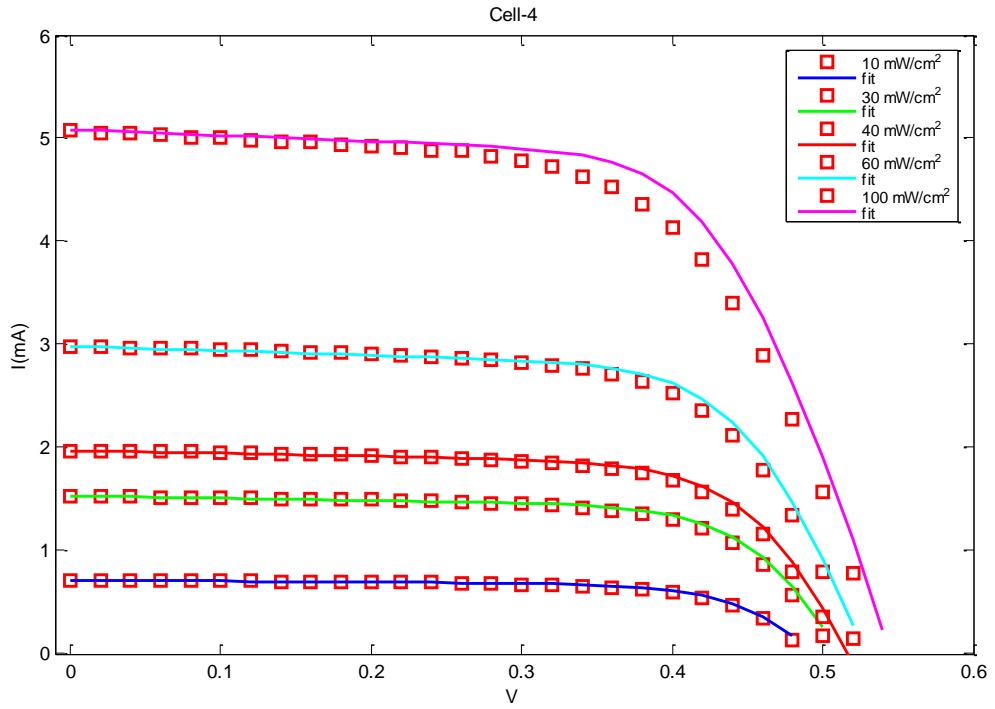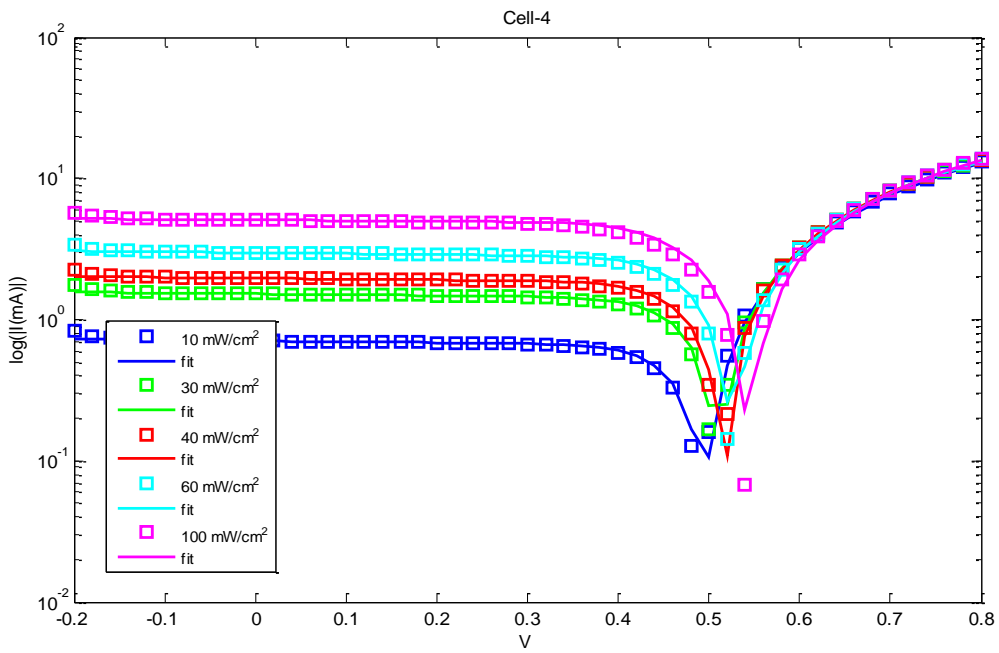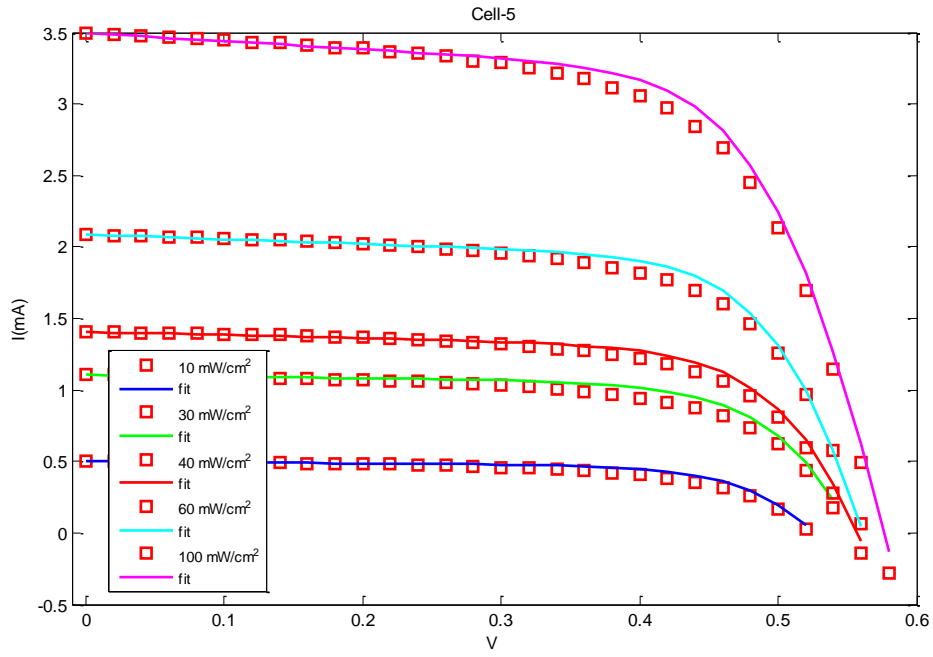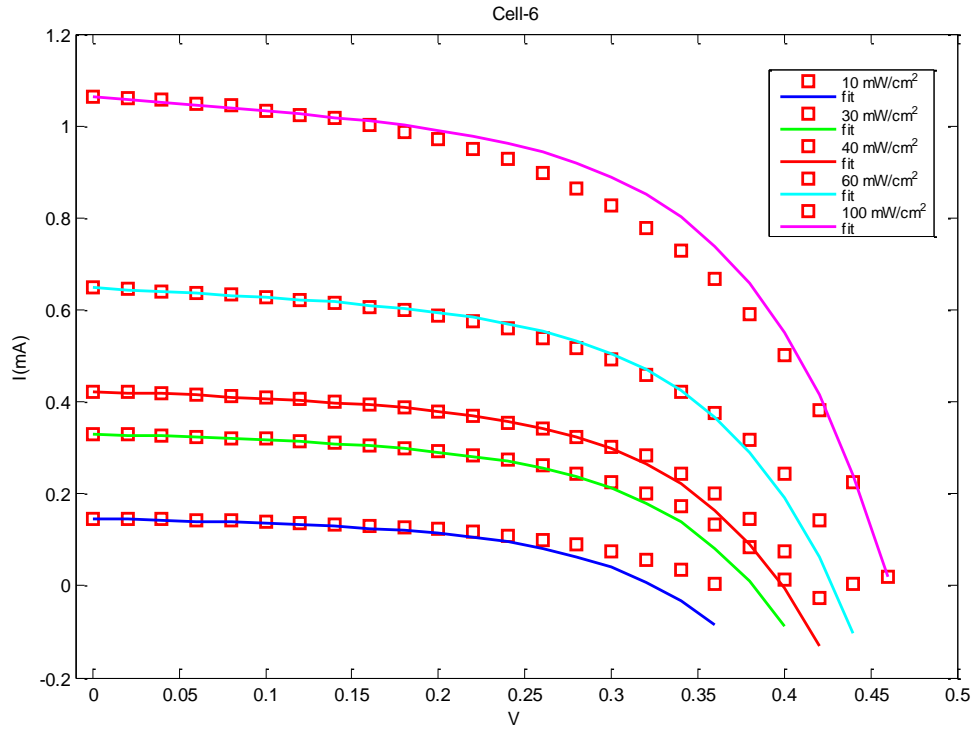
Figure 5.25 : I-V fitting results of positive part for Cell-6.
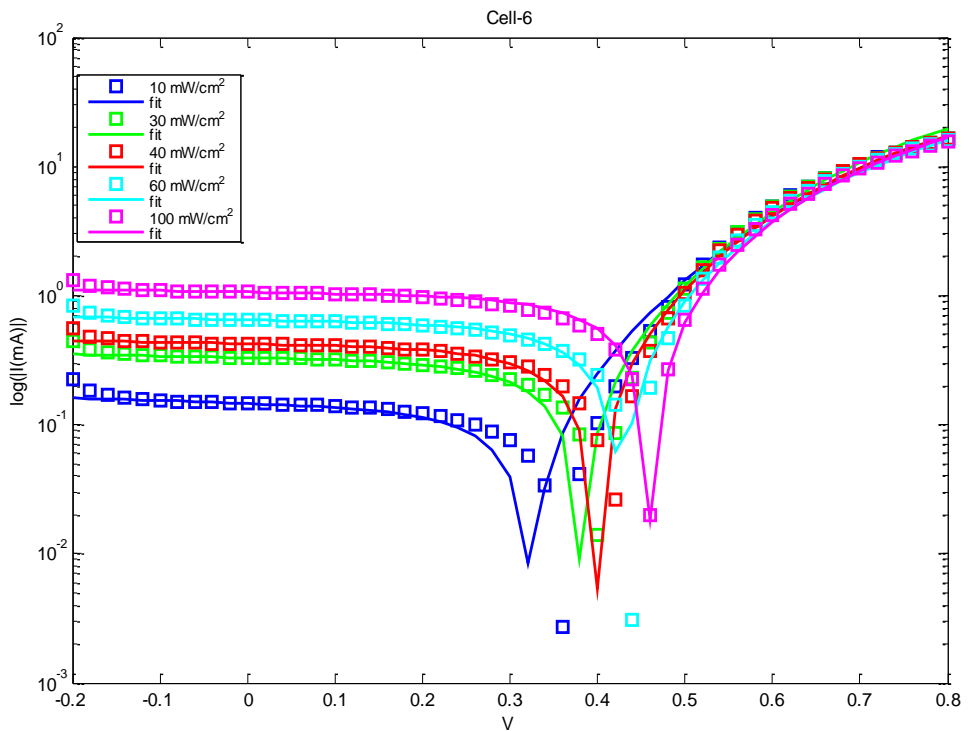
Figure 5.26 : Logarithmic I-V fitting result of complete experimental data of Cell-6.

Although our model is not valid for dark and very low irradiance measurements and results of dark is not illustrated in this study, result of $R_{sh\text{-}dark}$ is added in I_L-R_{sh}

graphics to show inversely propotional relation of shunted resistance with intensity
(Figure 5.27- Figure 5.32).
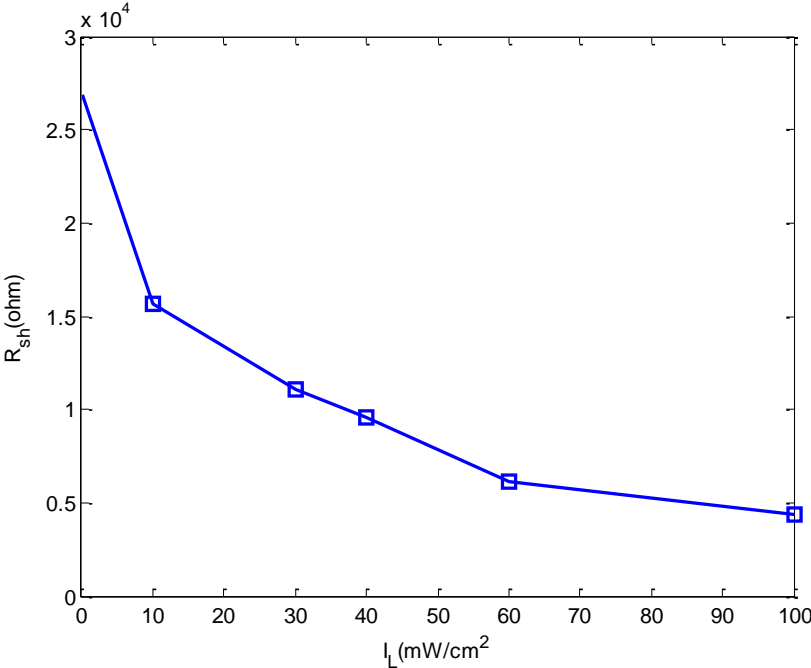
Figure 5.27 : I_L-R_{sh} demonstration of Cell-1.
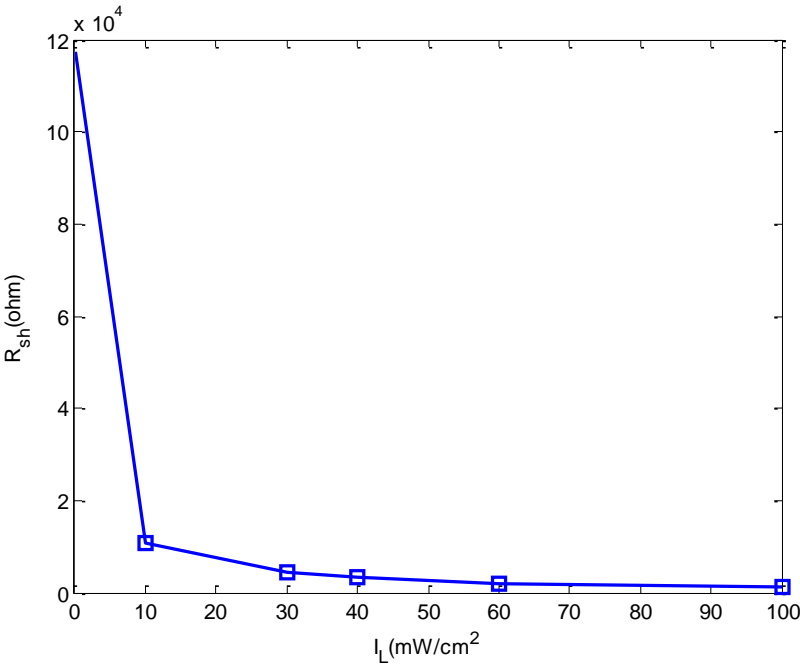
Figure 5.28 : I_L-R_{sh} demonstration of Cell-2.
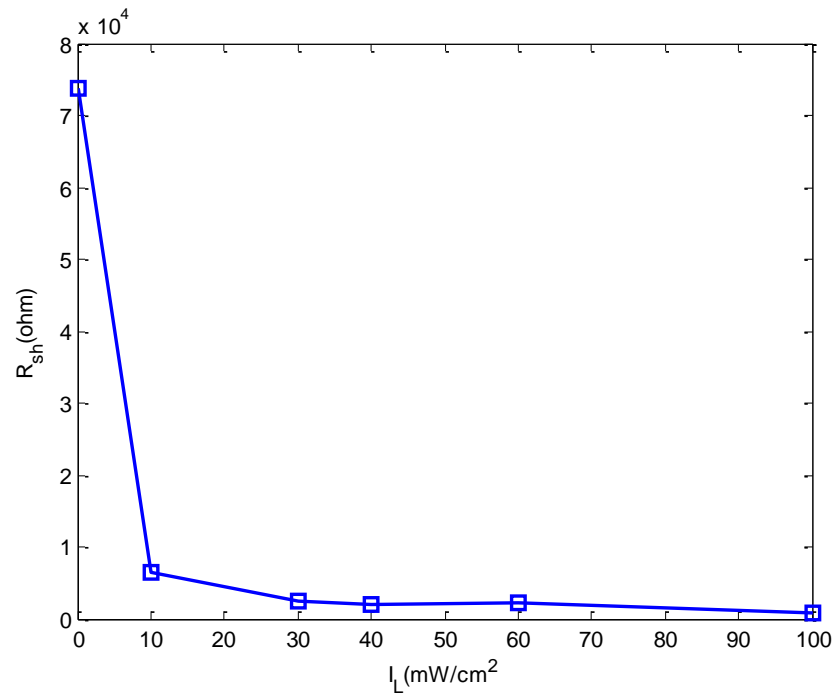
Figure 5.29 : I_L-R_{sh} demonstration of Cell-3.
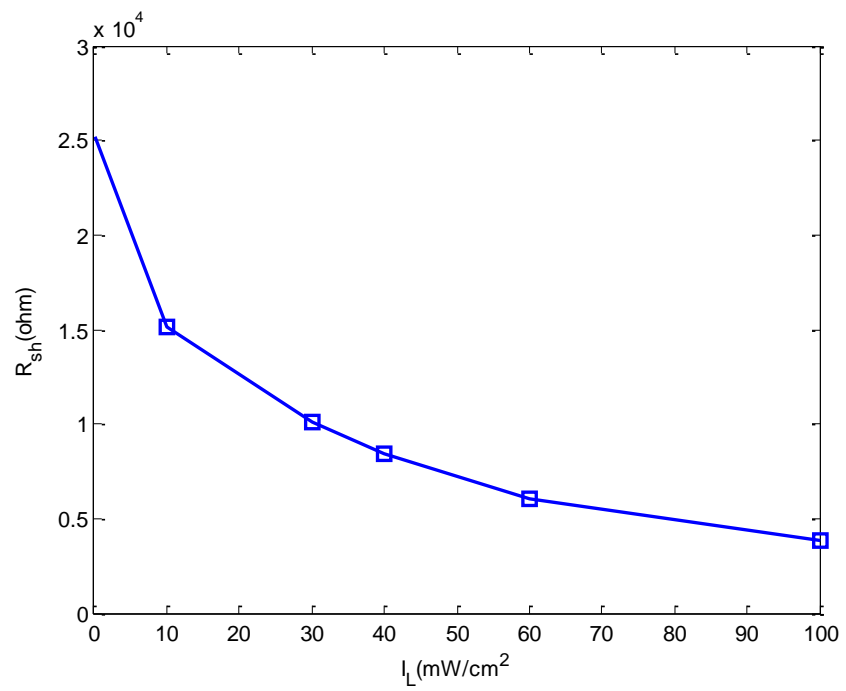
Figure 5.30 : I_L-R_{sh} demonstration of Cell-4.

49
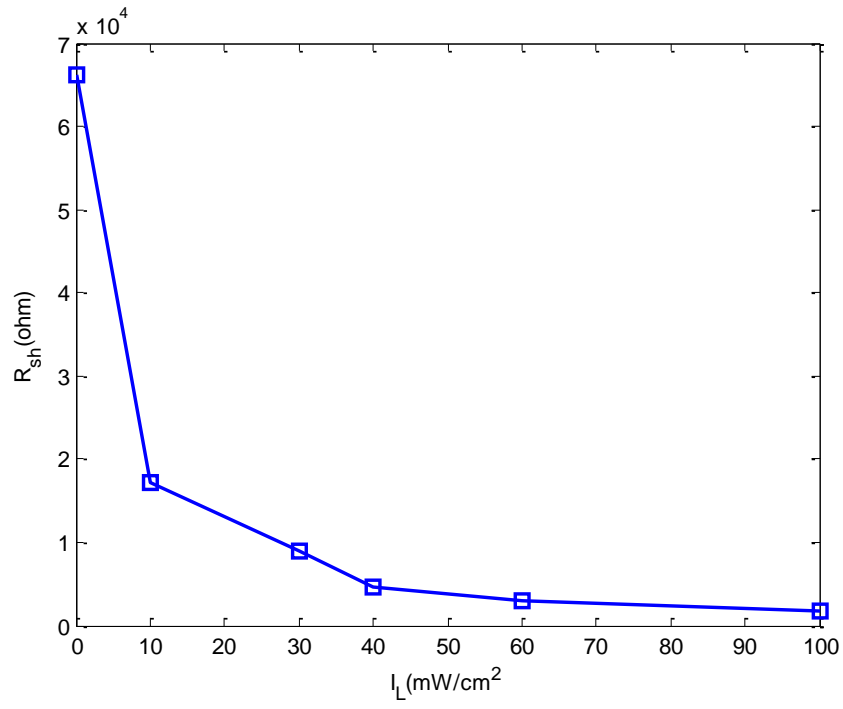
Figure 5.31 : I_L-R_{sh} demonstration of Cell-5.
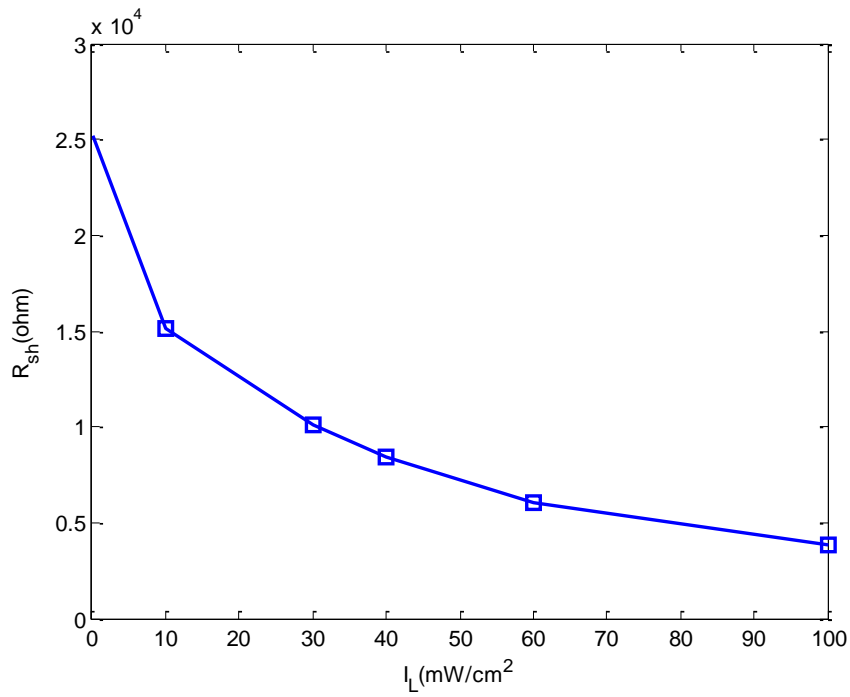
Figure 5.32 : I_L-R_{sh} demonstration of Cell-6.

5.4 "Individul Cell Simulator (ICS)"s Results

Illumination dependence of circuit parameters are illustrated in chapter 4.2 and 4.3. Individual Cell Simulator (ICS) stems from these illumination dependencies of circuit parameters. It is demonstrated in Chapter 4.2.3 that these dependencies are neither irregular nor random. We found the linear dependency equation of I_{sc} and illumination dependant equation of Rsh for each cell individually. We assumed that an approximate R_s is effective for all illuminations.

As it is mentioned in chapter 4.2.3.1 $I_{sc}^{\gamma \approx 1} \alpha I_L$ relationship is proposed between short circuit current and irradiance in literature. We used the same relationship in our simulators with an addition of an error constant "e" which is written as an equation:

$$I_{sc} = aI_L + e \qquad (5.1)$$

In Equation 5.1 "a" and "e" are constant values found by using extracted I_{sc} values from the experimental curve by using improved model via MATLAB curve fitting tool (cftool). I_L is the irradiance value as it is described previous chapters, which is variable value inside the equation.

The relationship between R_{sh} and irradiance is more complicated. Although, the equation used in this study is inspired from the proportional relationship in literature, which is showed in Equation 4.11, after numerous experiments applied by using cftool onto resistance values extracted from the thirty different I-V data of the six cells, the fitting equation of the shunted resistance is decided as:

$$R_{sh} = 1/(aI_L{}^c + b) \qquad (5.2)$$

The constant values of the equations are named "a, b, c" that are found via cftool.

To have an ICS simulator for each cell the constant values of the Equation 5.1 and 5.2 is extracted and put into the circuit equation (Equation 4.13). The values of ideality factor, saturation current and serial resistance must be inserted too. The constant values of the simulator equation found for six DSSC that we used in our study is listed in Table 5.7.

Table 5.7 : Constant values of the equivalent circuit extracted to create ICS of the six cell.

	n	I_0	$I_{sc} = aI_L + e$		$R_{sh} = 1/(aI_L{}^c + b)$			$mean(R_s)$
			a	e	a	b	c	
C1	1.5053	6.7340e-9	0.0402e-3	0.1011e-3	1.041e-6	6.239e-5	1.478	13.2336
C2	1.7083	4.3042e-8	0.0880e-4	0.2984e-4	2.622e-7	5.679e-5	1.431	13.0397
C3	1.1850	2.9876e-11	0.0674e-3	0.2351e-3	2.848e-5	1.463e-6	0.7443	16.8052
C4	1.5693	7.5527e-9	0.4913e-4	0.9246e-4	6.23e-6	3.623e-5	0.9921	17.2099
C5	1.5074	1.1871e-9	0.0335e-3	0.1113e-3	6.655e-8	5.082e-5	2.049	17.5294
C6	2.6260	1.0536e-6	0.1030e-4	0.2783e-4	5.128e-7	5.554e-5	1.307	8.7471

The output results of ICS simulators of six DSSC named from C1 to C6 are demonstrated in linear and logarithmic scale similar to the previous chapter between Figure 5.33 – 5.44. The impressive advantage of the ICS simulators are prediction of the I-V respond of cell under unknown illuminations. as it is illustrated in figures with simulated I-V curve of 50W/cm² and 80 W/cm² illuminations sketched with red lines.
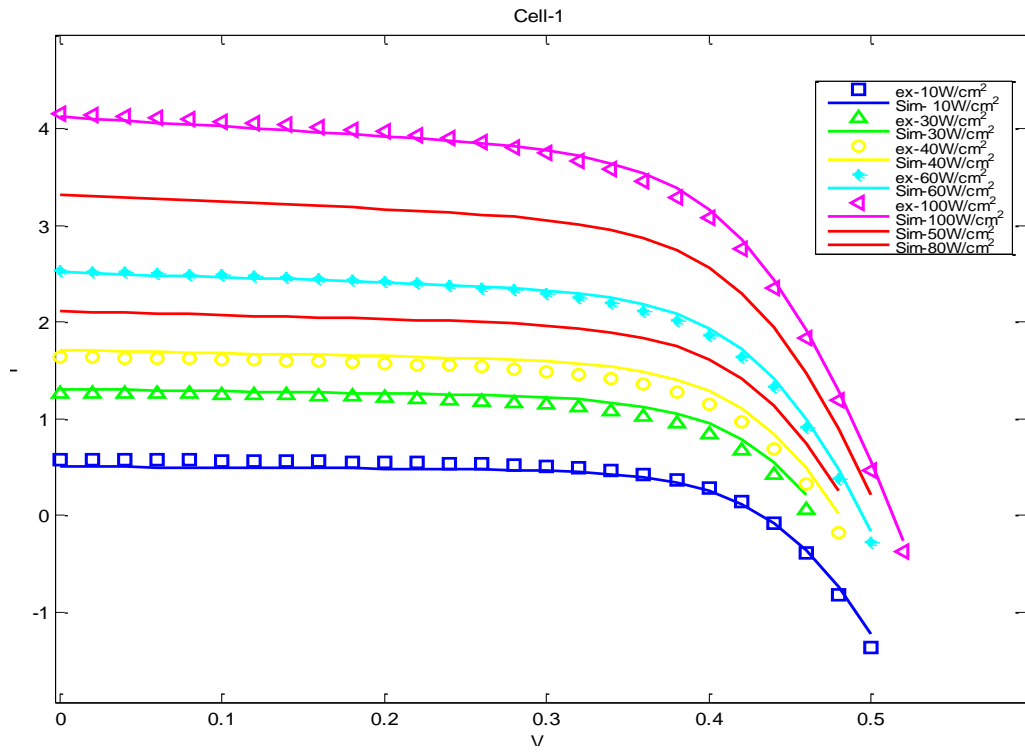
Figure 5.33 : I-V obtained from ICS-C1simulator compared to the I-V data of Cell-1.
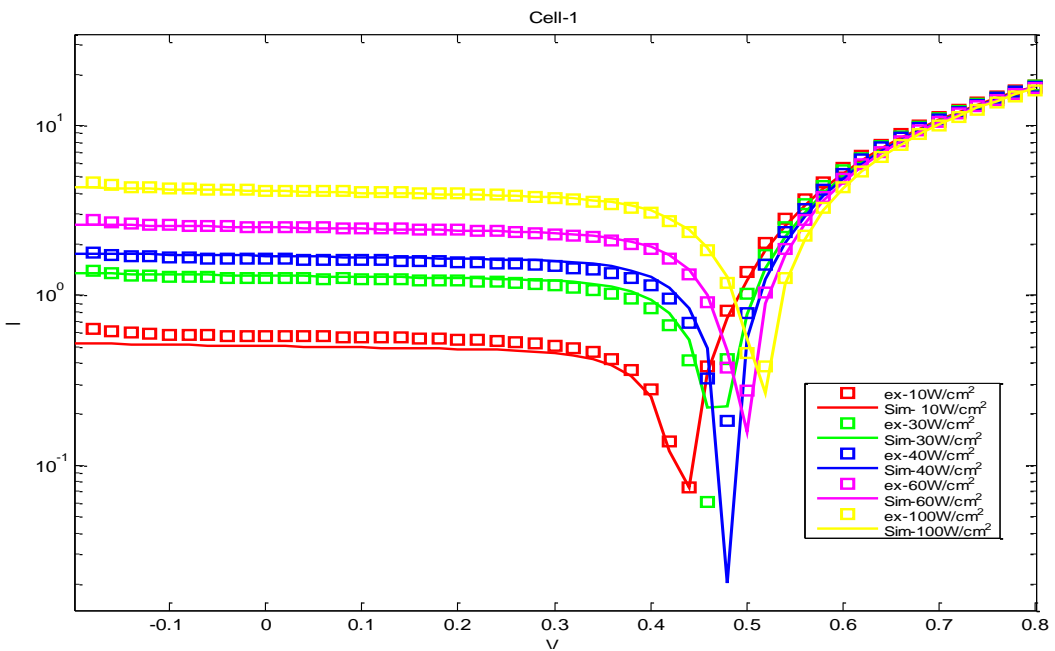
Figure 5.34 : Logarithmic demonstration of the accuracy of simulator on the complete I-V data of Cell-1
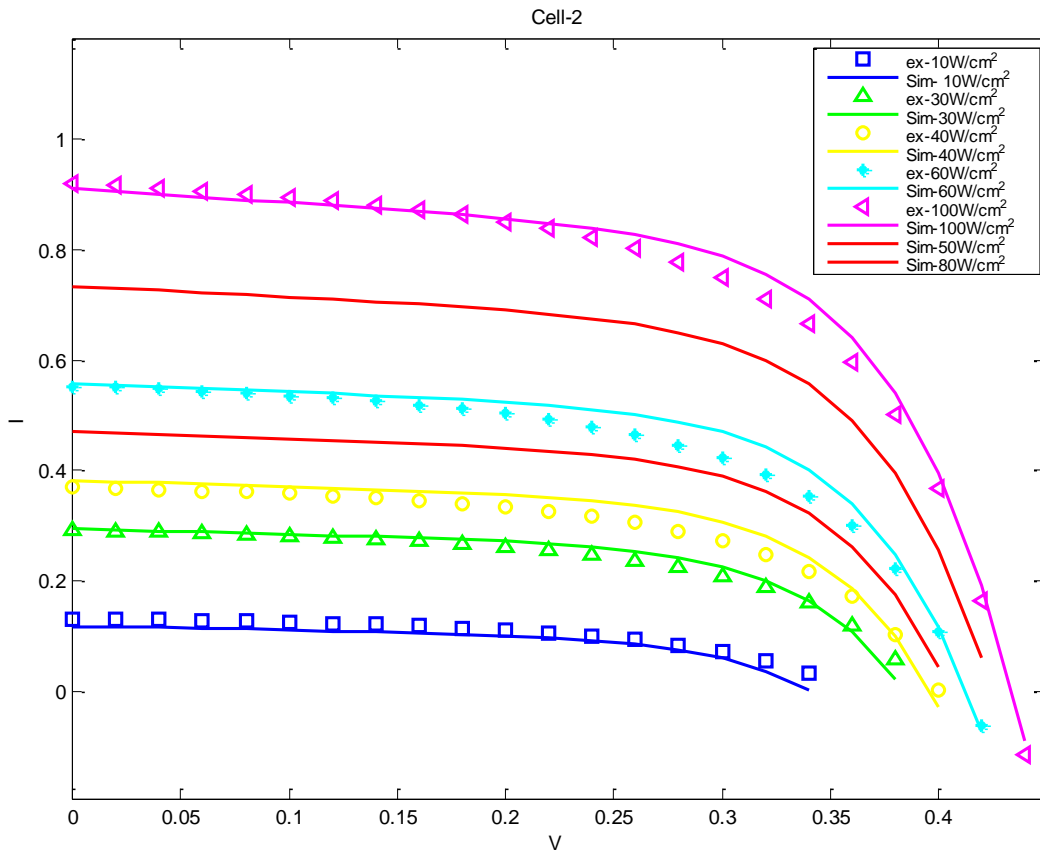
Figure 5.35 : I-V obtained from ICS-C2simulator compared to the I-V data of Cell-2.
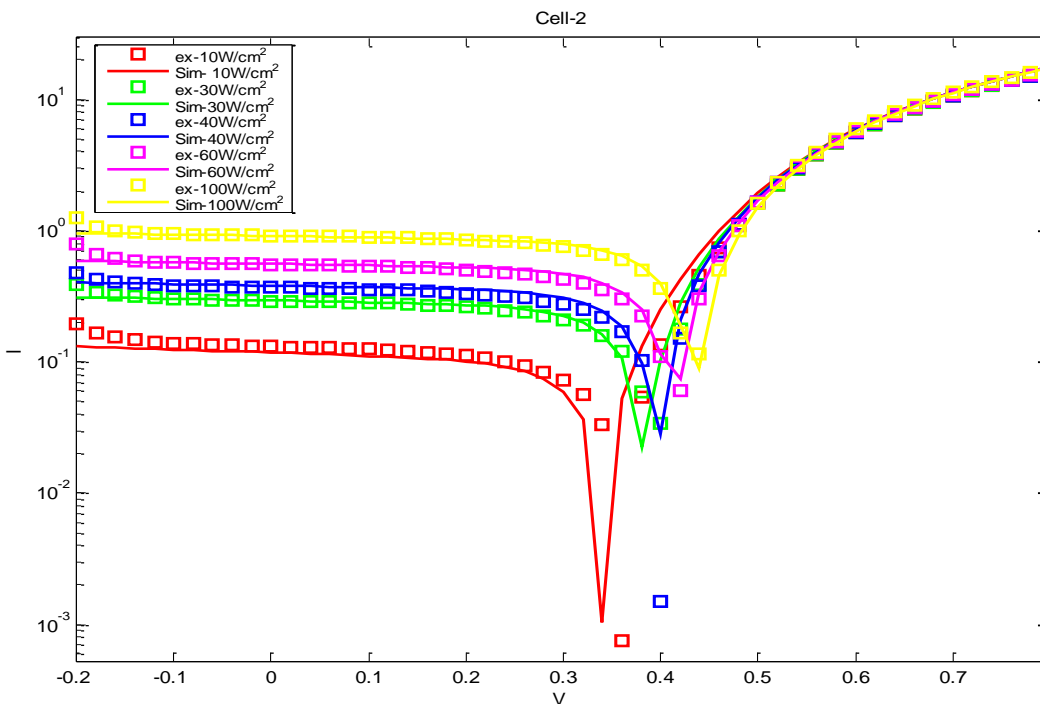
Figure 5.36 : Logarithmic demonstration of the accuracy of simulator on the complete I-V data of Cell-2.
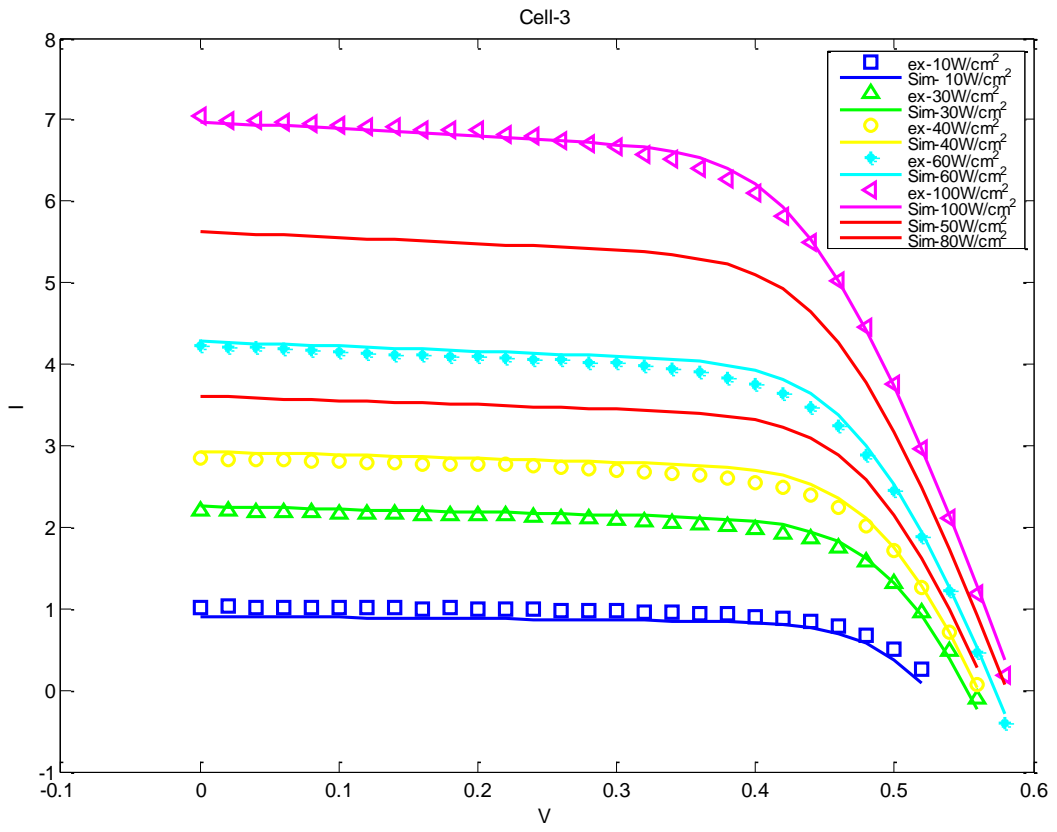
Figure 5.37 : I-V obtained from ICS-C3simulator compared to the I-V data of Cell-3.
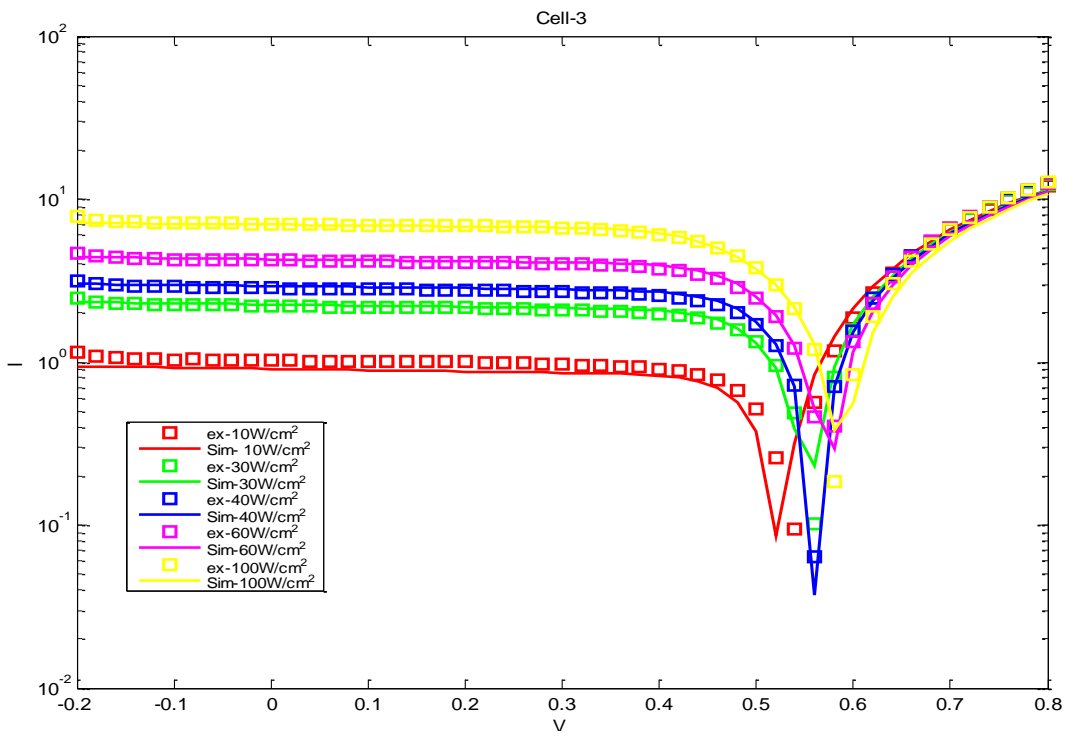
Figure 5.38 : Logarithmic demonstration of the accuracy of simulator on the complete I-V data of Cell-3.
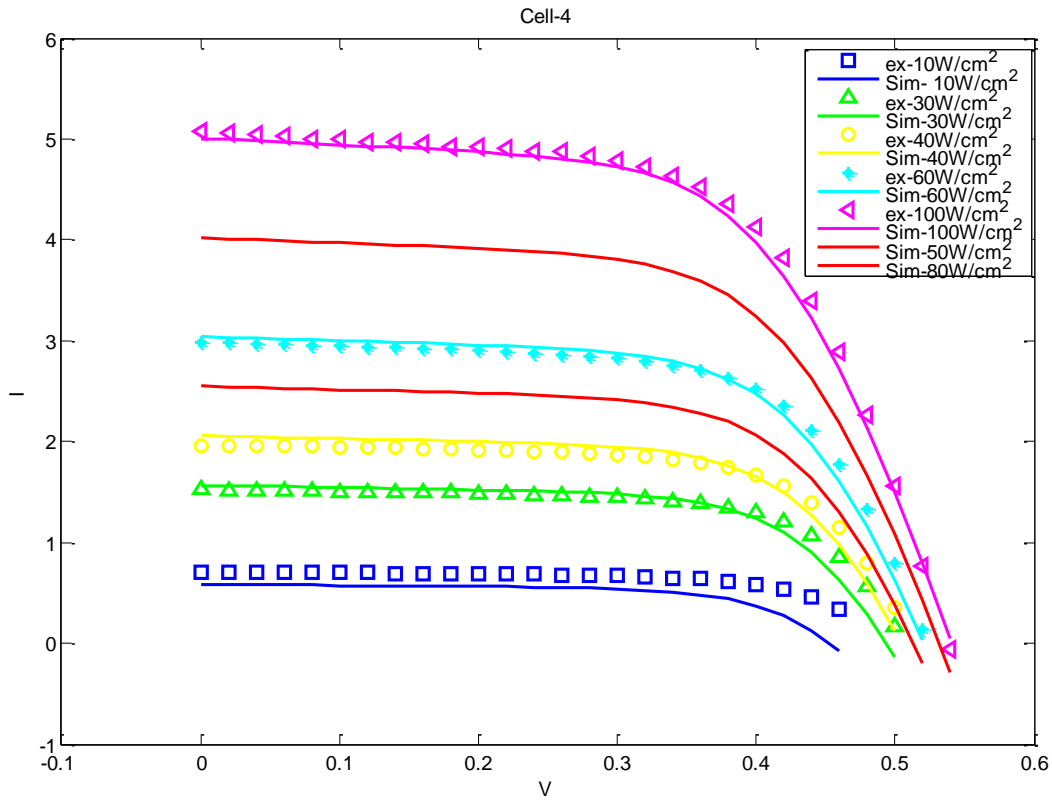
Figure 5.39 : I-V obtained from ICS-C4simulator compared to the I-V data of Cell-4.
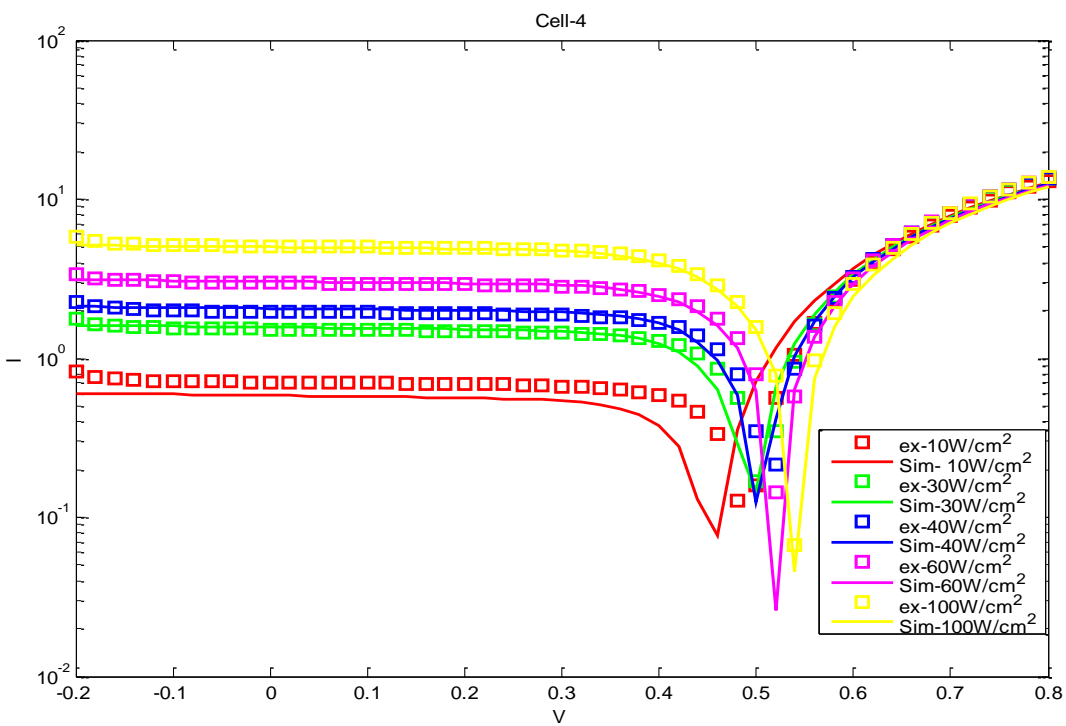
Figure 5.40 : Logarithmic demonstration of the accuracy of simulator on the complete I-V data of Cell-4.
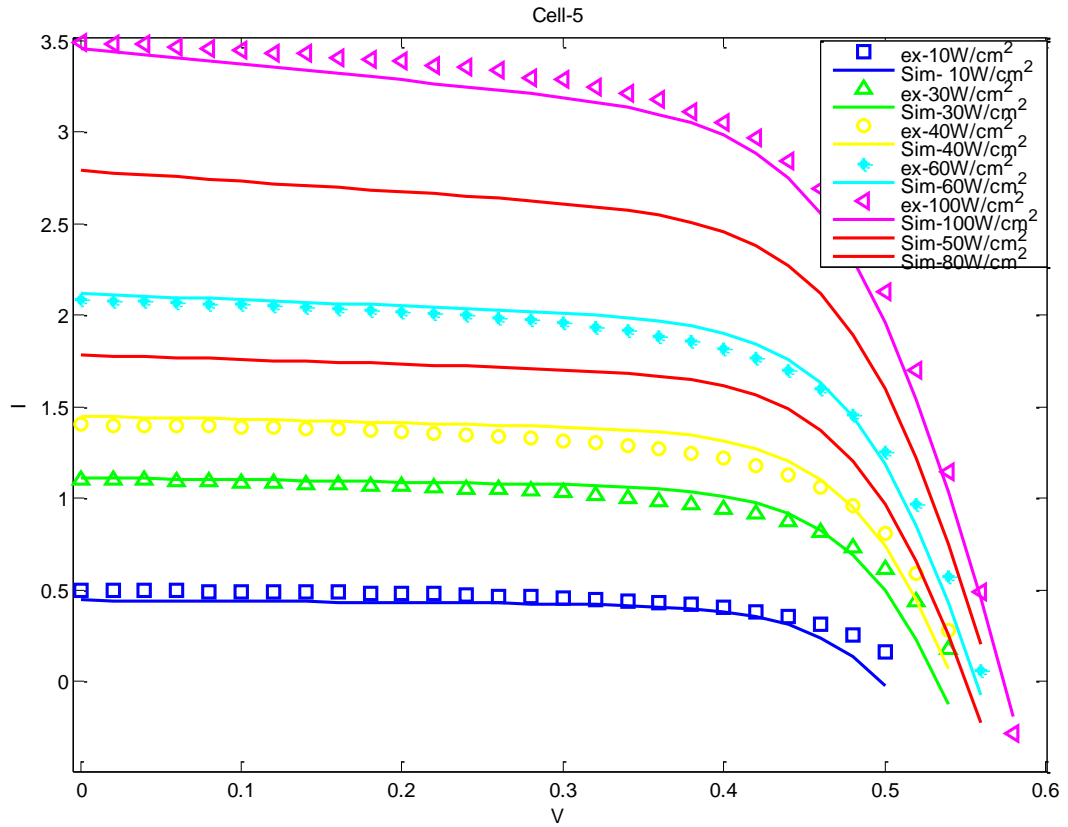
Figure 5.41 : I-V obtained from ICS-C5simulator compared to the I-V data of Cell-5.
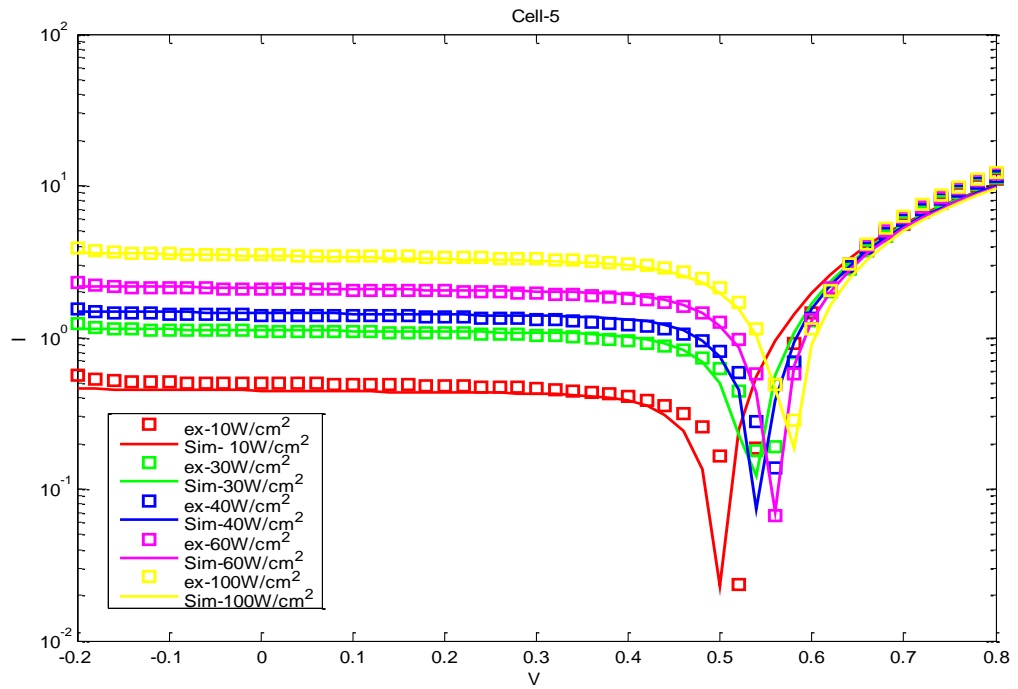
Figure 5.42 : Logarithmic demonstration of the accuracy of simulator on the complete I-V data of Cell-5.
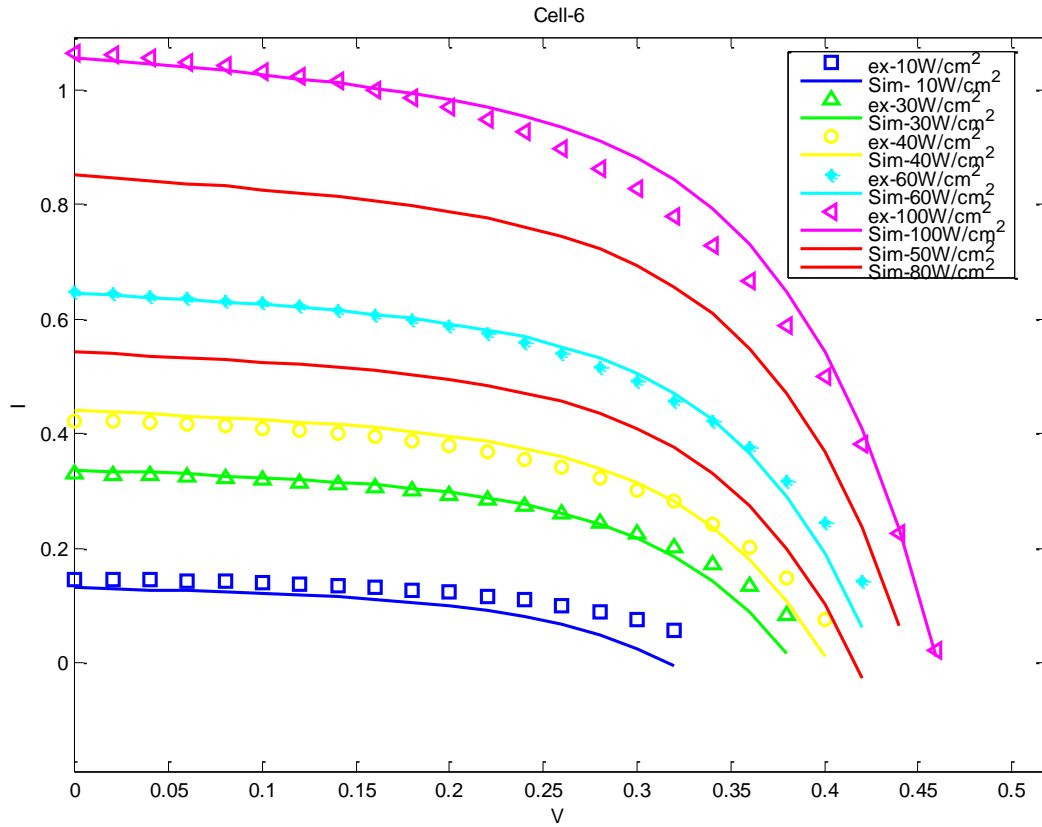
Figure 5.43 : I-V obtained from ICS-C6simulator compared to the I-V data of Cell-6.
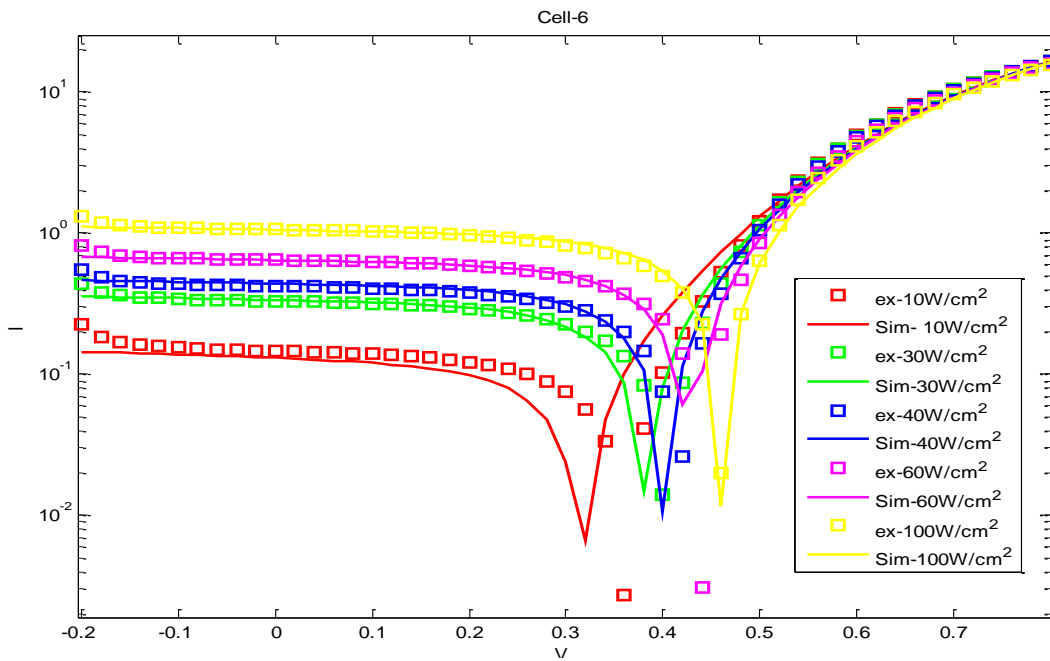
Figure 5.44 : Logarithmic demonstration of the accuracy of simulator on the complete I-V data of Cell-6.

The flow chart in Figure 5.45 demonstrates the processes to create an ICS for a cell by using improved method and model and measured I-V datas for different illumunations. The key point must be considered is that while currents are measured wide scale of the irrediance powers must be choosen to have accurate results. In our study this scale is optimized over 10 W/cm² and below 100 W/ cm² (STC), since as it can be seen 10 W/cm² does not provide te completely accurate I-V results. However, it still has acuracy in low voltages.
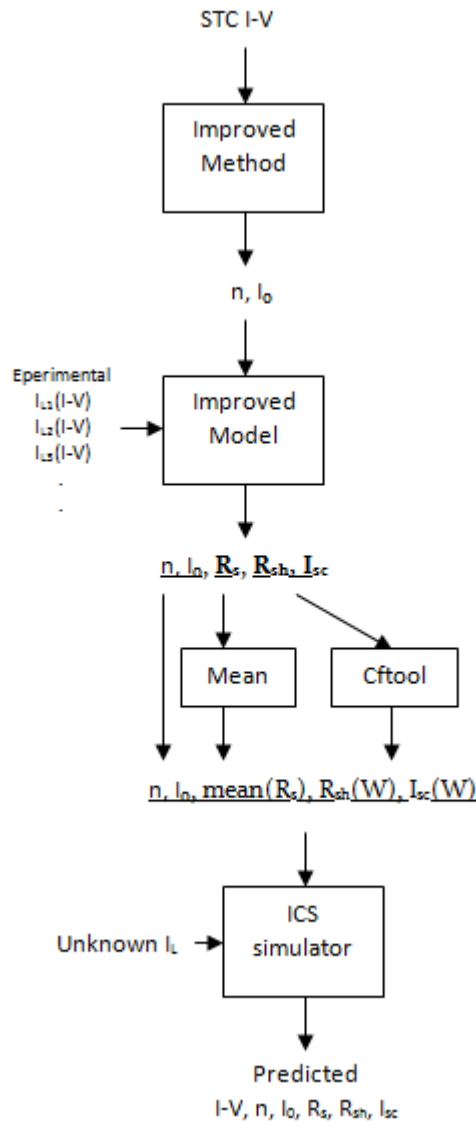
Figure 5.45 : The processes to create the improved model and an ICS of a cell with the inputs and outputs.

5.5 Comparison of The Results

As it is shown in tables below, parameter results obtained from improved method and model is nearly same. That approves the accuracy of the results we obtained from both improvements.

Table 5.8 : Cell-1 Fitting parameters comparison of method and model improvement.

Cell-1 Irradiance	R_s Met. Im.	R_s Mod. Im.	R_{sh} Met. Im.	R_{sh} Mod. Im.	n Met. Im.	n Mod. Im.	I_0 Met. Im.	I_0 Mod. Im.
10mW/cm²	12.7581	12.6382	10671	10670	1.5451	1.5053	0.9555 e-8	6.7340e-009
30mW/cm²	13.2483	12.9099	4507	4510	1.5014		0.7104 e-8	
40mW/cm²	13.2349	12.6994	3352	3350	1.5261		0.8554 e-8	
60mW/cm²	13.3453	13.4620	1822	1820	1.5304		0.8321 e-8	
100mW/cm²	13.8290	13.8290	1106	1110	1.5053		0.6734 e-8	

Table 5.9 : Cell-2 Fitting parameters comparison of method and model improvement.

Cell-2 Irradiance	R_s Met. Im.	R_s Mod. Im.	R_{sh} Met. Im.	R_{sh} Mod. Im.	n Met. Im.	n Mod. Im.	I_0 Met. Im.	I_0 Mod. Im.
10mW/cm²	12.4730	16.3462	15625	15625	1.7329	1.7083	0.3290 e-7	4.3042e-008
30mW/cm²	12.7643	15.6716	11041	11041	1.7496		0.3994 e-7	
40mW/cm²	14.7058	15.8739	9538	9538	1.6269		0.2284 e-7	
60mW/cm²	12.8606	14.5993	6171	6171	1.7999		0.6313 e-7	
100mW/cm²	13.6063	13.6063	4361	4361	1.7083		0.4304 e-7	

Table 5.10 : Cell-3 Fitting parameters comparison of method and model improvement

Cell-3 Irradiance	R_s Met. Im.	Mod. Im.	R_{sh} Met. Im.	Mod. Im.	n Met. Im.	Mod. Im.	I_0 Met. Im.	Mod. Im.
10mW/cm²	14.6462	18.8377	6416.1	6416	1.3265		0.1396 e-9	
30mW/cm²	14.9998	18.1136	2417.1	2417	1.2534		0.0605 e-9	
40mW/cm²	15.0150	17.2114	1964.6	1965	1.2253	1.1850	0.0454 e-9	2.9876e-011
60mW/cm²	14.8800	15.4856	2305.7	2306	1.2860		0.1243 e-9	
100mW/cm²	14.7727	14.7727	776.4	0776	1.1850		0.0299 e-9	

Table 5.11 : Cell-4 Fitting parameters comparison of method and model improvement

Cell-4 Irradiance	R_s Met. Im.	Mod. Im.	R_{sh} Met. Im.	Mod. Im.	n Met. Im.	Mod. Im.	I_0 Met. Im.	Mod. Im.
10mW/cm²	15.2201	19.6698	10259	10260	1.4003		0.7996 e-9	
30mW/cm²	15.9716	17.6649	4657	4660	1.3159		0.4304 e-9	
40mW/cm²	15.9846	13.1605	3614	3610	1.3112	1.5693	0.4424 e-9	7.5527e-009
60mW/cm²	16.5721	15.6126	2254	2250	1.1988		0.1115 e-9	
100mW/cm²	16.1246	14.7500	1774	1770	1.1295		0.0374 e-9	

Table 5.12 : Cell-5   Fitting parameters comparison of method and model improvement

Cell-5 Irradiance	R_s		R_{sh}		n		I_0	
	Met. Im.	Mod. Im.	Met. Im.	Mod. Im.	Met. Im.	Mod. Im.	Met. Im.	Mod. Im.
10mW/cm²	12.7050	21.4958	17157	17157	1.6505		0.2069 e-8	
30mW/cm²	12.1320	19.4673	8895	8895	1.7074		0.3699 e-8	
40mW/cm²	12.5195	16.3626	4531	4531	1.6520	1.5074	0.2739 e-8	1.1871e-009
60mW/cm²	14.9223	16.4370	3049	3049	1.4269		0.0465 e-8	
100mW/cm²	13.5629	13.5629	1766	1766	1.5074		0.1187 e-8	

Table 5.13 : Cell-6   Fitting parameters comparison of method and model improvement for

Cell-6 Irradiance	R_s		R_{sh}		n		I_0	
	Met. Im.	Mod. Im.	Met. Im.	Mod. Im.	Met. Im.	Mod. Im.	Met. Im.	Mod. Im.
10mW/cm²	8.4287	8.4563	15161	15161	2.2023		0.0215 e-5	
30mW/cm²	8.4089	6.6702	10120	10120	2.3229		0.0372 e-5	
40mW/cm²	8.8188	7.9726	8386	8386	2.2434	2.6260	0.0274 e-5	1.0536e-006
60mW/cm²	7.7214	9.0379	6048	6048	2.4602		0.0546 e-5	
100mW/cm²	8.4169	8.4169	3808	3808	2.6260		0.1054 e-5	

Table 5.14 : Elapsed time comparison for method, model improvement and simulator

	Method Improvement	Model Improvement	Simulator
Cell-1	323.498023 seconds	87.007248 seconds	4.313525 seconds
Cell-2	257.967132 seconds	63.070596 seconds	5.330890 seconds
Cell-3	335.995141 seconds	85.950575 seconds	5.291351 seconds
Cell-4	335.748234 seconds	43.363058 seconds	5.406006 seconds
Cell-5	347.334942 seconds	83.041698 seconds	4.279682 seconds
Cell-6	312.055578 seconds	92.350473 seconds	5.873948 seconds

Using improved model brings us obtaining parameters in four times shorter then improved method as it is depicted in Table 5.14. Moreover, the speed of ICS simulators are astonishing which is at least ten times speedy then improved model. That means also forty times faster then improved method. However, It is heavily dependent to the accurate results obtained from the improved method and model.

6. DISCUSSION AND FUTURE PLAN

Although, we managed to create an accurate model and a way to design predictive simulators for different solar cells individually, modelling a device to use in practice is an issue and needs plenty of experimental data and gathering analyzing them is a matter of time. Therefore, there are some points need to be discussed about this study and future works are needed.

First of all, our approach requires some revisions in order to get comprehensive understanding on AC behaviors and temperature dependancy as well as to get accurate results under dark conditions. Dark conditions are not included in our study because of the lack of time and data. However, slight inconsistancy of the fitting results and apparent difference between simulator results and measured data give an impress about the improved model that there might be shortcoming components necessary under dark condition such as an additional diode to represent dark saturation current. Nevertheless, our model satisfy the needs for DC illumunated conditions which is the most common state of a solar cell on to the operation.

Another point is that the CSDM which is the basic of our model is valid model for DC analyses of other type of solar cells such as organic and inorganic solar cells as it is shown in literature (See Chapter 3). In our opinion, this inclusive qualification of CSDM must be the same for our improved model too. Thus, to approve this forecast measured data of different type of solar cells is needed.

There is also a future project might be considered so as to improve invented ICS simulator and create a GUI called "ICS generator" to let researchers to generate individual simulators of their cells with a few easy steps. In order to do that, simulator must be well defined and written with intersected and interrelated optimization codes and these codes must be composed as a GUI.

Although, these improvements and project requires a big study group and plenty of data and effort, if a ICS generator can be achieved, it will be an outstanding contribution to iterature as well as industry.

REFERENCES

[1] **Whitesides, G. M., Crabtree, G. W.,** (2009). Don't Forget Long-Term Fundamental Research in Energy. Science, **Vol. 315**, pp. 796-798

[2] **Jasim, K. E.,** (2011). Dye Sensitized Solar Cells - Working Principles, Challenges and Opportunities, Solar Cells - Dye-Sensitized Devices, Kosyachenko, L. A. (Ed.), ISBN: 978-953-307-735-2, InTech

[3] **Madougou, S., Kaka, M., Sissoko, G.** (2010). Silicon Solar Cells: Recombination and Electrical Parameters, Solar Energy, Radu D Rugescu (Ed.), ISBN: 978-953-307-052-0, InTech Retrieved from: http://www.intechopen.com/books/solar-energy/silicon-solar-cells-recombination-and-electricalparameters

[4] **Nunzi, J-M,** (2002). Organic photovoltaic materials and devices C. R. Physique, 3, pp. 523–542

[5] **Stathatos, E.,** (2012). Dye Sensitized Solar Cells: A New Prospective to the Solar to Electrical Energy Conversion. Issues to be Solved for Efficient Energy Harvesting. J. of Engin. Sci. and Tech. Review, 5, no. 4, pp. 9 -13

[6] Retrieved from http://i0.wp.com/solarlove.org/wp-content/uploads/2013/06/nrel-solar-cell-efficiency-graph.jpg

[7] **Bonkoungou, D., Koalaga, Z., Donatien Njomo , D.,** (2013). Modelling and Simulation of photovoltaic module considering single -diode equivalent circuit model in MATLAB. International J. of Emerging Technology and Adv. Eng., Vol. 3, Is. 3, pp. 493-502

[8] **Zeman, M., Krc, J.,** (2007). Electrical and Optical Modelling of Thin-Film Silicon Solar Cells. Mater. Res. Soc. Symp. Proc., Vol. 989

[9] **BISHOP , J. W.,(1988).** Compute Ssimulation of the Effects of Electrical Mismaches in Photovoltaic Cell Interconnection Circuit. Solar Cells, Vol. **25** , pp. 73 – 89

[10] **J. Merten,J., Asensi, J. M., Voz, C., Shah, A.V., Platz, R., Andreu,J.,** (1998). Improved Equivalent Circuit and Analytical Model for Amorphous Silicon Solar Cells and Modules. IEEE Transection on Electron Devices, **Vol. 45,** no. 2, pp. 423-429.

[11] **Cheknane, A., Hilal, H. S., Djeffal, F., Benyoucef, B., Charlese, J. P.,** (2008). An equivalent circuit approach to organic solar cell modelling. Microelectronics J., **39**, 1173–1180 doi:10.1016/j.mejo.2008.01.053

[12] **Yoo, S., Domercq, B., Kippelen, B.,** (2005). Intensity-dependent equivalent circuit parameters of organic solar cells based on pentacene and C60. J. Appl. Phys., 97, no. 103706 doi: 10.1063/1.1895473

[13] **Pallarès, J., Cabré, R., Marsal, L. F.,** (2006). A compact equivalent circuit for the dark current-voltage characteristics of nonideal solar cells. Journal of Applied Physics, Vol. 100, 084513

[14] **Tripathi, B., Yadav, P., Kumar, M.,** (2013). Effect of Varying Illumination and Temperature on Steady-State and Dynamic Parameters of Dye-Sensitized Solar Cell Using AC Impedance Modeling. International Journal of Photoenergy, **Vol. 2013**, ID 646407

[15] **Choi, S., Potscavage, W. J., Jr., Kippelen, B.,** (2009). Area-scaling of organic solar cells. Journal of Applied Physics, Vol. 106, 054507

[16] **Moliton, A., Nunzi, J.-M.,** (2006). Review How to model the behaviour of organic photovoltaic cells. Polym Int., Vol. 55, pp. 583–600

[17] **Guliania, R., Jain, A., Kapoora, A.,** (2012). Exact Analytical Analysis of Dye-Sensitized Solar Cell: Improved Method and Comparative Study. The Open Renewable Energy J., Vol. **5**, 49-60

[18] **Koide, N., Islam, A., Chiba, Y., Han, L.,** (2006). Improvement of efficiency of dye-sensitized solar cells based on analysis of equivalent circuit. Journal of Photochemistry and Photobiology A: Chemistry, Vol. 182, pp. 296–305

[19] **Han, L., Koide, N., Chiba, Y., Islam, A., Mitate, T.,** (2006) . Diode I-U Curve Fitting with Lambert W Function. C. R. Chimie, **9**, 645–651 doi:10.1016/j.crci.2005.02.046

[20] **Hanmin, T., Zhao Danyang, Z.,** (2012). High Precise Diagnosis of DSSCs Electrical Parameters based on the Equivalent Circuit Analysis. Inter. Con. on Envir. Eng. and Tech. Adv. in Biomed. Eng., Vol.**8**, pp. 64-68.

[21] **Tian, H., Zhang, J., Wang, X., Yu, T., Zou, Z.,** (2011). Influence of capacitance characteristic on I–V measurement of dye-sensitized solar cells. Measurement, Vol. 44, pp. 1551–1555

[22] **Romero ,B., Pozo, G. del, Arredondo, B.,** (2012). Exact analytical solution of a two diode circuit model for organic solar cells showing S-shape using Lambert W-functions. Solar Energy, Vol. **86**, pp. 3026–3029

[23] **Breitenstein, O.,** (2013). Understanding the current-voltage characteristics of industrial crystalline silicon solar cells by considering inhomogeneous current distributions. Opto−Electron. Rev., 21, no. 3, pp. 259–282 Doi:10.2478/s11772−013−0095−5

[24] **Mazhari, B.,** (2006). An improved solar cell circuit model for organic solar cells. Solar Energy Materials & Solar Cells, 90, pp. 1021–1033

[25] **Chegaar , M. , Azzouzi , G., Mialhe,P.,** (2006). Simple parameter extraction method for illuminated solar cells. Solid-State Electronics, Vol. **50**, pp. 1234–1237

[26] **Chegaar, M., Ouennoughi, Z., Guechi, F.,** (2004). Extracting dc parameters of solar cells under illumination. Vacuum, **75**, pp. 367–372

[27] **Villalva, M. G., Gazoli, J. R., and Filho, E. R.,** (2009). Comprehensive Approach to Modeling and Simulation of Photovoltaic Arrays. IEEE Transactions on Power Electronics, Vol. **24**, no. 5, pp. 1198-1207

[28] **Phang, J. C. H., Chang, D. S. H.,Phillips, J. R.,** (1984). Accurate Analytical Method for The Extraction of Solar Cell Model Parameters. Elec. Let., Vol. **20**, no. 10, pp. 406-408

[29] **Saleem, H., Karmalkar, S.,** (2009). An Analytical Method to Extract the Physical Parameters of a Solar Cell From Four Points on the Illuminated J–V Curve. IEEE Electron Device Letters, Vol. 30, no. 4,pp. 349-352

[30] **Villanueva-Cab, J., Oskam, G., Anta, J. A.,** (2010). A simple numerical model for the charge transport and recombination properties of dye-sensitized solar cells: A comparison of transport-limited and transfer-limited recombination. Solar Energy Materials & Solar Cells, Vol. 94, pp. 45–50

[31] **Ortiz-Conde, A., Sa´ nchez, F. J. G., Muci, J.,** (2006). Solar Energy Materials & Solar Cells, **90**, pp. 352–361

[32] **Hruska, P., Chobola, Z., Grmela, L.,** (2006). Diode I-U Curve Fitting with Lambert W Function. PROC. 25th International Conference on Microelectronics (MIEL), Belgrade, Serbia and Montenegro, May 14-17

[33] **Can, M.,** (2012). Organik Işik Yayan Diyotlar ve Boyar Maddeli Fotovoltaik Hücreler İçin Organik Malzeme Sentezi ve Uygulamalari. PhD thesis, Ege University, Izmir

[34] **Unger, E.,** (2012). XDSC: Excitonic Dye Solar Cells. PhD thesis, Uppsala University, Uppsala, Sweden

[35] **GRätzel, M.,** (2009). Recent Advances in Sensitized Mesoscopic Solar Cells. Accounts of Chemical Research, Vol. 42, No. 11, pp. 1788-1798

[36] **Tang, C. W.,** (1986). Twolayer organic photovoltaic cell. Applied Physics Letters, 48, pp. 183-185 doi: 10.1063/1.96937

[37] **O'Regan, B., Grätzel, M.,** (1991). A low cost, high efficiency solar cell based on dye sensitized colloidal TiO_2 films. Nature, Vol. 353, pp. 737-740

[38] **Chapin, D. M., Fuller, C. S., Pearson, G. L.,** (1954). A New Silicon pn Junction Photocell for Converting Solar Radiation into Electrical Power. Journal of Applied Physics, Vol. 25, 676 doi: 10.1063/1.1721711

[39] **Fraas, L., Partain, L.,** (2010). Solar Cells and Their Applications (Second Edition). New Jersey: John Wiley & Sons

[40] **Reynolds, D. C., Leies, G., Antes, L. L., Marburger, R. E., (**1954). Photovoltaic Effect in Cadmium Sulfide. Physical Review, **96**, 533-534.

[41] **Green, M. A., Emery, K., Hishikawa, Y., Warta, W., Dunlop, E. D**., (2012). Progress in Photovoltaics: Research and Applications, **Vol. 20**, pp. 12-20.

[42] **Gregg, B. A., Hanna, M. C.,** (2003). Journal of Applied Physics, **Vol. 93**, 3605-3614.

[43] Encyclopedia of Nanoscience and Nanotechnology Volume 3 Number 1 2004

[44] **Kasap, S., Capper, P.,** (2006). Handbook of Electronic and Photonic Materials. Springer pg 1099

[45] **B. Kippelen,B., Bredas, J-L.,** (2009). Organic Photovoltaics. Energy & Environmental Science, **Vol. 2**, pp. 241-332.

[46] **Yu, G., Gao, J., Hummelen, J. C., Wudl, F., Heeger, A. J.,** (1995). Polymer Photovoltaic Cells: Enhanced Efficiencies via a Network of Internal Donor-Acceptor Heterojunctions. Science, Vol. 270, pp. 1789-1791

[47] **Service, R. F.,** (2011). Outlook Brightens for Plastic Solar Cells. Science, Vol. 332, pp. 293

[48] **Waldauf, C., Schilinsky, P., Hauch, J., Brabec, C. J.,** (2004). Material and device concepts for organic photovoltaics: towards competitive efficiencies. Thin Solid Films 451 –452, pp. 503–507

[49] **J. Nelson, J.,** (2002). Organic Photovoltaic Films. Current Opinion in Solid State and Materials Science, **Vol. 6**, 87-95.

[50] **Hoppe, H., Sariciftci, N. S.,** (2004). Organic Solar Cells: An Overview. J. Mater. Res., **Vol. 19**, pp. 1924-1945

[51] **Vlachopoulos, N., Liska, P., Augustynski, J., Graetzel, M.,** (1988). Very efficient visible light energy harvesting and conversion by spectral sensitization of high surface area polycrystalline titanium dioxide films. J. Am. Chem. Soc., **Vol. 110**, no. 4, 1216–1220.

[52] **Chen, C., Wang, M., Li, J., Pootrakulchote, N., Alibabaei, L., Ngoc-le, C., J. Decoppet, J., Tsai, J., Grätzel, C., Wu, C., Zakeeruddin, S. M., Grätzel, M.,** (2009). Highly Efficient Light-Harvesting Ruthenium Sensitizer for Thin-Film Dye-Sensitized Solar Cells., ACS Nano, **Vol. 3**, 3103-3109.

[53] **Yella, A., Lee, H., Tsao, H., Yi, C., Chandiran, A., Nazeeruddin, M. K., Diau, E., Yeh, C., Zakeeruddin, S., Grätzel, M.,** (2011). Porphyrin-Sensitized Solar Cells with Cobalt (II/III)-Based Redox Electrolyte Exceed 12 Percent Efficiency. Science, **Vol. 334**, pp. 629-634 DOI: 10.1126/science.1209688

[54] **Grätzel, M.,** (2006). The Advent of Mesoscopic Injection Solar Cells. Progress in Photovoltaics: Research and Applications, **Vol. 14**, pp. 429-442 DOI: 10.1002/pip.712

[55] **Barber, J., Andersson, B.,** (1994). Revealing the blueprint of photosynthesis, Nature, **Vol. 370**, pp. 31-34.

[56] **Khan, Md I.,** (2013). A Study on the Optimization of Dye-Sensitized Solar Cells. MS thesis, University of South Florida

[57] **Xin, X.,** (2012). Dye- and quantum dot-sensitized solar cells based on nanostructured wide-bandgap semiconductors via an integrated experimental and modeling study. PhD Thesis, Iowa State University, Ames, Iowa

[58] **Barbé, C. J., Arendse, F., Comte, P., Jirousek, M., Lenzmann, F., Shklover, V., Grätzel, M.,** (1997). Nanocrystalline Titanium Oxide Electrodes for Photovoltaic Applications. J. Am. Ceram. Soc., Vol. 80, no. 12, pp. 3157–3171

[59] **Hiren Patel, H., Agarwal, V., Member, S.,** (2008). MATLAB-Based Modeling to Study the Effects of Partial Shading on PV Array Characteristics. IEEE Transactions on Energy Conversion, Vol. **23**, no. 1, pp. 302-310

[60] **Chegaar, M., Nehaoua, N., Bouhemadou, A.,** (2008). Organic and inorganic solar cells parameters evaluation from single I–V plot. Energy Conversion and Management 49, pp. 1376–1379

[61] **Firoz Khan, F., Singh, S. N., Husain, M.,** (2010). Effect of illumination intensity on cell parameters of a silicon solar cell. Solar Energy Materials & Solar Cells, **Vol. 94**, pp. 1473–1476

[62] **Khan, F., Singh, N., Husain, M.,** (2010). Determination of diode parameters of a silicon solar cell from variation of slopes of the I–V curve at open circuit and short circuit conditions with the intensity of illumination. Semicond. Sci. Technol., Vol. 25, 015002 (8pp) doi:10.1088/0268-1242/25/1/015002

[63] **KEITHLEY INSTUMENTS** Inc. Electrical Characterization of Photovoltaic Materials and Solar Cells with the Model 4200-SCS Semiconductor Characterization System   I-V, C-V, C-f, DLCP, Pulsed I-V, Resistivity, andHall Voltage Measurements. Application Note Series, no. 3026

[64] **Kumar, P., Jain, S. C., Kumar, V., Chand, S., Tandon, R.P.,** (2009). A model for the current–voltage characteristics of organic bulk heterojunction solar cells. J. Phys. D: Appl. Phys. 42, 055102 (7pp) doi:10.1088/0022-3727/42/5/055102

[65] **Nehaou, N., Chergui, Y., Mekki, D. E.,** (2010). Determination of organic solar cell parameters based on single or multiple pin structures. Vacuum, **84**, pp. 326–329

[66] **Schilinsky, P., Waldauf, C., Jens Hauch, J., Brabec, C. J.,** (2004). Simulation of light intensity dependent current characteristics of polymer solar cells. Journal of Applied Physics Vol. 95, no. 5, pp. 2816- 2819 DOI: 10.1063/1.1646435

[67] **Tian Hanmin, T., Xiaobo, Z., Yuan Shikui,Y., Wang Xiangyan, W., Zhipeng, T., Bin, L., Ying, W., Tao, Y., Zhigang, Z.,** (2009). An improved method to estimate the equivalent circuit parameters in DSSCs. Solar Energy, Vol. 83, pp. 715–720

[68] **Murayama, M., Mori, T.,** (2006). Evaluation of treatment effects for high-performance dye-sensitized solar cells using equivalent circuit analysis. Thin Solid Films, Vol. 509, pp. 123 – 126

[69] **Hoshikawa, T., Kikuchi, R., Eguchi, K.,** (2006). Impedance analysis for dye-sensitized solar cells with a reference electrode. Journal of

Electroanalytical Chemistry, 588, pp. 59–67 doi:10.1016/j.jelechem.2005.12.017

[70] **William J. Potscavage, W. J.,** (2011). Physıcs and Engıneerıng of Organıc Solar Cells, PhD Thesis, Georgia Institute of Technology.

[71] **Labat, F., Bahers, T. L., Ciofini, I., Adamo, C.,** (2012). First-Principles Modeling of Dye-SensitizedSolar Cells: Challenges and Perspectives. Accounts of Chemıcal Research, Vol. 45, no. 8, , pp. 1268–1277

[72] **Guliani, R., Jain, A., Sharma, S., Kaur, D., Guliani, A., Kapoor, A.,** (2013). Analysis of Electrical Characteristics using a Lambert W-Function Technique and MATLAB Simulation for Dye Sensitised ZnO Solar Cell. The Open Renewable Energy Journal, Vol. 6, pp. 23-28

[73] **Chan, D. S. H., PHANG, J. C.H.,** (1987). Analytical Methods for the Extraction of Solar-Cell Single- and Double-Diode Model Parameters from I- V Characteristics. IEEE Transactions on Electron Devices, Vol. Ed. 34, no. 2, pp. 286-293

[74] **Mawyin, J. A.,** (2009). Characterization of Anthocyanin Based Dye-Sensitized Organic Solar Cells (DSSC) and Modifications Based on Bio-Inspired Ion Mobility Improvements. PhD Thesis. Stony Brook University, Stony Brook

[75] **Wolf, M., Rauschenbacht, H.,** (1963). series resistance effects on solar cell measurements. Advanced Energy Conversion., Vol. 3, pp. 455-479.

[76] **Araujo, G. L., Sanchez, E.,** (1982). A New Method for Experimental Determination of the Series Resistance of a Solar Cell. IEEE Transactions on Electron Devices, Vol. 29, no. 10, pp. 1511-1513

[77] **Koster, L. J., Mihailetchi, V., D., Xie, H., Blom, P. W.,** (2005). Origin of the light intensity dependence of the short-circuit current of polymer/fullerene solar cells. Appl. Phys. Lett., 87, 203502 doi: 10.1063/1.2130396

[78] **Park, Y., Noh, S., Lee, D., Kim, J. Y., Lee, C**., (2011). Temperature and Light Intensity Dependence of Polymer Solar Cells with MoO_3 and PEDOT:PSS as a Buffer Layer. Journal of the Korean Physical Society, Vol. 59, No. 2, pp. 362-366

[79] **Riedel, I., Parisi, J., Dyakonov, V., Lutsen, L., Vanderzande, D**., (2004). Effect of Temperature and Illumination on the Electrical Characteristics of Polymer-Fullerene Bulk-Heterojunction Solar Cells. Adv. Funct. Mater., Vol. 14, no. 1, pp. 38-44 doi:10.1002/adfm.200304399

[80] **Moulé, A. J., Meerholz, K**., (2008). Intensity-dependent photocurrent generation at the anode in bulk-heterojunction solar cells. Appl. Phys. B, DOI: 10.1007/s00340-008-3081-8

[81] **Kyocera Solar.** KC200GT high efficiency multicrystal photovoltaic module [Datasheet]. Retrieved from http://www.kyocerasolar.com/assets/001/5195.pdf

APPENDICES

APPENDIX A: Matlab codes of method

APPENDIX A

Codes of Improved Method Kernel Functions

Method function codes

```matlab
function [ Voc FF Rs Rsh_ n I0 Isc_ Ipred I_ V_] =
Omer2013(IVData,b)

%% I must be A
global I V Isc Rsh
q = 1.602*10^-19;
k = 1.38*10^-23;
T = 300;
beta = q./(k.*T);
Vth = 1./beta;

IVData(:,2)=-IVData(:,2);
I=IVData(:,2);
V=IVData(:,1);
%Breaking apart input matrix

%Finding the Isc (foo is a dummy variable)
[foo, SCindex] = min(abs(V));
Isc = I(SCindex);
Isc_=Isc*1e3;%mA

%Finding the Voc
[foo, OCindex] = min(abs(I));
Voc = V(OCindex);

%Defining initial guess value of Rsh as the slope at V<=0
Vlin=IVData(SCindex-4:SCindex,1);
Ilin=IVData(SCindex-4:SCindex,2);
 [f,err] = polyfit(Vlin, Ilin,1);
Gsh = -f(1); %Defining the shunt resistance as the slope
Rsh = 1./Gsh;
Rsh_=Rsh;

%Defining initial guess value of Rs as the slope around V>>0
Vlin_oc=IVData(end-10:end,1);
Ilin_oc=IVData(end-10:end,2);
 [f,err] = polyfit(Vlin_oc, Ilin_oc,1);
Gs = -f(1); %Defining the shunt resistance as the slope
Rs = 1./Gs;

n = b(1);
I0 =b(2); %for organic and DSSC
% I0=1e-5;%for single crystal cell
a= [Rs n I0];

%Calculating the modelling variables by minimizing SSE (using a
%user-defined function that takes the input data + initial guesses
and
%outputs the sum of squared error)
solved = fminsearch(@diode_minerr_2, a);

%---------------------------------
```

```
%Fill factor and power calculations
V=IVData(:,1);
I=IVData(:,2);
Vmod = V(SCindex:OCindex);
Imod = I(SCindex:OCindex);

P = Vmod.*Imod;
[Pmax,Pmaxpt] = max(abs(P));
Vprime = Vmod(Pmaxpt);
Iprime = Imod(Pmaxpt);

FF = (Iprime.*Vprime)./(Voc.*Isc);
%---------------------------------
%Outputting relevant data
clear V I
V_=IVData(:,1);
I_=IVData(:,2);
I= I_;
V=V_;
Rs = solved(1);
 n = solved(2);
I0 = solved(3);

Ipred = -V./(Rs+Rsh)-
lambertw(((Rs.*I0.*Rsh).*exp((Rsh.*(Rs.*Isc*(Rsh+Rs)/Rsh+Rs.*I0+V)).
/(n.*Vth.*(Rs+Rsh))))./(Rs.*n.*Vth+Rsh.*n.*Vth)).*(n.*Vth)./Rs +
Rsh.*(I0+Isc*(Rsh+Rs)/Rsh)./(Rs+Rsh);

Ipred=Ipred*1e3;
I_=I*1e3;
```

Optimization function of the improved Method

```
function SSE = diode_minerr_2(a)
%This function requires the (global) data from the IV
characteristics and
%the intial guesses for the fitting parameters.  It calculates the
%error between the the diode-Rs-Rsh model and the experimental IV
values.
%Variables
q = 1.602*10^-19;
k = 1.38*10^-23;
T = 298;
beta = q./(k.*T);
Vth = 1./beta;

global I V Isc Rsh

%Exploding the a variable
Rs = a(1);
n = a(2);
I0 = a(3);

%Prediction of the current based using the Lambert W function
Ipred = -V./(Rs+Rsh)-
lambertw(((Rs.*I0.*Rsh).*exp((Rsh.*(Rs.*Isc*(Rsh+Rs)/Rsh+Rs.*I0+V)).
/(n.*Vth.*(Rs+Rsh))))./(Rs.*n.*Vth+Rsh.*n.*Vth)).*(n.*Vth)./Rs +
Rsh.*(I0+Isc*(Rsh+Rs)/Rsh)./(Rs+Rsh);
%Calculating sum of square errors
% SSE = sum((Ipred-I).^2);
SSE = sum((log(abs(Ipred))-log(abs(I))).^2+(Ipred-I).^2);
```

```
end
```

Codes of Improved Model Kernel Functions

Improved model function codes

```matlab
function [ Voc FF Rs Rsh_ Isc_ Ipred I_ V_] = Seyda2013_3(IVData,b)

%%!!I must be A
global I V Isc n I0 Rsh
q = 1.602*10^-19;
k = 1.38*10^-23;
T = 300;
beta = q./(k.*T);
Vth = 1./beta;

IVData(:,2)=-IVData(:,2);
I=IVData(:,2);
V=IVData(:,1);
%Breaking apart input matrix

%Finding the Isc (foo is a dummy variable)
[foo, SCindex] = min(abs(V));
Isc = I(SCindex);
Isc_ =Isc*1e3;%mA
%Finding the Voc
[foo, OCindex] = min(abs(I));
Voc = V(OCindex);

%Using the slope at V=0V as Rsh (otherwise the fitting is
underdefined and
%diverges)
Vlin=IVData(SCindex--4:SCindex,1);
Ilin=IVData(SCindex--4:SCindex,2);
 [f,err] = polyfit(Vlin, Ilin,1);
Gsh = -f(1); %Defining the shunt resistance from slope
Rsh = 1./Gsh;
Rsh_=Rsh;

%Initial guess value of Rs
Vlin_oc=IVData(end-10:end,1);
Ilin_oc=IVData(end-10:end,2);
 [f,err] = polyfit(Vlin_oc, Ilin_oc,1);
Gs = -f(1); %Defining the shunt resistance as the slope
Rs = 1./Gs;

n = b(1);
I0 =b(2); %for organic and DSSC
% I0=1e-5;%for single crystal cell

a= Rs;

%Calculating the modelling variables by minimizing SSE (using a
%user-defined function that takes the input data + initial guesses
and
%outputs the sum of squared error)
```

```matlab
solved = fminsearch(@diode_minerr_n, a);
%----------------------------------
%Fill factor and power calculations
V=IVData(:,1);
I=IVData(:,2);
Vmod = V(SCindex:OCindex);
Imod = I(SCindex:OCindex);


P = Vmod.*Imod;
[Pmax,Pmaxpt] = max(abs(P));
Vprime = Vmod(Pmaxpt);
Iprime = Imod(Pmaxpt);


FF = (Iprime.*Vprime)./(Voc.*Isc);
%----------------------------------
%Outputting relevant data
clear V I
V_=IVData(:,1);
I_=IVData(:,2);
I= I_;
V=V_;
Rs = solved;


Ipred = -V./(Rs+Rsh)-
lambertw(((Rs.*I0.*Rsh).*exp((Rsh.*(Rs.*Isc*(Rsh+Rs)/Rsh+Rs.*I0+V)).
/(n.*Vth.*(Rs+Rsh))))./(Rs.*n.*Vth+Rsh.*n.*Vth)).*(n.*Vth)./Rs +
Rsh.*(I0+Isc*(Rsh+Rs)/Rsh)./(Rs+Rsh);


Ipred=Ipred*1e3;
I_=I*1e3;
```
……

Optimization function of the improved model

```matlab
function SSE = diode_minerr_n(a)
%This function requires the (global) data from the IV
characteristics and
%the intial guesses for the fitting parameters.  It calculates the
%error between the the diode-Rs-Rsh model and the experimental IV
values.

%Variables
q = 1.602*10^-19;
k = 1.38*10^-23;
T = 298;
beta = q./(k.*T);
Vth = 1./beta;

global I V Isc n I0 Rsh

%Exploding the a variable

Rs=a(1);


%Prediction of the current based using the Lambert W function
Ipred = -V./(Rs+Rsh)-
lambertw(((Rs.*I0.*Rsh).*exp((Rsh.*(Rs.*Isc*(Rsh+Rs)/Rsh+Rs.*I0+V)).
/(n.*Vth.*(Rs+Rsh))))./(Rs.*n.*Vth+Rsh.*n.*Vth)).*(n.*Vth)./Rs +
Rsh.*(I0+Isc*(Rsh+Rs)/Rsh)./(Rs+Rsh);
```

```
%Calculating sum of square errors
% SSE = sum((Ipred-I).^2);
SSE = sum((log(abs(Ipred))-log(abs(I))).^2+(Ipred-I).^2);
end
```

An Example of the Driver Codes for Cell-1

Driver codes of method improvement:
```
tic
clc
clear all

disp('SolarCell 1')
fid_2='C:\Users\Arif\Documents\MATLAB\13.05.14\1\1-10.dat';
fid_3='C:\Users\Arif\Documents\MATLAB\13.05.14\1\1-30.dat';
fid_4='C:\Users\Arif\Documents\MATLAB\13.05.14\1\1-40.dat';
fid_5='C:\Users\Arif\Documents\MATLAB\13.05.14\1\1-60.dat';
fid_6='C:\Users\Arif\Documents\MATLAB\13.05.14\1\1-100.dat';

%readoled is a function written to extract datas from exe files
easily.
Mydat_2=readoled(fid_2,2,inf);
Mydat_3=readoled(fid_3,2,inf);
Mydat_4=readoled(fid_4,2,inf);
Mydat_5=readoled(fid_5,2,inf);
Mydat_6=readoled(fid_6,2,inf);

Mydat_2(:,2)=1e-3*Mydat_2(:,2);%Make mA->A
Mydat_3(:,2)=1e-3*Mydat_3(:,2);
Mydat_4(:,2)=1e-3*Mydat_4(:,2);
Mydat_5(:,2)=1e-3*Mydat_5(:,2);
Mydat_6(:,2)=1e-3*Mydat_6(:,2);

a=[1.5 1e-9];

[ Voc(1) FF(1) Rs(1) Rsh(1) n(1) I0(1) Isc(1) Ipred1_2 I2 V2] =
Omer2013(Mydat_2,a);

[ Voc(2) FF(2) Rs(2) Rsh(2) n(2) I0(2) Isc(2) Ipred1_3 I3 V3] =
Omer2013(Mydat_3,a);

[ Voc(3) FF(3) Rs(3) Rsh(3) n(3) I0(3) Isc(3) Ipred1_4 I4 V4] =
Omer2013(Mydat_4,a);

[ Voc(4) FF(4) Rs(4) Rsh(4) n(4) I0(4) Isc(4) Ipred1_5 I5 V5] =
Omer2013(Mydat_5,a);
[ Voc(5) FF(5) Rs(5) Rsh(5) n(5) I0(5) Isc(5) Ipred1_6 I6 V6] =
Omer2013(Mydat_6,a);

figure
semilogy(V2,abs(I2),'bs',V2,abs(Ipred1_2),'b','linewidth',2);
hold on
semilogy(V3,abs(I3),'gs',V3,abs(Ipred1_3),'g','linewidth',2);
hold on
semilogy(V4,abs(I4),'rs',V4,abs(Ipred1_4),'r','linewidth',2);
hold on
```

```
semilogy(V5,abs(I5),'cs',V5,abs(Ipred1_5),'c','linewidth',2);
hold on
semilogy(V6,abs(I6),'ms',V6,abs(Ipred1_6),'m','linewidth',2);
hold off
title('Cell-1')
xlabel('V')
ylabel('log(|I(mA)|)')
legend('10 mW/cm^2','fit','30 mW/cm^2','fit','40 mW/cm^2','fit','60
mW/cm^2','fit','100 mW/cm^2','fit')


figure
 [foo, SCindex] = min(abs(V2));
[foo, OCindex] = min(abs(I2));
plot(V2(SCindex:OCindex),I2(SCindex:OCindex),'rs',V2(SCindex:OCindex
),Ipred1_2(SCindex:OCindex),'b','linewidth',2)
hold on
 [foo, SCindex] = min(abs(V3));
[foo, OCindex] = min(abs(I3));
plot(V3(SCindex:OCindex),I3(SCindex:OCindex),'rs',V3(SCindex:OCindex
),Ipred1_3(SCindex:OCindex),'g','linewidth',2)
hold on
 [foo, SCindex] = min(abs(V4));
[foo, OCindex] = min(abs(I4));
plot(V4(SCindex:OCindex),I4(SCindex:OCindex),'rs',V4(SCindex:OCindex
),Ipred1_4(SCindex:OCindex),'r','linewidth',2)
hold on
 [foo, SCindex] = min(abs(V5));
[foo, OCindex] = min(abs(I5));
plot(V5(SCindex:OCindex),I5(SCindex:OCindex),'rs',V5(SCindex:OCindex
),Ipred1_5(SCindex:OCindex),'c','linewidth',2)
hold on
 [foo, SCindex] = min(abs(V6));
[foo, OCindex] = min(abs(I6));
plot(V6(SCindex:OCindex),I6(SCindex:OCindex),'rs',V6(SCindex:OCindex
),Ipred1_6(SCindex:OCindex),'m','linewidth',2)
hold off
title('Cell-1')
xlabel('V')
ylabel('I(mA)')
legend('10 mW/cm^2','fit','30 mW/cm^2','fit','40 mW/cm^2','fit','60
mW/cm^2','fit','100 mW/cm^2','fit')
toc
```

Driver codes of model improvement:
```
tic
clc
clear all

disp('SolarCell 1')
fid_1='C:\Users\Arif\Documents\MATLAB\13.05.14\1\1 dark.dat';
fid_2='C:\Users\Arif\Documents\MATLAB\13.05.14\1\1-10.dat';
fid_3='C:\Users\Arif\Documents\MATLAB\13.05.14\1\1-30.dat';
fid_4='C:\Users\Arif\Documents\MATLAB\13.05.14\1\1-40.dat';
fid_5='C:\Users\Arif\Documents\MATLAB\13.05.14\1\1-60.dat';
fid_6='C:\Users\Arif\Documents\MATLAB\13.05.14\1\1-100.dat';
Mydat_1=readoled(fid_1,2,inf);
Mydat_2=readoled(fid_2,2,inf);
```

```matlab
Mydat_3=readoled(fid_3,2,inf);
Mydat_4=readoled(fid_4,2,inf);
Mydat_5=readoled(fid_5,2,inf);
Mydat_6=readoled(fid_6,2,inf);

Mydat_1(:,2)=1e-3*Mydat_1(:,2);%Make mA->A
Mydat_2(:,2)=1e-3*Mydat_2(:,2);%Make mA->A
Mydat_3(:,2)=1e-3*Mydat_3(:,2);
Mydat_4(:,2)=1e-3*Mydat_4(:,2);
Mydat_5(:,2)=1e-3*Mydat_5(:,2);
Mydat_6(:,2)=1e-3*Mydat_6(:,2);

mydat_1(:,2)=-Mydat_1(:,2);%Make mA->A
mydat_2(:,2)=-Mydat_2(:,2);%Make mA->A
mydat_3(:,2)=-Mydat_3(:,2);
mydat_4(:,2)=-Mydat_4(:,2);
mydat_5(:,2)=-Mydat_5(:,2);
mydat_6(:,2)=-Mydat_6(:,2);

mydat_1(:,1)=Mydat_1(:,1);
mydat_2(:,1)=Mydat_2(:,1);
mydat_3(:,1)=Mydat_3(:,1);
mydat_4(:,1)=Mydat_4(:,1);
mydat_5(:,1)=Mydat_5(:,1);
mydat_6(:,1)=Mydat_6(:,1);

b=[1.5 1e-9];

[ Voc(5) FF(5) Rs(5) Rsh(5) n I0 Isc(5) Ipred1_6 I6 V6] =
Omer2013(Mydat_6,b);

a=[n I0];

[ Voc(1) FF(1) Rs(1) Rsh(1) Isc(1) Ipred1_2 I2 V2] =
Seyda2013_3(Mydat_2,a);

[ Voc(2) FF(2) Rs(2) Rsh(2) Isc(2) Ipred1_3 I3 V3] =
Seyda2013_3(Mydat_3,a);

[ Voc(3) FF(3) Rs(3) Rsh(3) Isc(3) Ipred1_4 I4 V4] =
Seyda2013_3(Mydat_4,a);

[ Voc(4) FF(4) Rs(4) Rsh(4) Isc(4) Ipred1_5 I5 V5] =
Seyda2013_3(Mydat_5,a);

figure
semilogy(V2,abs(I2),'bs',V2,abs(Ipred1_2),'b','linewidth',2);
hold on
semilogy(V3,abs(I3),'gs',V3,abs(Ipred1_3),'g','linewidth',2);
hold on
semilogy(V4,abs(I4),'rs',V4,abs(Ipred1_4),'r','linewidth',2);
hold on
semilogy(V5,abs(I5),'cs',V5,abs(Ipred1_5),'c','linewidth',2);
hold on
semilogy(V6,abs(I6),'ms',V6,abs(Ipred1_6),'m','linewidth',2);
hold off
title('Cell-1')
xlabel('V')
ylabel('log(|I(mA)|)')
```

```matlab
legend('10 mW/cm^2','fit','30 mW/cm^2','fit','40 mW/cm^2','fit','60
mW/cm^2','fit','100 mW/cm^2','fit')

figure
 [foo, SCindex] = min(abs(V2));
[foo, OCindex] = min(abs(I2));
plot(V2(SCindex:OCindex),I2(SCindex:OCindex),'rs',V2(SCindex:OCindex
),Ipred1_2(SCindex:OCindex),'b','linewidth',2)
hold on
 [foo, SCindex] = min(abs(V3));
[foo, OCindex] = min(abs(I3));
plot(V3(SCindex:OCindex),I3(SCindex:OCindex),'rs',V3(SCindex:OCindex
),Ipred1_3(SCindex:OCindex),'g','linewidth',2)
hold on
 [foo, SCindex] = min(abs(V4));
[foo, OCindex] = min(abs(I4));
plot(V4(SCindex:OCindex),I4(SCindex:OCindex),'rs',V4(SCindex:OCindex
),Ipred1_4(SCindex:OCindex),'r','linewidth',2)
hold on
 [foo, SCindex] = min(abs(V5));
[foo, OCindex] = min(abs(I5));
plot(V5(SCindex:OCindex),I5(SCindex:OCindex),'rs',V5(SCindex:OCindex
),Ipred1_5(SCindex:OCindex),'c','linewidth',2)
hold on
 [foo, SCindex] = min(abs(V6));
[foo, OCindex] = min(abs(I6));
plot(V6(SCindex:OCindex),I6(SCindex:OCindex),'rs',V6(SCindex:OCindex
),Ipred1_6(SCindex:OCindex),'m','linewidth',2)
hold off
title('Cell-1')
xlabel('V')
ylabel('I(mA)')
legend('10 mW/cm^2','fit','30 mW/cm^2','fit','40 mW/cm^2','fit','60
mW/cm^2','fit','100 mW/cm^2','fit')

toc
```

CURRICULUM VITAE

Name Surname: Elif Şeyda Çakmak (updated: Elif Şeyda Aydın)

Place and Date of Birth: Aksaray 05/07/1988

E-Mail: elifseydacakmak@gmail.com

B.Sc.: Electronic Engineering

Professional Experience and Rewards: R&D Engineer at Lazer Market Ltd.

PUBLICATIONS/PRESENTATIONS ON THE THESIS

- Mustafa Can, A. Nuri Ozcivan, **Elif Şeyda Çakmak**, Ceylan Zafer, Sıddık İçli, Ömer Mermer, "Synthesis of novel organic sensitizers in dye-sensitized solar cells: photovoltaic characterization and equivalent circuit modeling" NanoTR-9 2013 - Nanoscience and Nanotechnology Conference June 24-28, Atatürk University, Turkey, 2013, (sunum)

- Mesude Zeliha Yigit, Mustafa Can, A. Nuri Ozcivan, **Elif Seyda Cakmak**, Hakan Bilgili, Sermet Koyuncu, Omer Mermer, "Photovoltaic Characterization and Electrical Modeling of Dye-Sensitized solar cells using novel synthesized organic dyes", ICWEE 2013- Second International Conference on Water, Energy, and Environment, September 21-24, 2013, Kusadası, Turkey (sunum)

- Ömer Mermer, **Elif Şeyda Çakmak**, Mustafa Can, A. Nuri Ozcivan, Ceylan Zafer, Sıddık İçli, "Analysis of Illumination Intensity Dependent Equivalent Circuit Parameters for Dye Sensitized Solar Cells", 3th International Symposium on Computing in Science & Engineering (ISCSE), October 24-25 2013, Kuşadası, Turkey (sunum)

- Mustafa Can, A. Nuri Ozcivan, **Elif Şeyda Çakmak**, Sıddık İçli, Ömer Mermer, "Modeling of Dye-Sensitized Solar Cells for Characterized Devices Manufactured Using New Synthesized Organic Dyes", 1st International Semiconductor Science and Technology Conference" (ISSTC-2014), January13-14 2014, Istanbul, Turkey (sunum)

- Mustafa Can, **Elif Şeyda Çakmak**, Ceylan Zafer, Ömer Mermer, "Analysis Of Illumination Intensity Dependent Equivalent Circuits Parameters For Dye Sensitized Solar Cells", accepted in Turkish Journal of Electrical Engineering & Computer Sciences